Fundamentals of Particle Detectors

Fulvio Tessarotto (I.N.F.N. – Trieste)

Introduction

particle detectors history

CERN accelerators

Some detector technologies

Gaseous Detectors

Signal formation

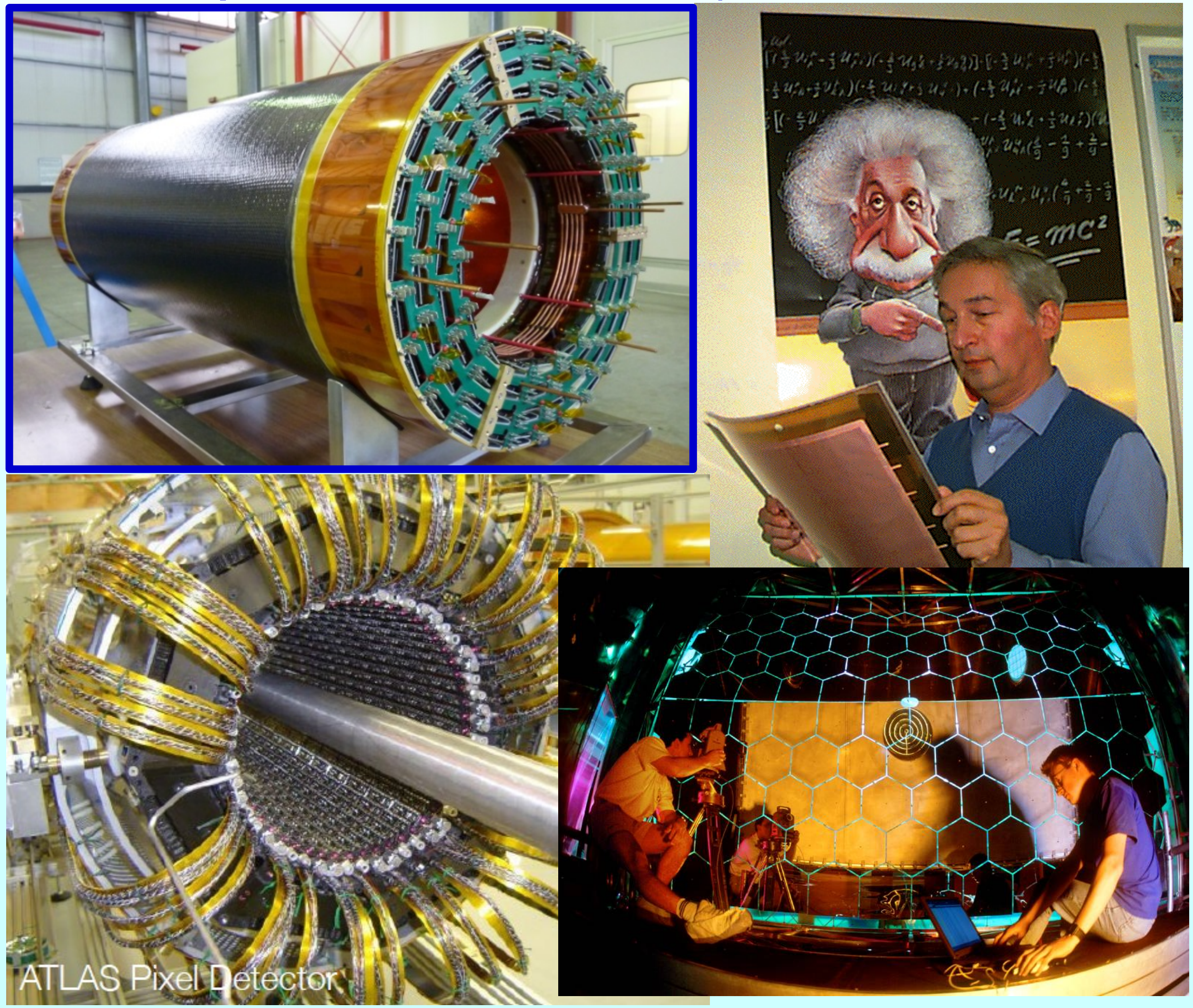

The constituents of matter

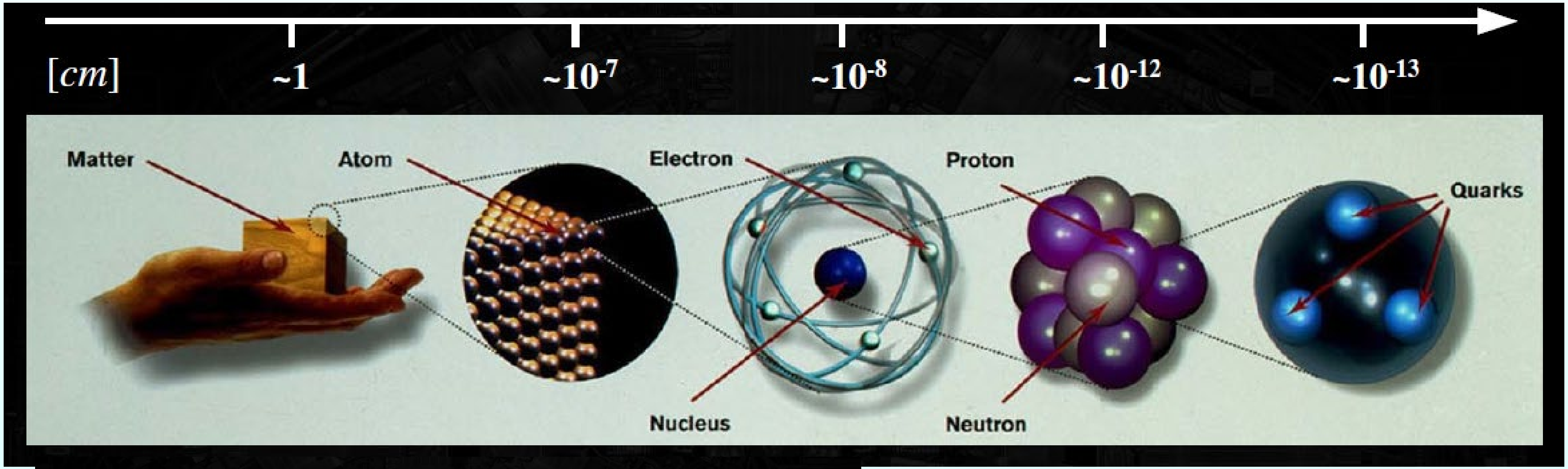

Two families

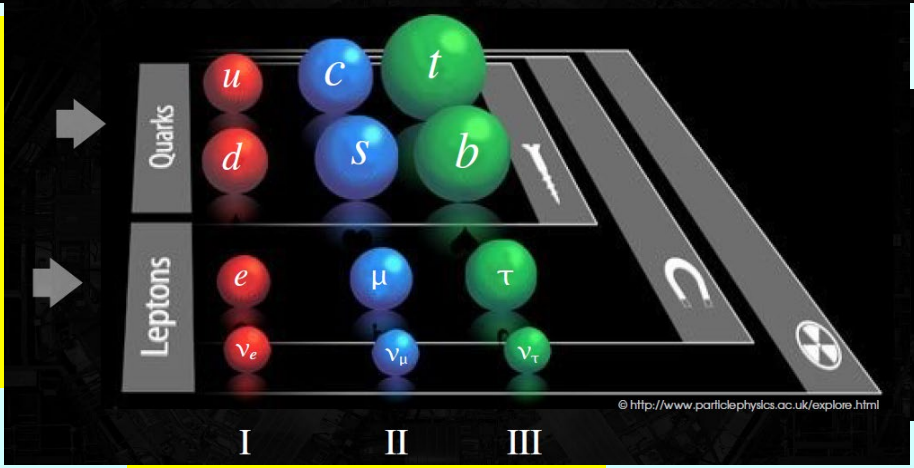

Three generations

Four interactions

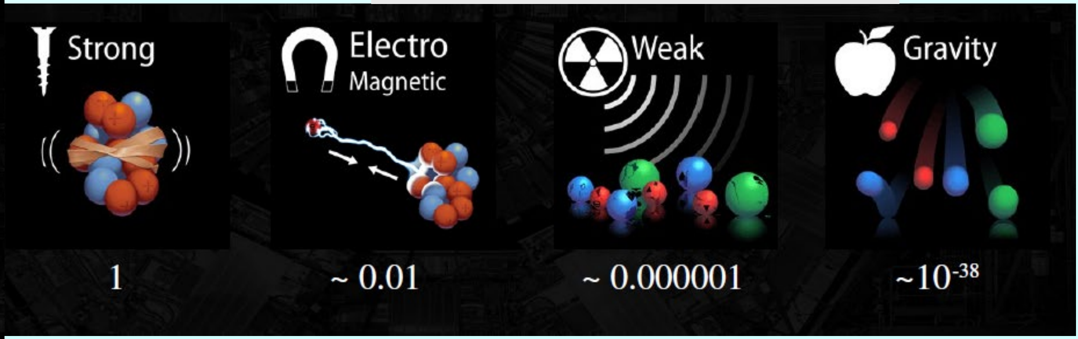

gluon **photon** **W-Z** **graviton**

Particles do what we cannot

The laws which hold at the microscopic level are different from ours

A particle or an atom can stay at the same time in two or more different places

A particle can move from a point to another in space without passing anywhere in between the two points

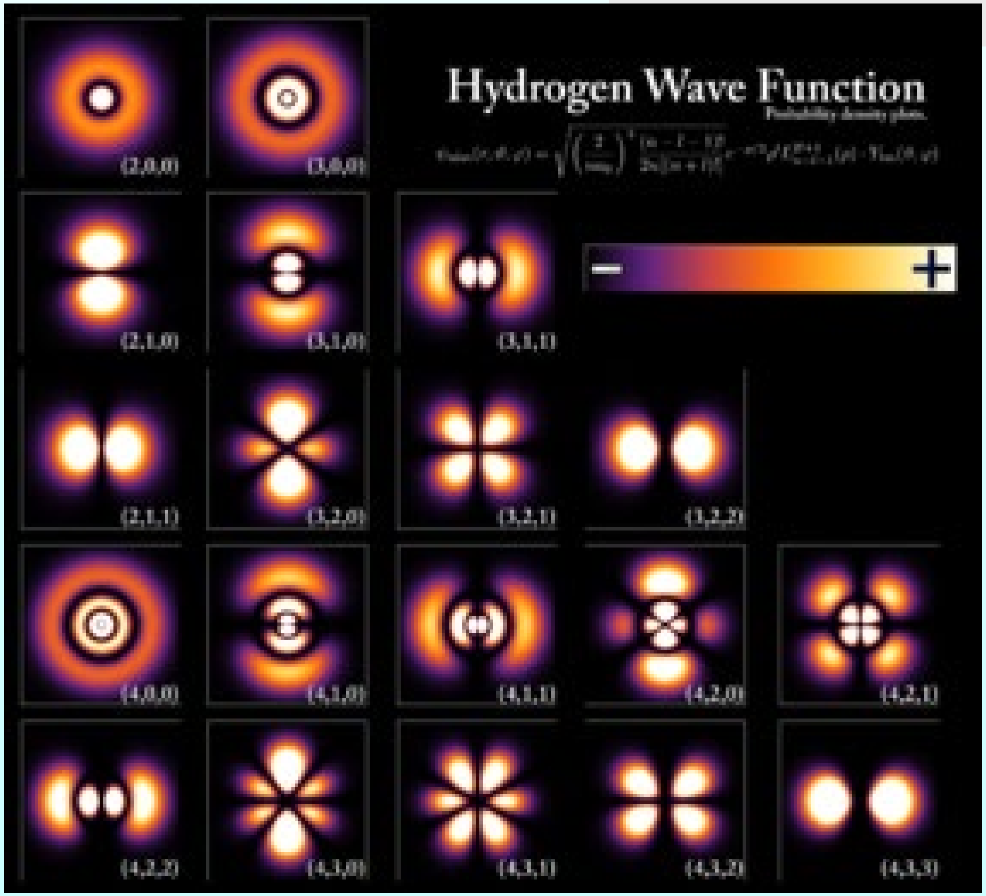

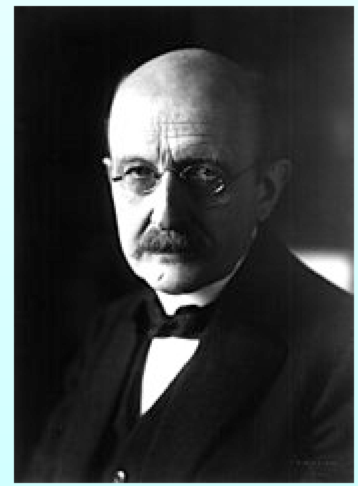

Max Plank is the father of the quantum theory

The Standard Model

Standard Model of

FUNDAMENTAL PARTICLES AND INTERACTIONS

The Standard Model summarizes the current knowledge in Particle Physics. It is the quantum theory that includes the theory of strong interactions (quantum chromodynamics or QCD) and the unified theory of weak and electromagnetic interactions (electroweak). Gravity is included on this chart because it is one of the fundamental interactions even though not part of the "Standard Model."

FERMIONS matter constituents spin = 1/2, 3/2, 5/2, ...

Leptons spin = 1/2

Flavor	Mass GeV/c²	Electric charge
ν_e electron neutrino	$<1\times10^{-8}$	0
e electron	0.000511	–1
ν_μ muon neutrino	<0.0002	0
μ muon	0.106	–1
ν_τ tau neutrino	<0.02	0
τ tau	1.7771	–1

Quarks spin = 1/2

Flavor	Approx. Mass GeV/c²	Electric charge
u up	0.003	2/3
d down	0.006	–1/3
c charm	1.3	2/3
s strange	0.1	–1/3
t top	175	2/3
b bottom	4.3	–1/3

Spin is the intrinsic angular momentum of particles. Spin is given in units of ħ, which is the quantum unit of angular momentum, where $\hbar = h/2\pi = 6.58\times10^{-25}$ GeV s = 1.05×10^{-34} J s.

Electric charges are given in units of the proton's charge. In SI units the electric charge of the proton is 1.60×10^{-19} coulombs.

The **energy** unit of particle physics is the electronvolt (eV), the energy gained by one electron in crossing a potential difference of one volt. **Masses** are given in GeV/c^2 (remember $E = mc^2$), where 1 GeV = 10^9 eV = 1.60×10^{-10} joule. The mass of the proton is 0.938 GeV/c^2 = 1.67×10^{-27} kg.

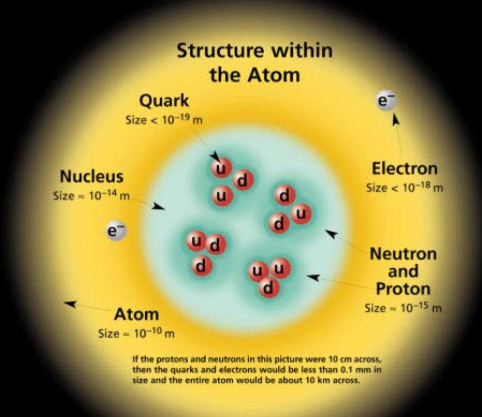

If the protons and neutrons in this picture were 10 cm across, then the quarks and electrons would be less than 0.1 mm in size and the entire atom would be about 10 km across.

BOSONS force carriers spin = 0, 1, 2, ...

Unified Electroweak spin = 1

Name	Mass GeV/c²	Electric charge
γ photon	0	0
W^-	80.4	–1
W^+	80.4	+1
Z^0	91.187	0

Strong (color) spin = 1

Name	Mass GeV/c²	Electric charge
g gluon	0	0

Color Charge

Each quark carries one of three types of "strong charge," also called "color charge." These charges have nothing to do with the colors of visible light. There are eight possible types of color charge for gluons. Just as electrically-charged particles interact by exchanging photons, in strong interactions color-charged particles interact by exchanging gluons. Leptons, photons, and ***W*** and ***Z*** bosons have no strong interactions and hence no color charge.

Quarks Confined in Mesons and Baryons

One cannot isolate quarks and gluons; they are confined in color-neutral particles called **hadrons**. This confinement (binding) results from multiple exchanges of gluons among the color-charged constituents. As color-charged particles (quarks and gluons) move apart, the energy in the color-force field between them increases. This energy eventually is converted into additional quark-antiquark pairs (see figure below). The quarks and antiquarks then combine into hadrons; these are the particles seen to emerge. Two types of hadrons have been observed in nature: **mesons** $q\bar{q}$ and **baryons** qqq.

Residual Strong Interaction

The strong binding of color-neutral protons and neutrons to form nuclei is due to residual strong interactions between their color-charged constituents. It is similar to the residual electrical interaction that binds electrically neutral atoms to form molecules. It can also be viewed as the exchange of mesons between the hadrons.

PROPERTIES OF THE INTERACTIONS

Property \ Interaction	Gravitational	Weak (Electroweak)	Electromagnetic (Electroweak)	Strong: Fundamental	Strong: Residual
Acts on:	Mass – Energy	Flavor	Electric Charge	Color Charge	See Residual Strong Interaction Note
Particles experiencing:	All	Quarks, Leptons	Electrically charged	Quarks, Gluons	Hadrons
Particles mediating:	Graviton (not yet observed)	W^+ W^- Z^0	γ	Gluons	Mesons
Strength relative to electromag for two u quarks at: 10^{-18} m	10^{-41}	0.8	1	25	Not applicable to quarks
Strength relative to electromag for two u quarks at: 3×10^{-17} m	10^{-41}	10^{-4}	1	60	
for two protons in nucleus	10^{-36}	10^{-7}	1	Not applicable to hadrons	20

Baryons qqq and Antibaryons $\bar{q}\bar{q}\bar{q}$

Baryons are fermionic hadrons. There are about 120 types of baryons.

Symbol	Name	Quark content	Electric charge	Mass GeV/c²	Spin
p	proton	uud	1	0.938	1/2
$\bar{p}$	anti-proton	$\bar{u}\bar{u}\bar{d}$	–1	0.938	1/2
n	neutron	udd	0	0.940	1/2
Λ	lambda	uds	0	1.116	1/2
Ω^-	omega	sss	–1	1.672	3/2

Mesons $q\bar{q}$

Mesons are bosonic hadrons. There are about 140 types of mesons.

Symbol	Name	Quark content	Electric charge	Mass GeV/c²	Spin
π^+	pion	$u\bar{d}$	+1	0.140	0
K^-	kaon	$s\bar{u}$	–1	0.494	0
ρ^+	rho	$u\bar{d}$	+1	0.770	1
B^0	B-zero	$d\bar{b}$	0	5.279	0
η_c	eta-c	$c\bar{c}$	0	2 .980	0

Matter and Antimatter

For every particle type there is a corresponding antiparticle type, denoted by a bar over the particle symbol (unless + or – charge is shown). Particle and antiparticle have identical mass and spin but opposite charges. Some electrically neutral bosons (e.g., Z^0, γ, and $\eta_c = c\bar{c}$, but not $K^0 = d\bar{s}$) are their own antiparticles.

Figures

These diagrams are an artist's conception of physical processes. They are ***not*** exact and have ***no*** meaningful scale. Green shaded areas represent the cloud of gluons or the gluon field, and red lines the quark paths.

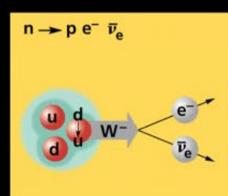

A neutron decays to a proton, an electron, and an antineutrino via a virtual (mediating) W boson. This is neutron β decay.

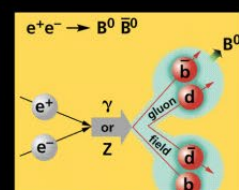

An electron and positron (antielectron) colliding at high energy can annihilate to produce B^0 and $\bar{B}^0$ mesons via a virtual Z boson or a virtual photon.

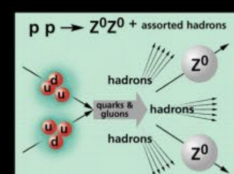

Two protons colliding at high energy can produce various hadrons plus very high mass particles such as Z bosons. Events such as this one are rare but can yield vital clues to the structure of matter.

The Particle Adventure

Visit the award-winning web feature *The Particle Adventure* at **http://ParticleAdventure.org**

This chart has been made possible by the generous support of:

U.S. Department of Energy
U.S. National Science Foundation
Lawrence Berkeley National Laboratory
Stanford Linear Accelerator Center
American Physical Society, Division of Particles and Fields
BURLE INDUSTRIES, INC.

History of the Universe

From Cosmic Microwave Background Radiation and other measurements

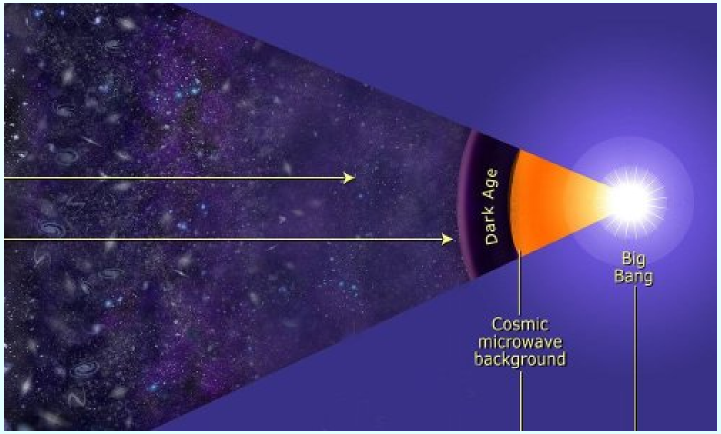

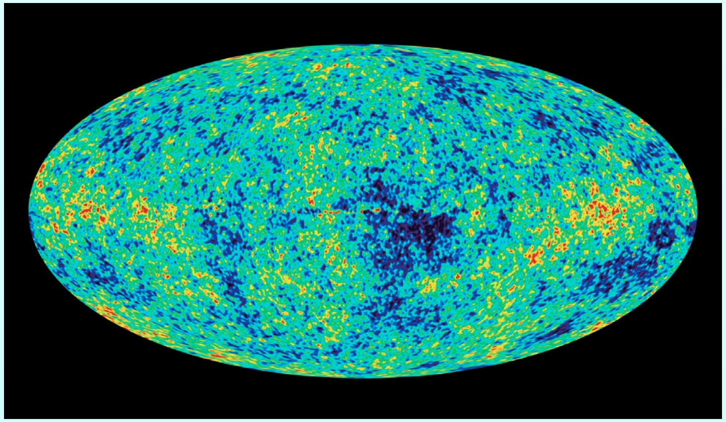

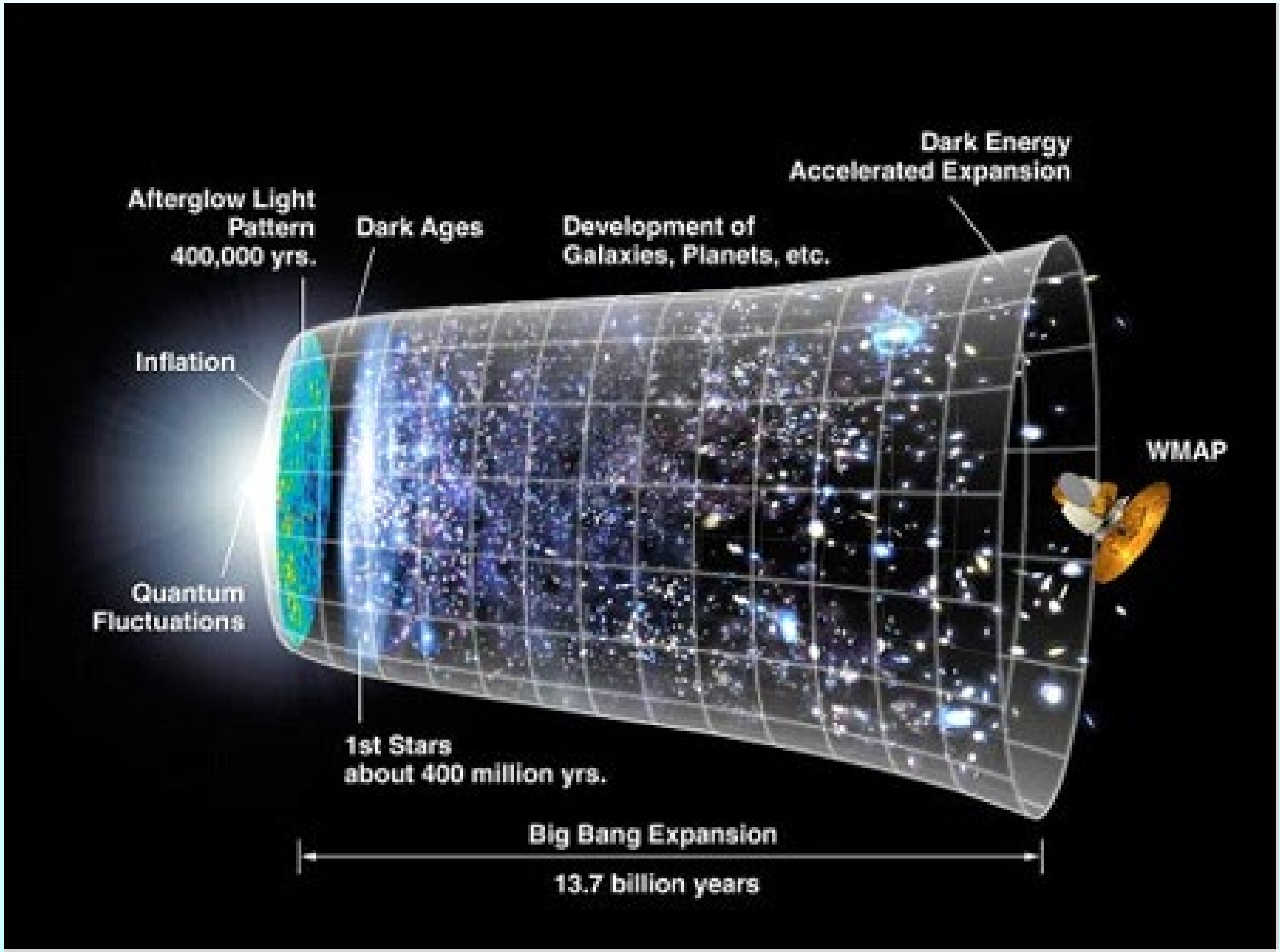

Theoretical panorama

The fundamental constants of nature and unified theories

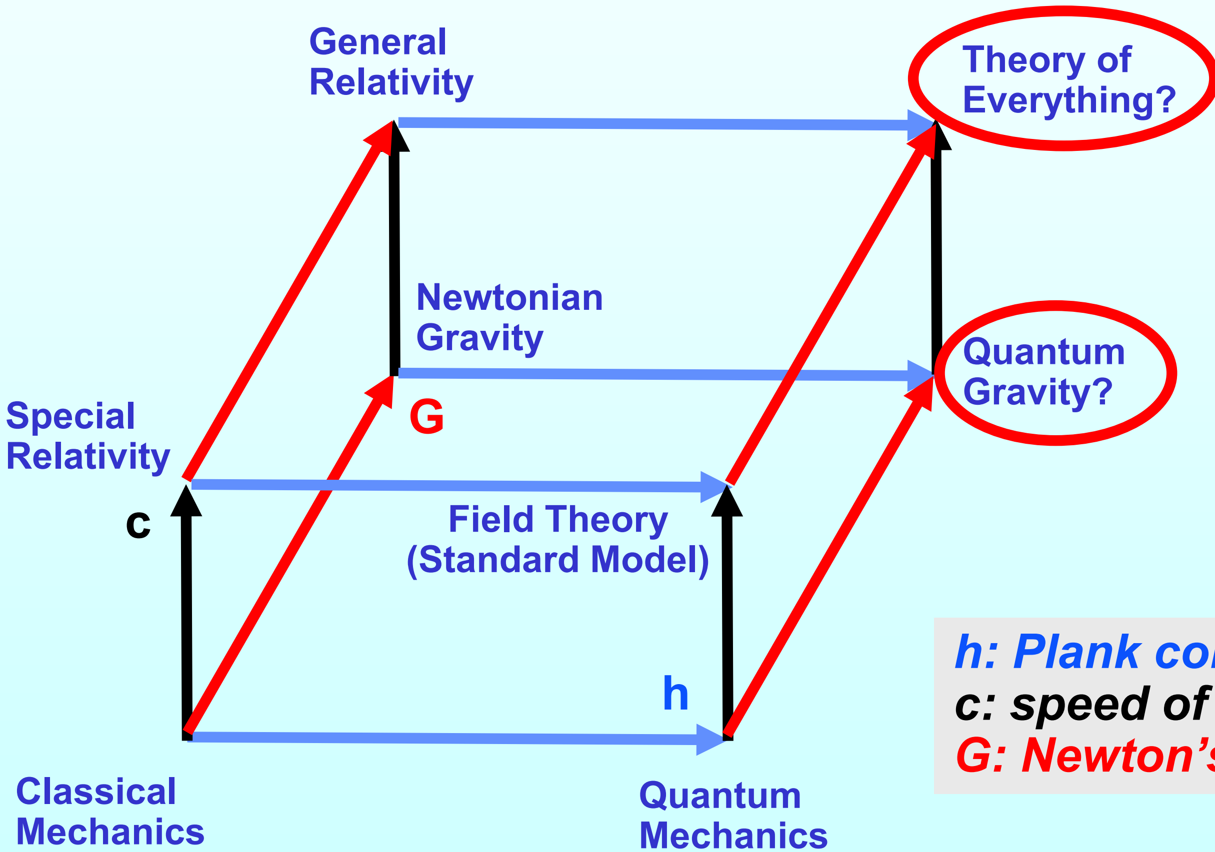

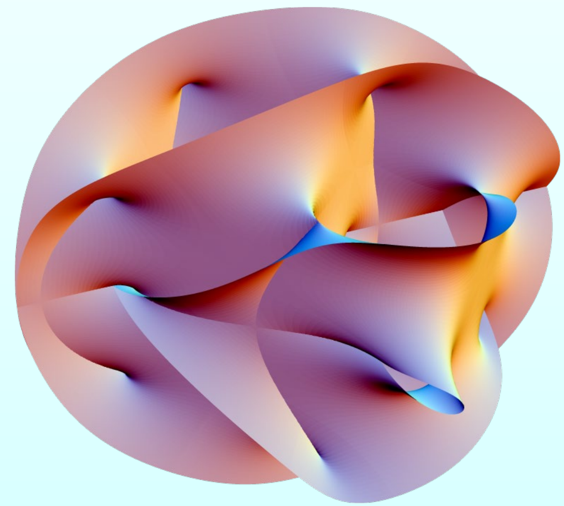

h: Plank constant
c: speed of light
G: Newton's constant

We know a lot about our world

Thanks to theoreticians and experimentalists

There is an ancient Chinese saying:

"He who labors with his mind rules over he who labors with his hand".

This kind of backward idea is very harmful to youngsters from developing countries.

Partly because of this type of concept, many students from these countries are inclined towards theoretical studies and avoid experimental work.

In reality, a theory in natural science can not be without experimental foundations; physics, in particular, comes from experimental work ...

Samuel Ting
December 10, 1976

Nobel Prizes 1974 for the J/ψ discovery

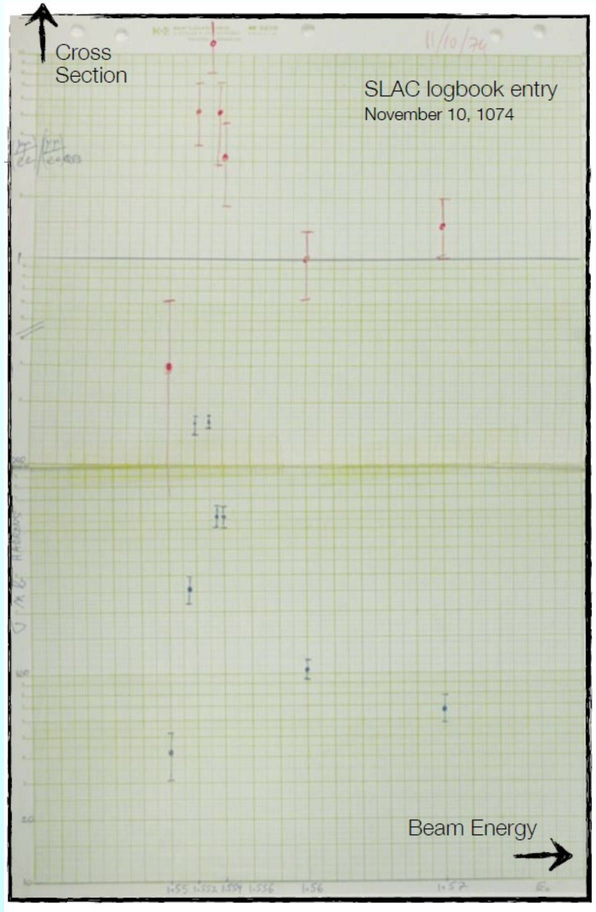

Discoveries and detector technologies

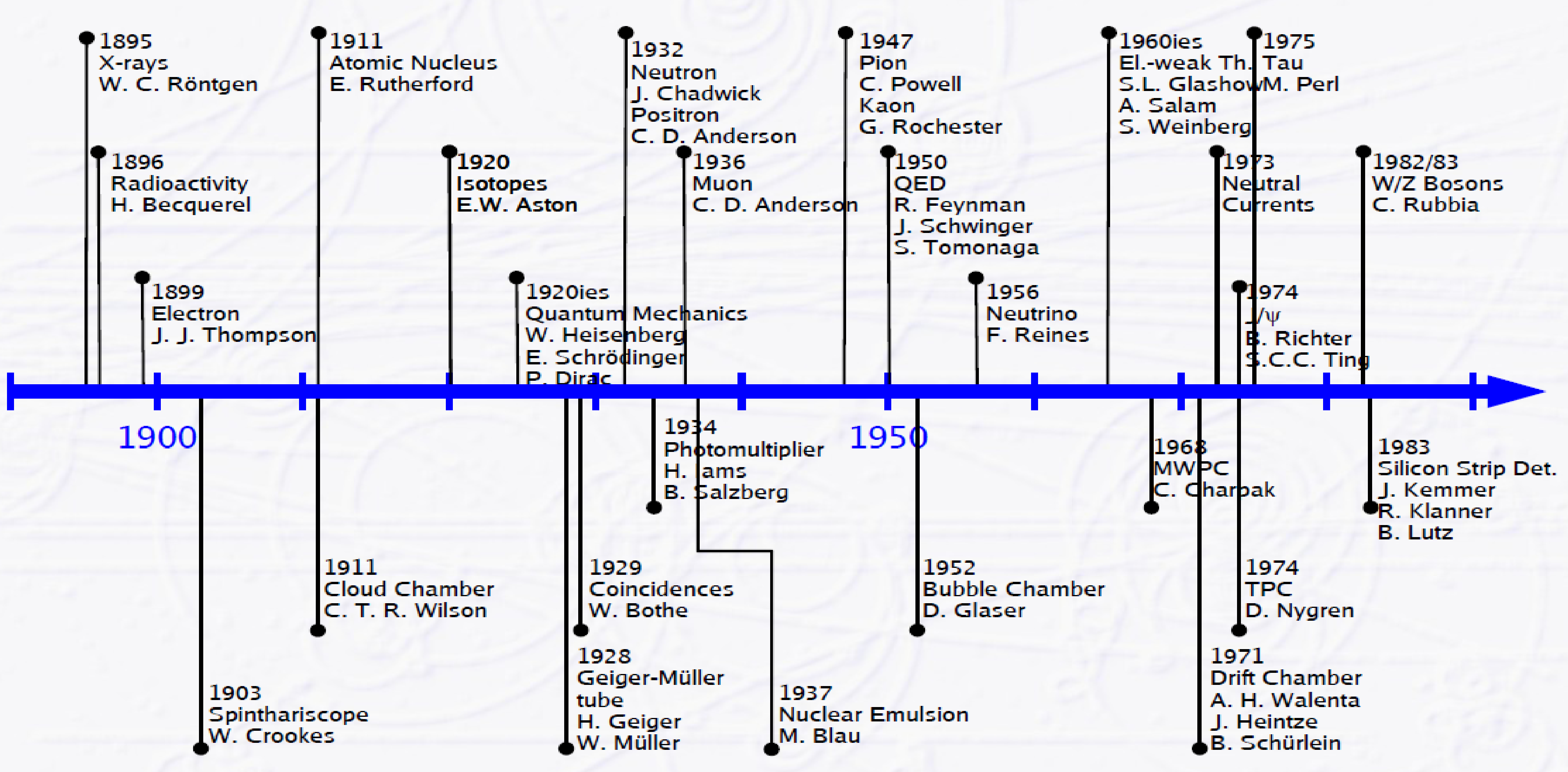

The history of discoveries and that of particle detectors are intimately interconnected

Radioactivity is everywhere

On average a human body has ~30 mg of Potassium 40, corresponding to ~ 4 kBq

$$\beta^- : {}^{40}_{19}K \rightarrow {}^{40}_{20}Ca + e^- + \overline{\nu}_e$$

$$EC : {}^{40}_{19}K + e^- \rightarrow {}^{40}_{18}Ar^* + \nu_e \rightarrow {}^{40}_{18}Ar^* + \nu_e \rightarrow {}^{40}_{18}Ar + \gamma + \nu_e$$

$$\beta^+ : {}^{40}_{19}K \rightarrow {}^{40}_{18}Ca + e^+ + \nu_e$$

My activity is ~ 5000 disintegrations per second

An average banana has 14 Bq

The average annual human exposure to natural background radiation is 2.4 mSv (from 0.4 to 4 mSv/y depending on the location)

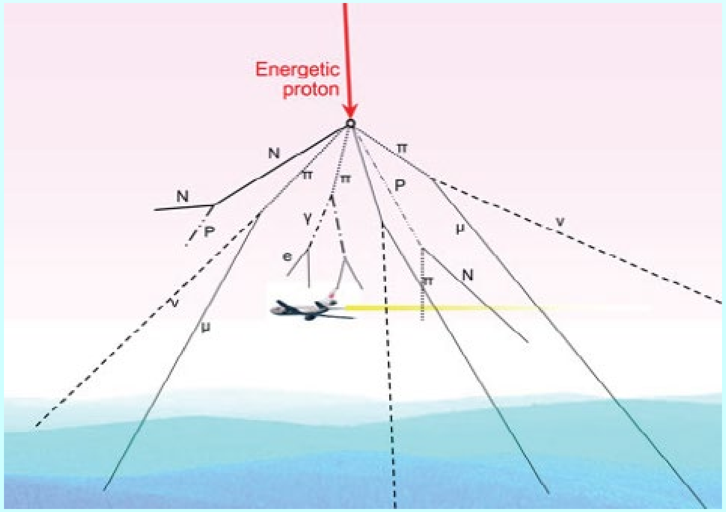

During a flight the background dose rate increases by a factor between 10 and 30

Charged particles:
- ***-heavy (μ, π, p, α, …)***
- ***-light (electrons and positrons)***

Neutral particles:
- ***-photons***
- ***-neutrons***
- ***-neutrinos***

The discovery of radiation

Photographic plates

First

Detection of

α-, β- and γ-rays

1896

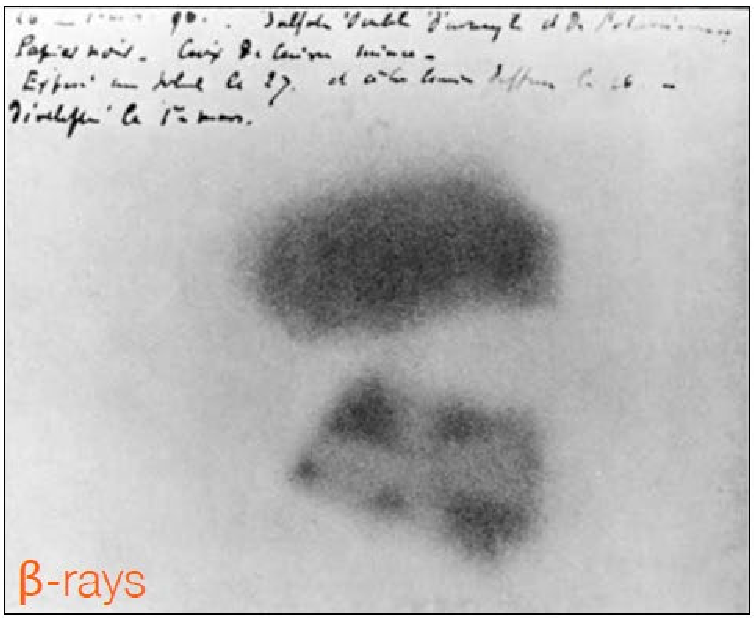

Image of Becquerel's photographic plate which has been fogged by exposure to radiation from a uranium salt.

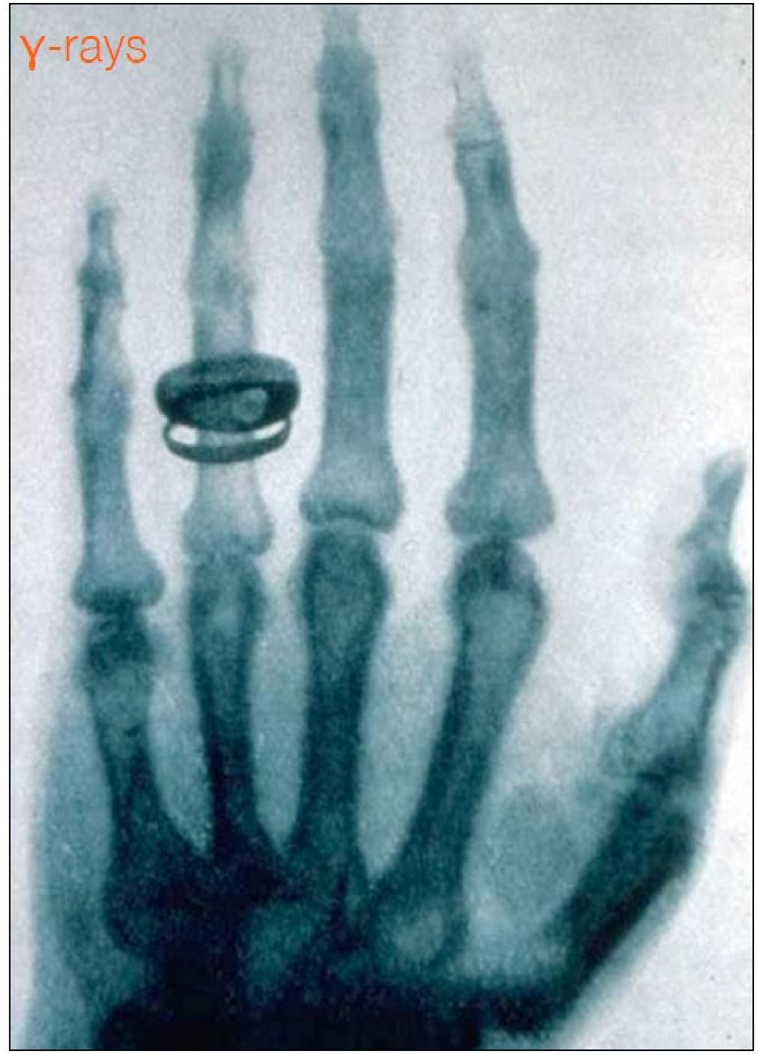

1896

An x-ray picture taken by Wilhelm Röntgen of Albert von Kölliker's hand at a public lecture on 23 January 1896.

The discovery of the atomic nucleus

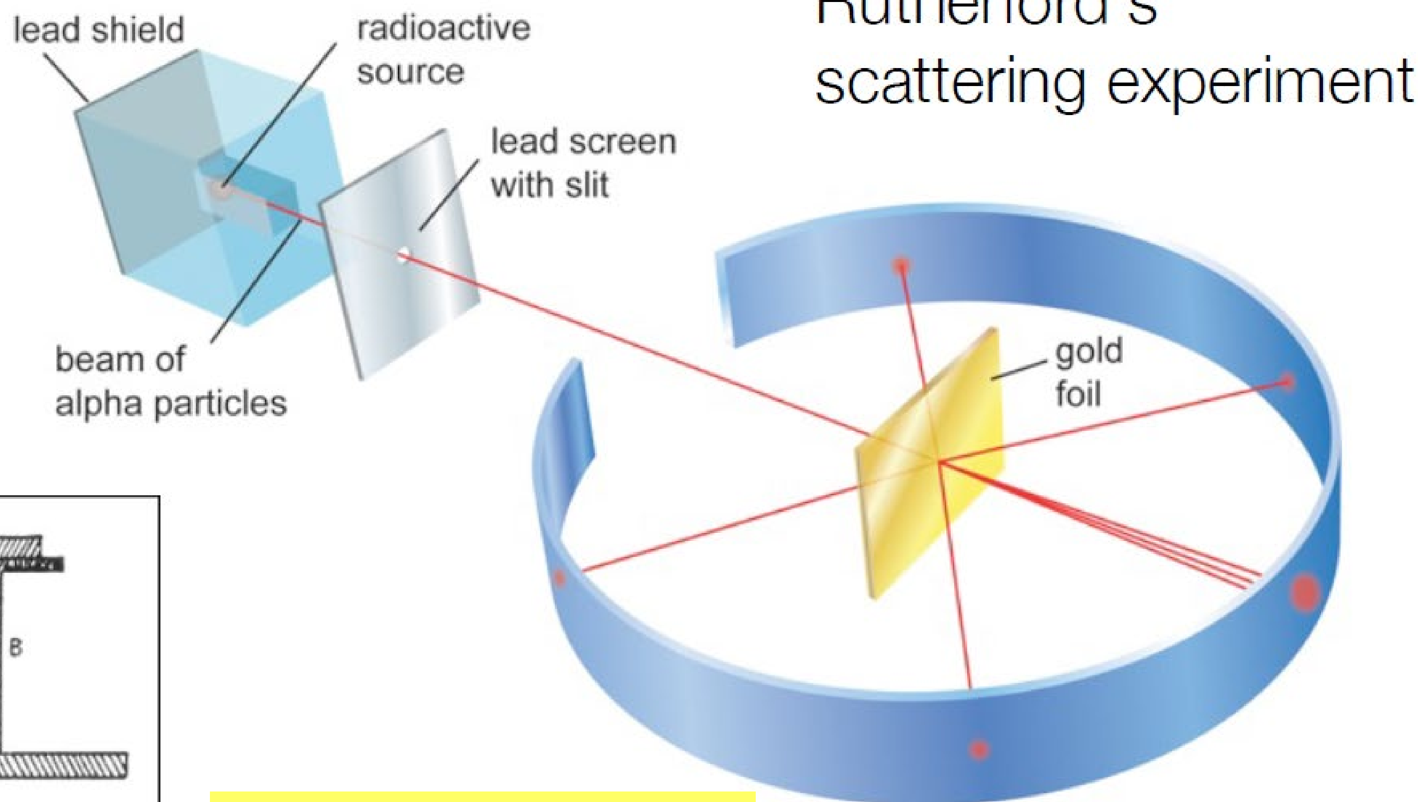

Schematic view
of Rutherford experiment

1911

Microscope +
Scintillating ZnS screen

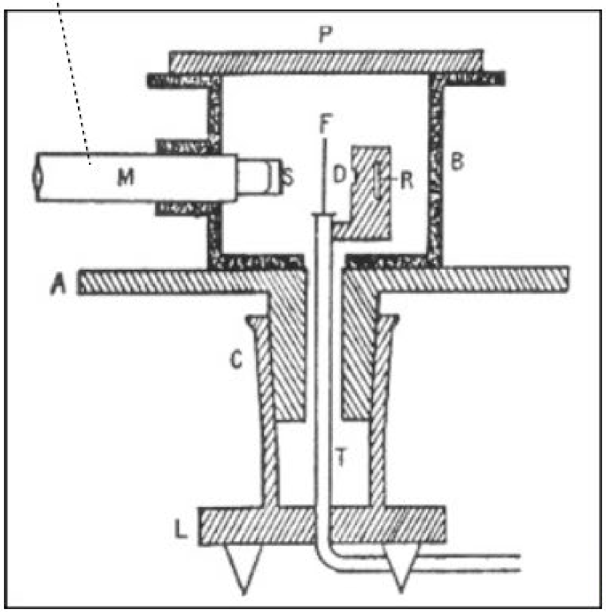

Rutherford's original
experimental setup

Scintillating screens:
William Crooks, 1903

1912: cosmic rays

Detection
of cosmic rays

[Hess 1912; Nobel prize 1936]

Wulf electroscope invented in 1909

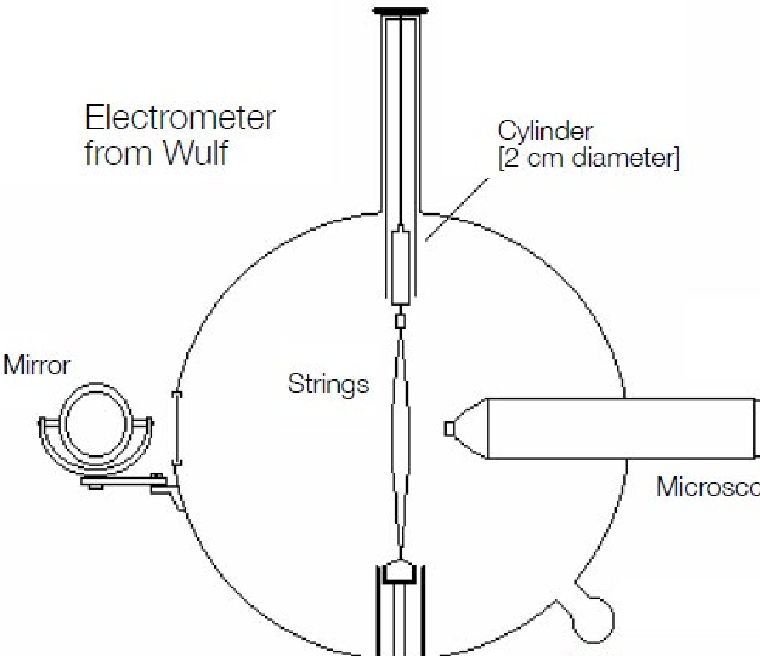

1912

Victor F. Hess before his 1912 balloon flight
in Austria during which he discovered cosmic rays.

1911: the cloud chamber

Cloud chamber (1911 by Charles T. R. Wilson, Noble Prize 1927)

- chamber with saturated water vapour
- charged particles leave trails of ions
  - water is condensing aound ions
- visible track as line of small water droplets

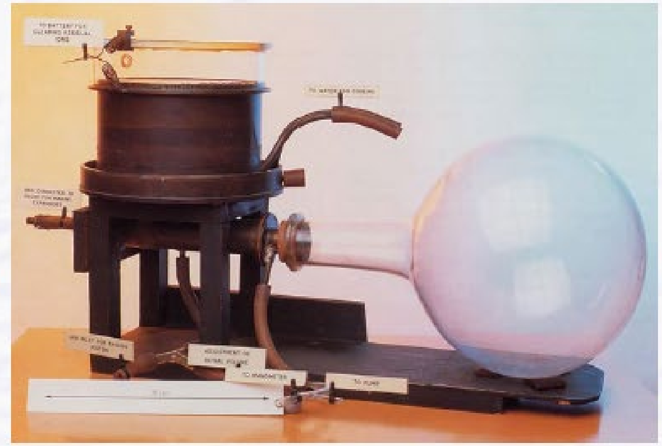

UK Science Museum

Also required

- high speed photographic methods
  - invented by Arthur M. Worthington 1908 to investigate the splash of a drop
  - ultra short flash light produced by sparks

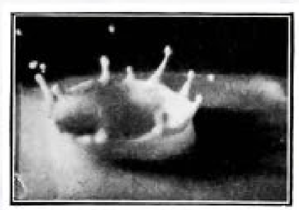

Charles T. R. Wilson

First photographs of α–ray particles 1912

1932: antimatter, 1936: muon

Was also used for the discovery of the positron

- predicted by Paul Dirac 1928 (Nobel Prize 1933)
- found in cosmic rays by Carl D. Anderson 1932 (Nobel Prize 1936)

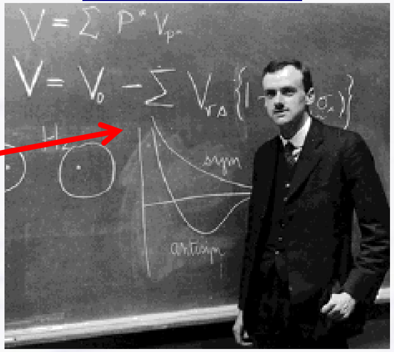

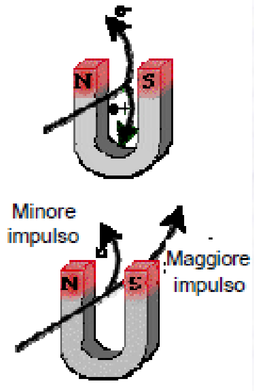

downward going positron, 63 MeV

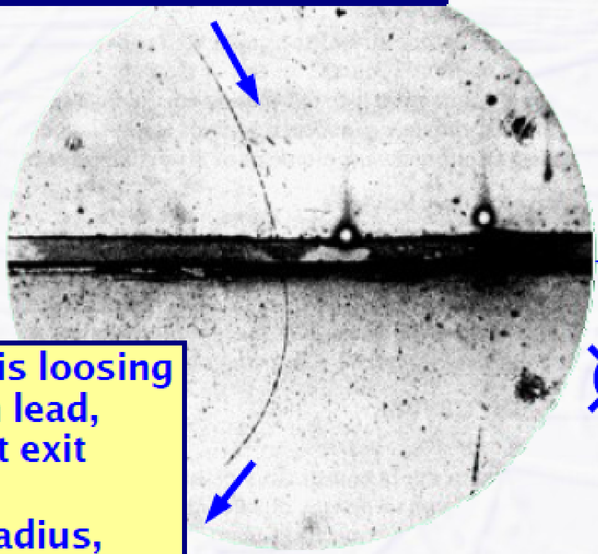

6 mm lead plate

1.5 T magnetic field

positron is loosing energy in lead, 23 MeV at exit → smaller radius, this defines the track direction!

Anderson also found the **muon** in 1936, the first 2nd generation particle in the Standard Model

Isidor Isaac Rabi said: "Who ordered that?"

Carl D. Anderson

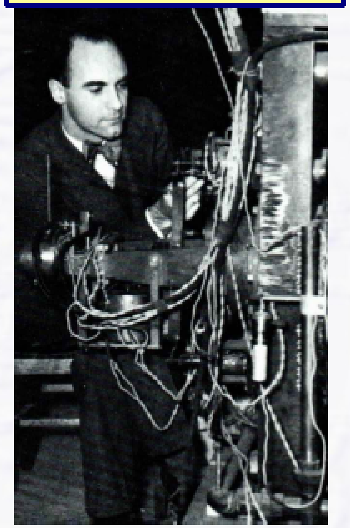

Nuclear emulsions

Marietta Blau:

she developed in Vienna the photographic nuclear emulsion technology for very accurate measurement of high energy nuclei and discovered the ”disintegration stars” of spallation events

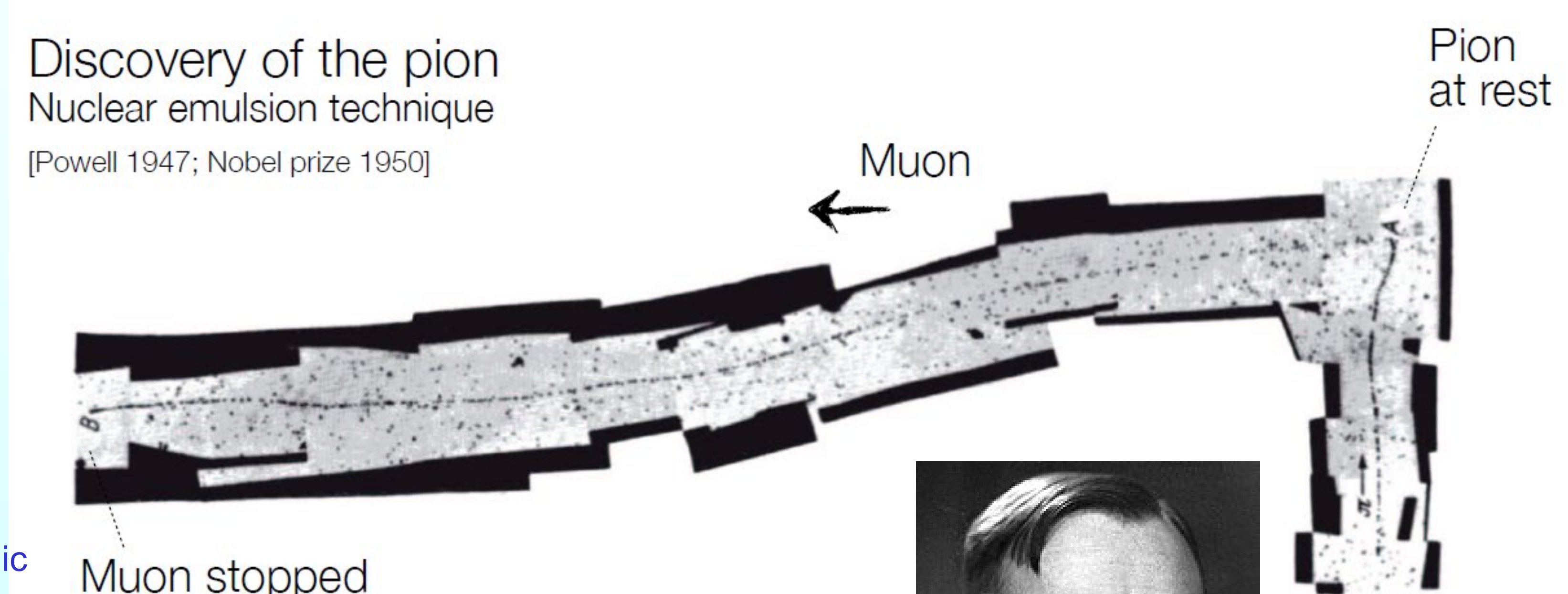

$\pi \rightarrow \mu\nu$

$\mu \rightarrow e\nu\nu$ [not seen]

Pion

emulsions are still the detectors with the highest intrinsic space resolution: < 1 μm

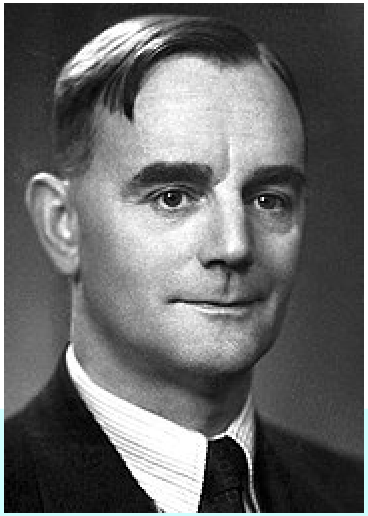

Cecil Frank Powell
Nobel Prizes 1950

1952: bubble chamber

The bubble chamber, invented by Donald Arthur Glaser in 1952, has been for many years the most powerful instrument of ionizing particles investigation.

BEBC (Big European Bubble Chamber)

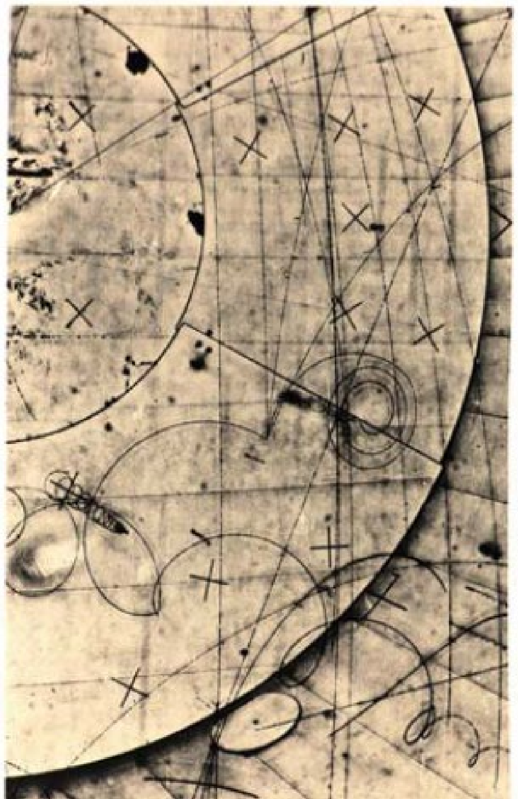

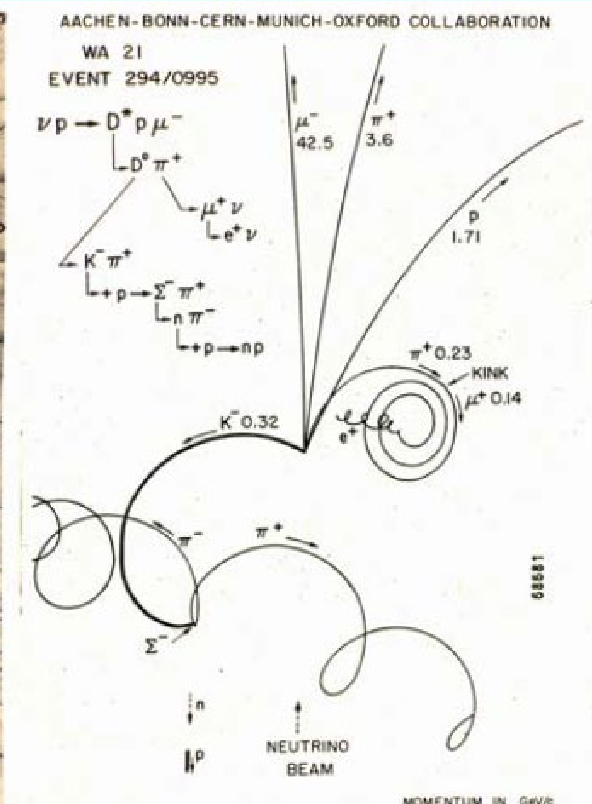

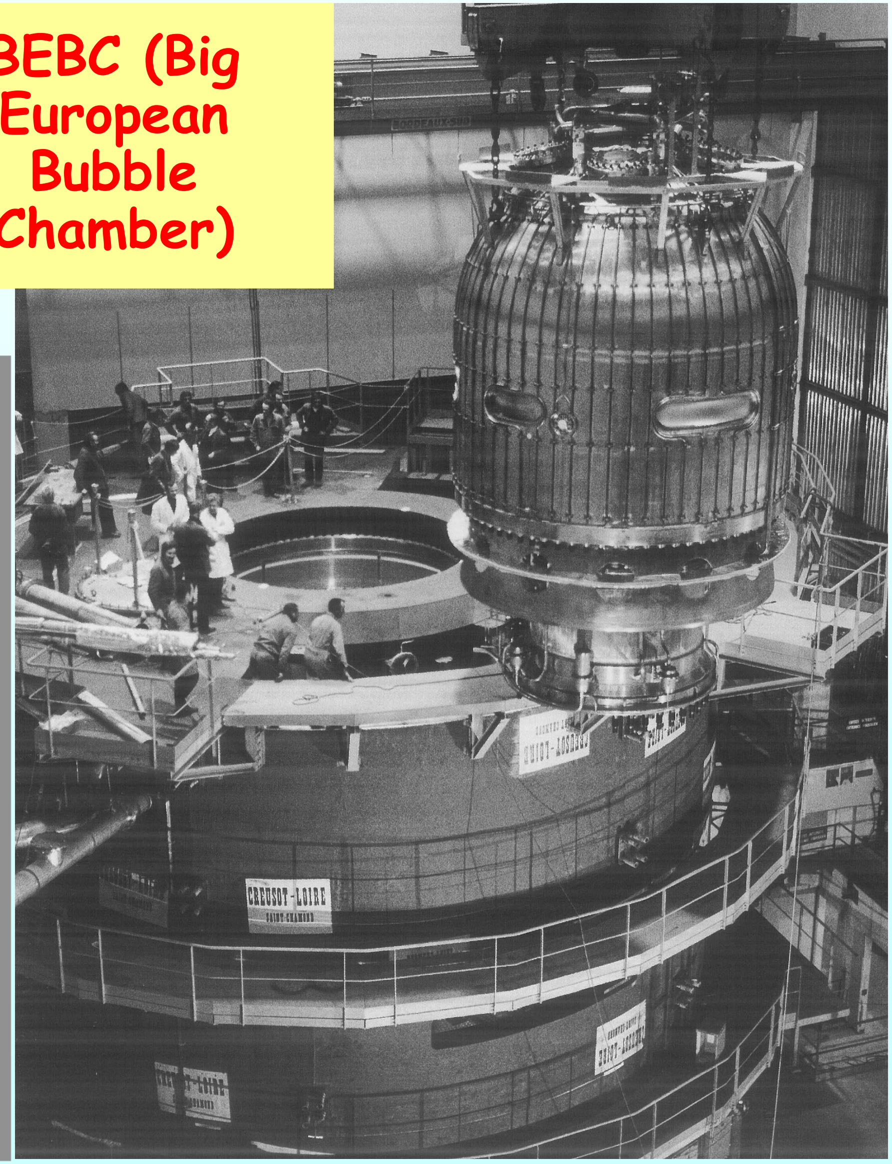

1964: the first predicted particle

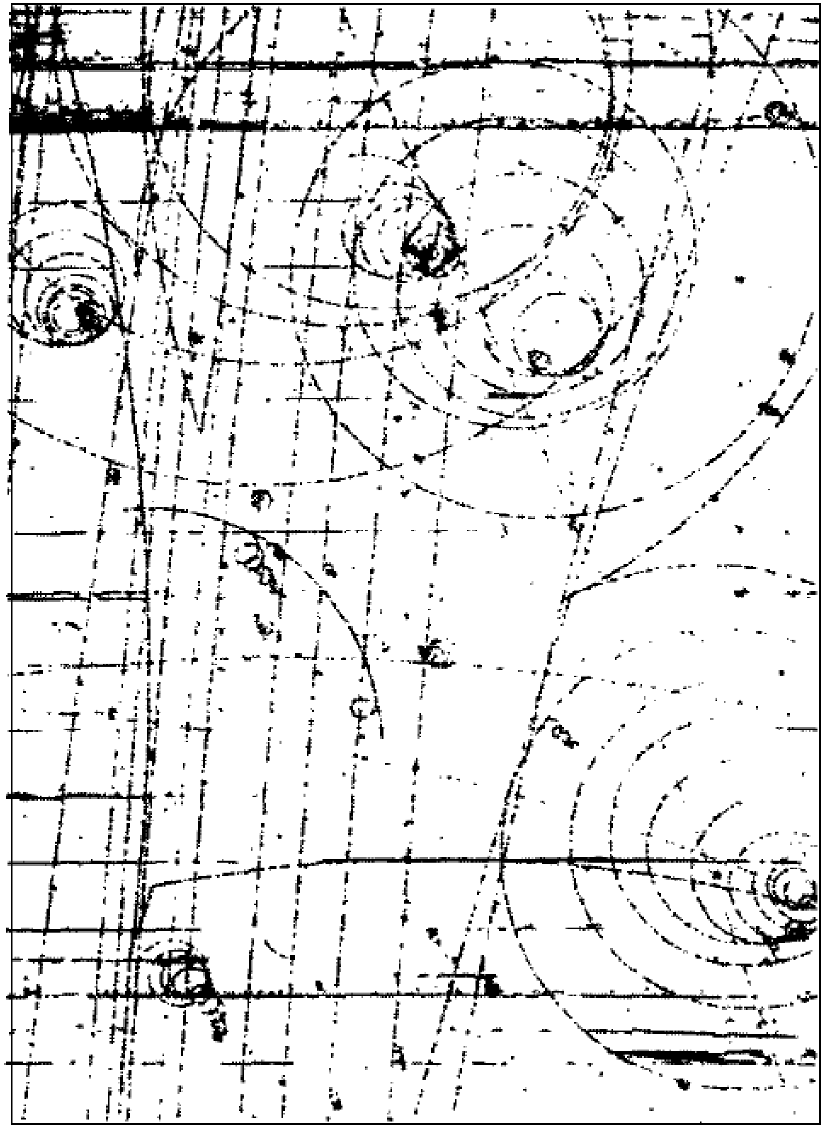

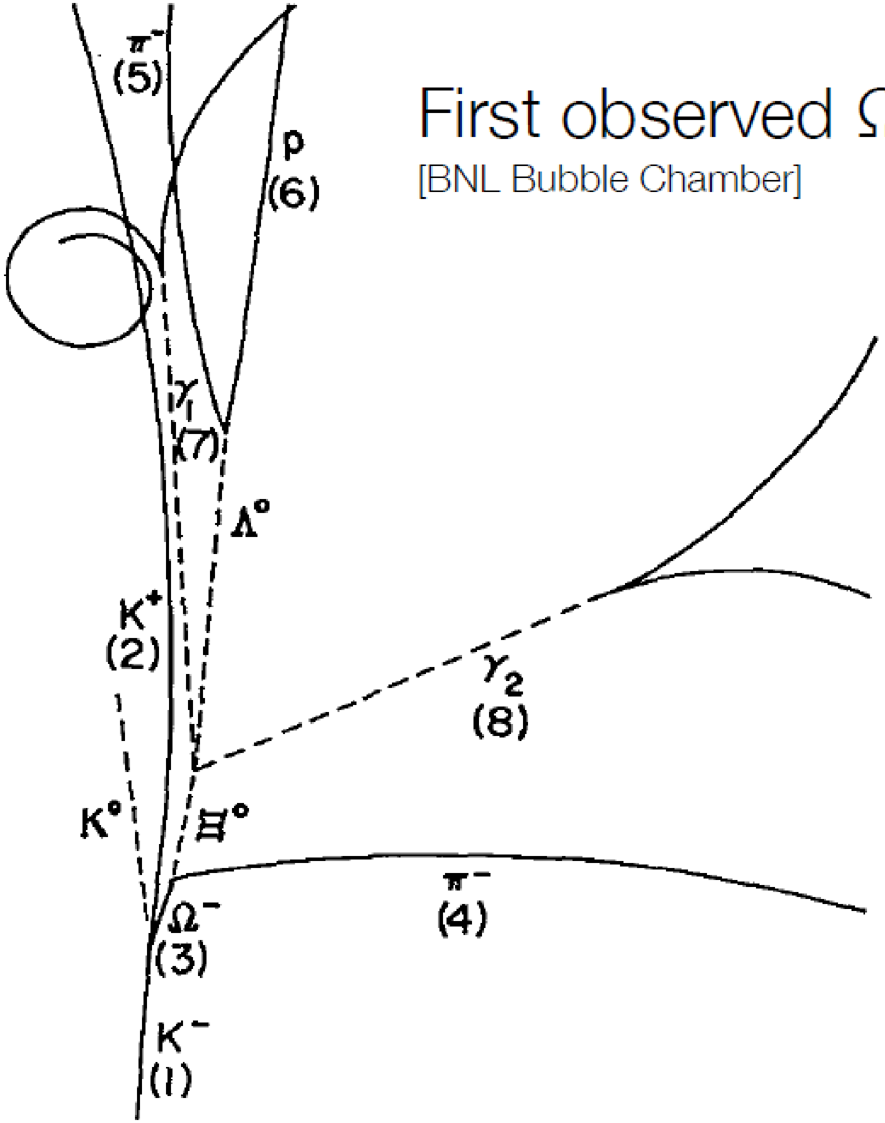

First observed Ω^- event

[BNL Bubble Chamber]

1973: the e.w. theory is confirmed

1973: a big discovery in Europe, at CERN.
Gargamelle detects weak neutral currents
The electroweak theory is confirmed

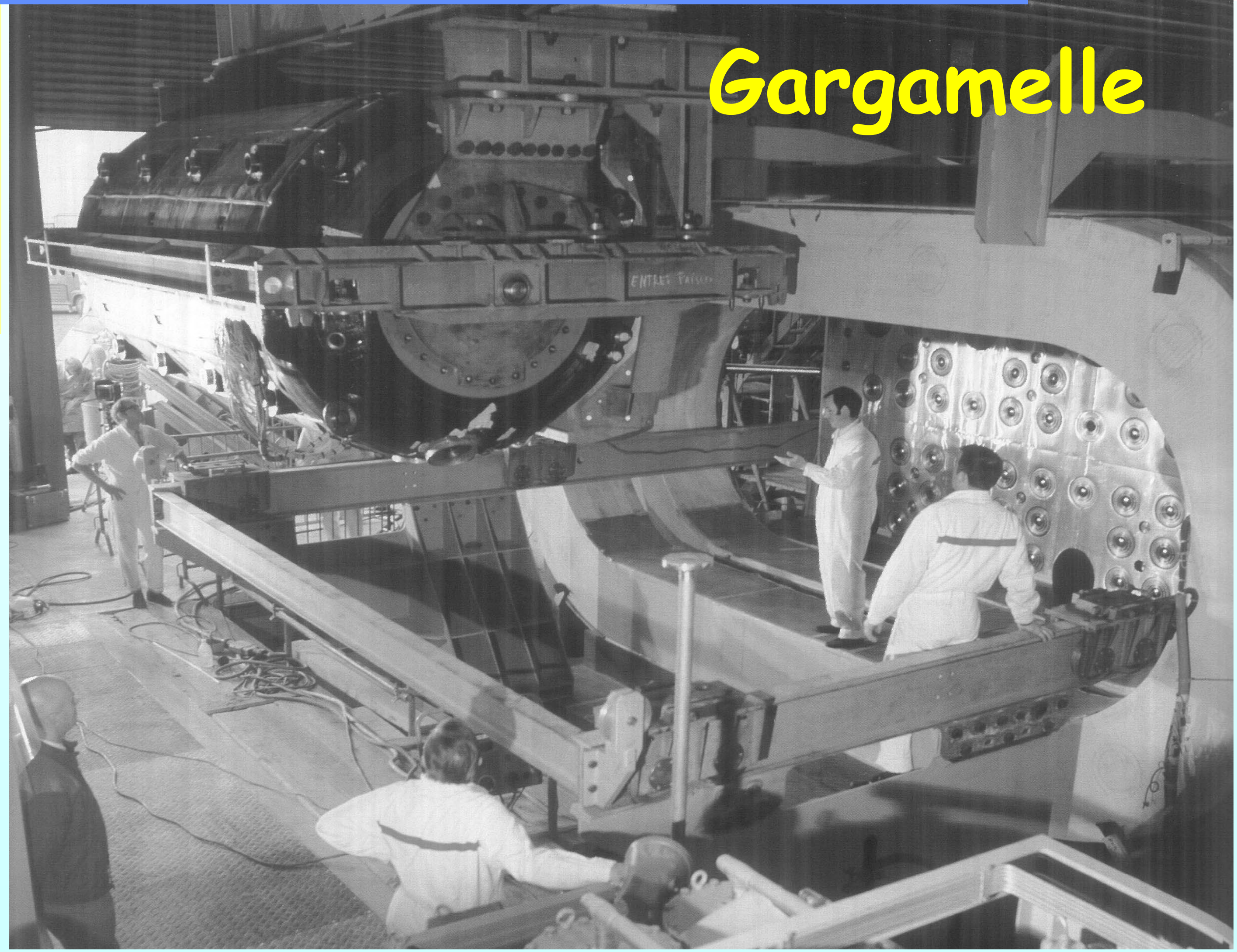

Salam receives the Nobel prize in 1979 together with Weinberg and Glashow

1983: the weak bosons

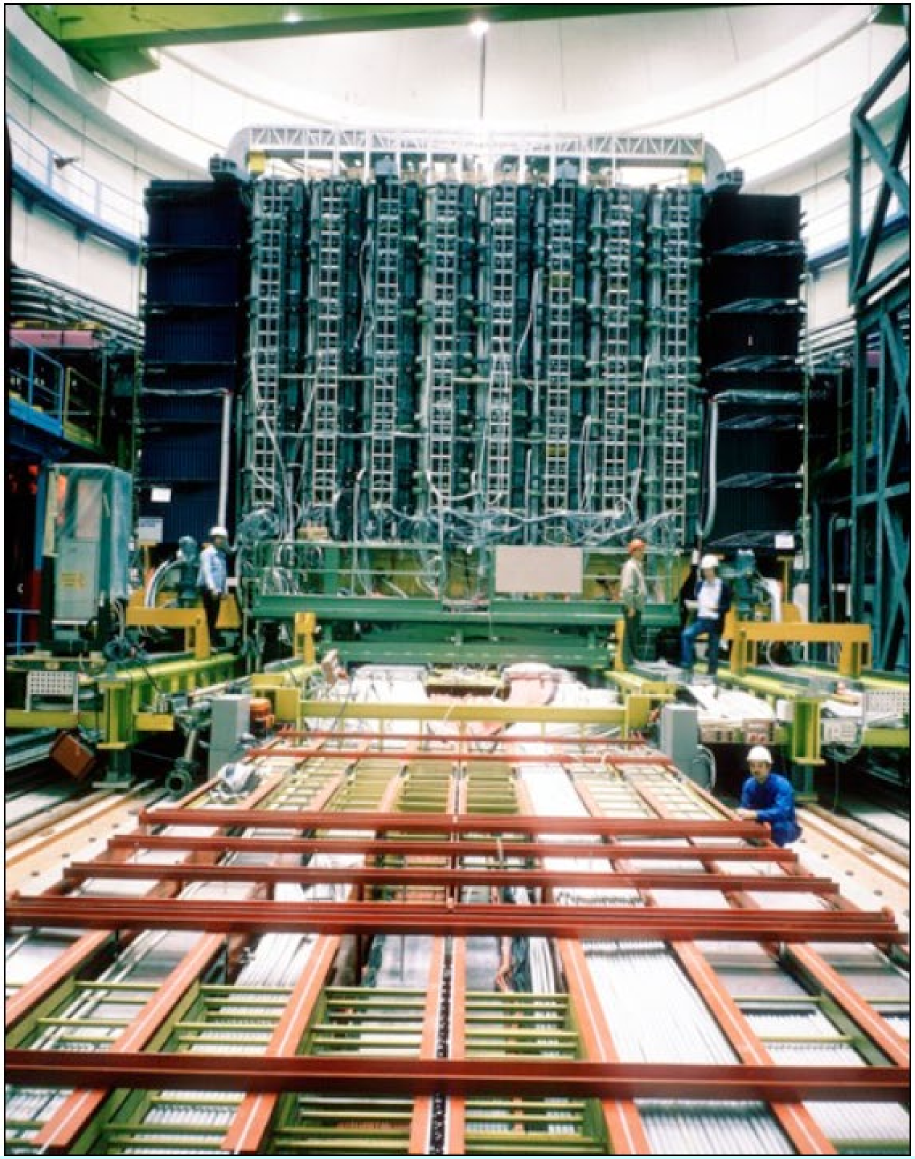

UA1 Detector

Discovery of the W/Z boson (1983)

Carlo Rubbia
Simon Van der Meer

[Nobel prize 1984]

First Z^0 particle seen by UA1

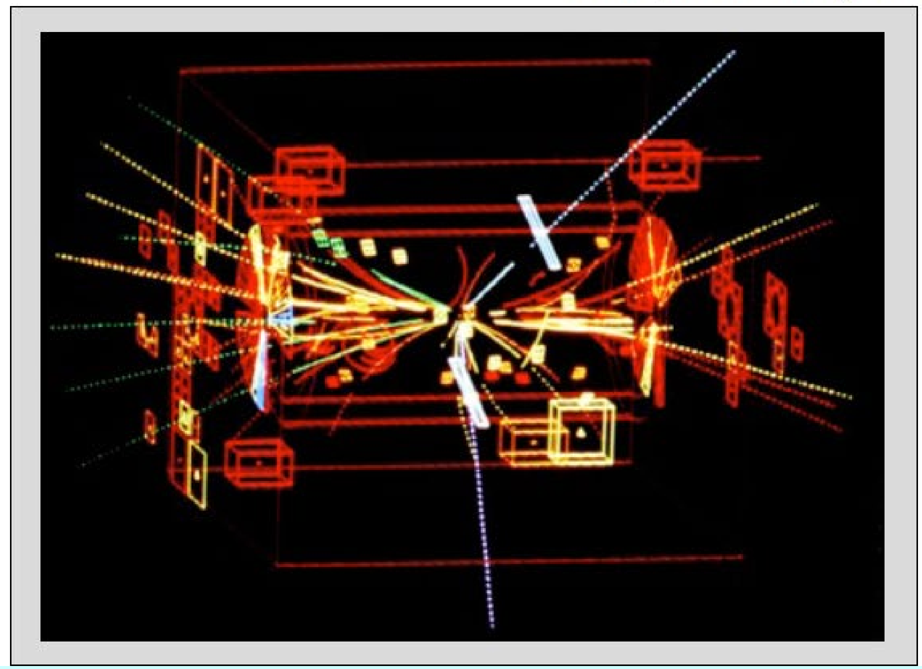

The discovery of W and Z bosons

Nobel Prize in Physics 1984

"for their decisive contributions to the large project, which led to the discovery of the field particles W and Z, communicators of weak interaction"

Carlo Rubbia and

Simon Van der Meer

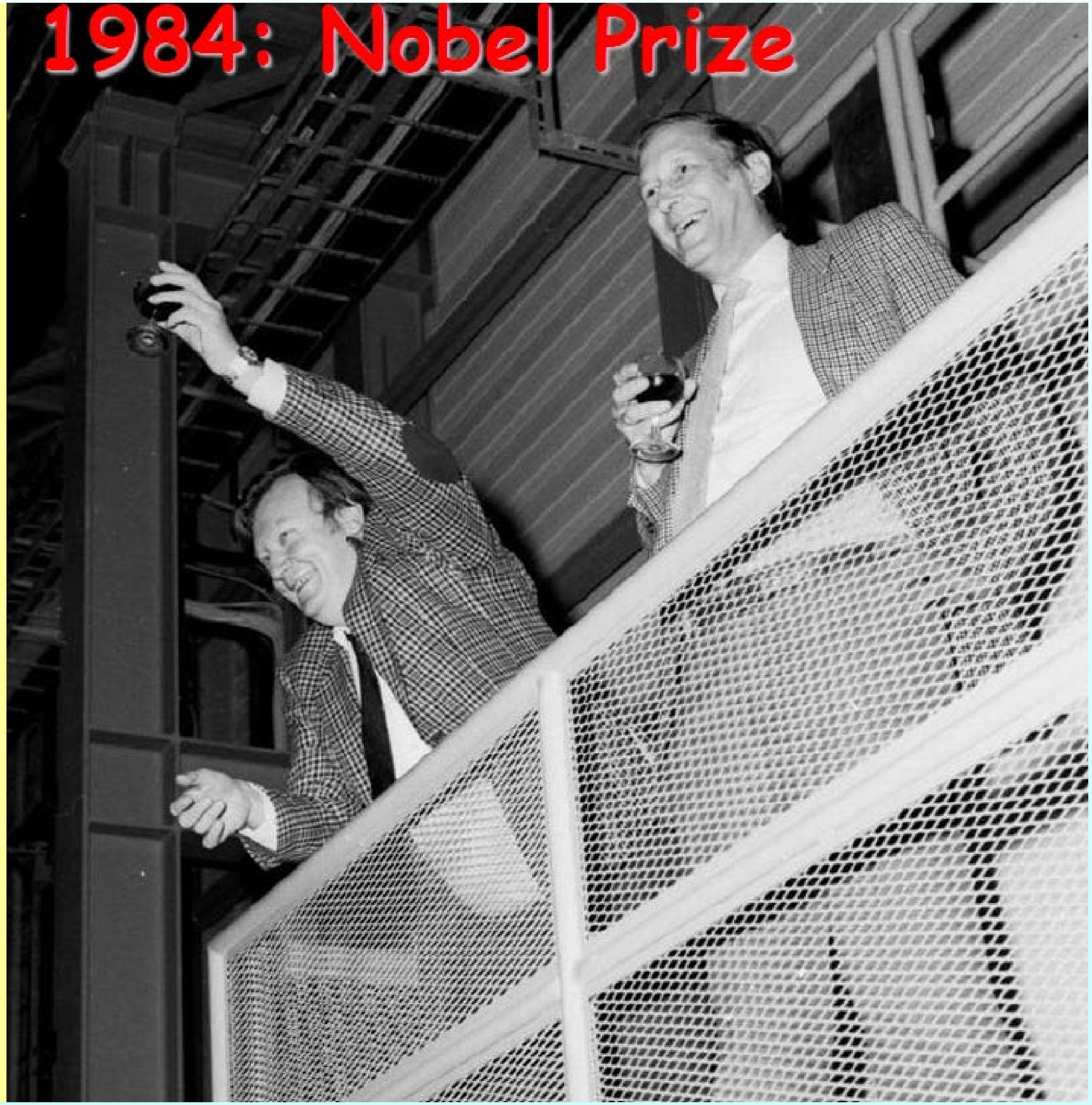

Thanks to the CERN accelerators

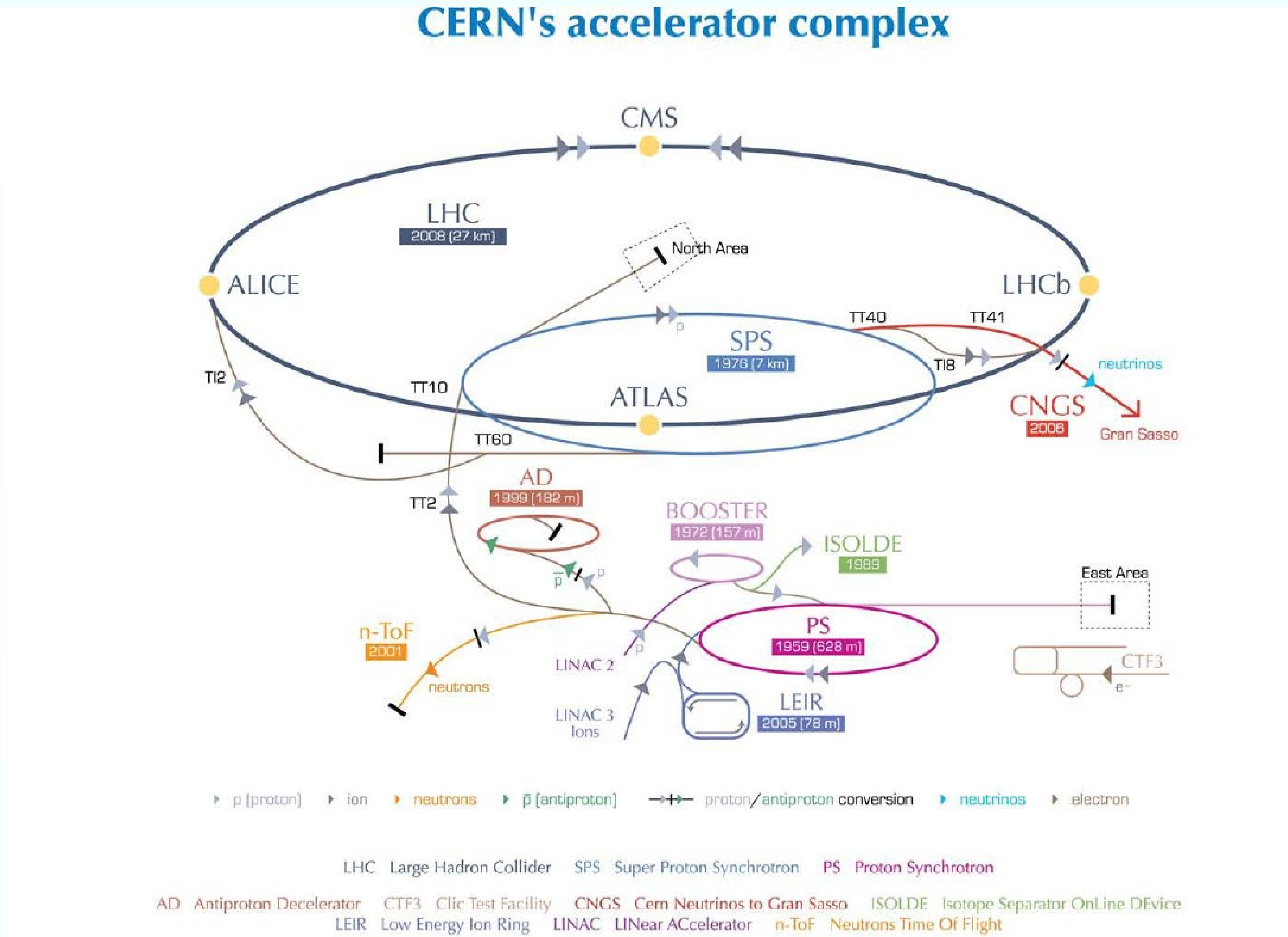

CERN:
European Organization for Nuclear Research

Is the largest particle physics laboratory in the world

It hosts ~2500 staff members and ~12000 users

Provides particle accelerators and infrastructures for particle physics research.

Founded in 1954 as a European common project

All results are published and universally accessible

P. Auger, E. Amaldi, L. Kowalski

15 May 1954

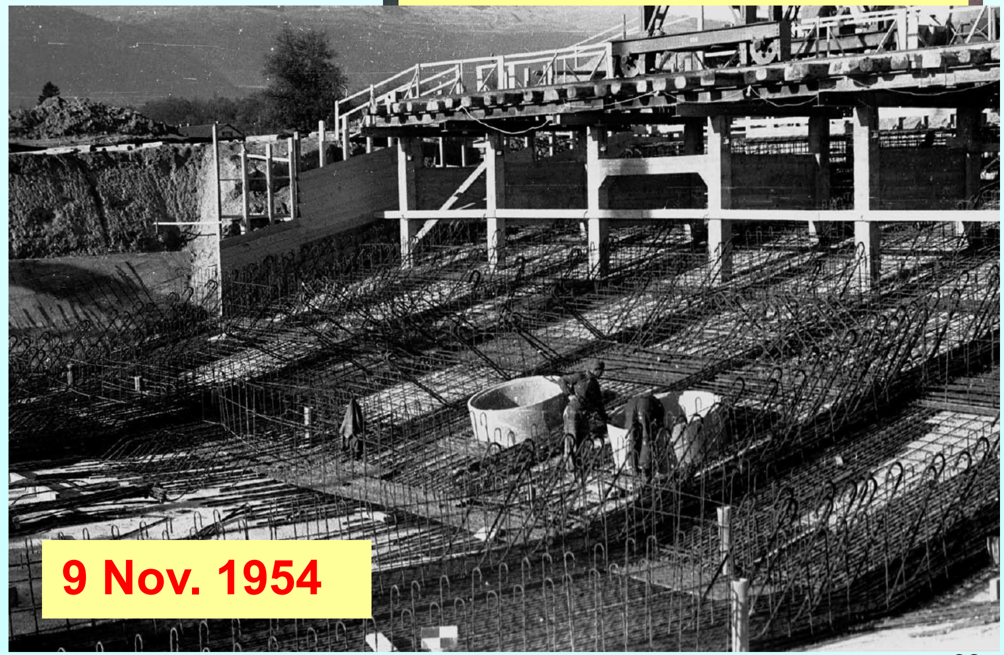

9 Nov. 1954

The 600 MeV Syncro-Cyclotron

1 Jan. 1956

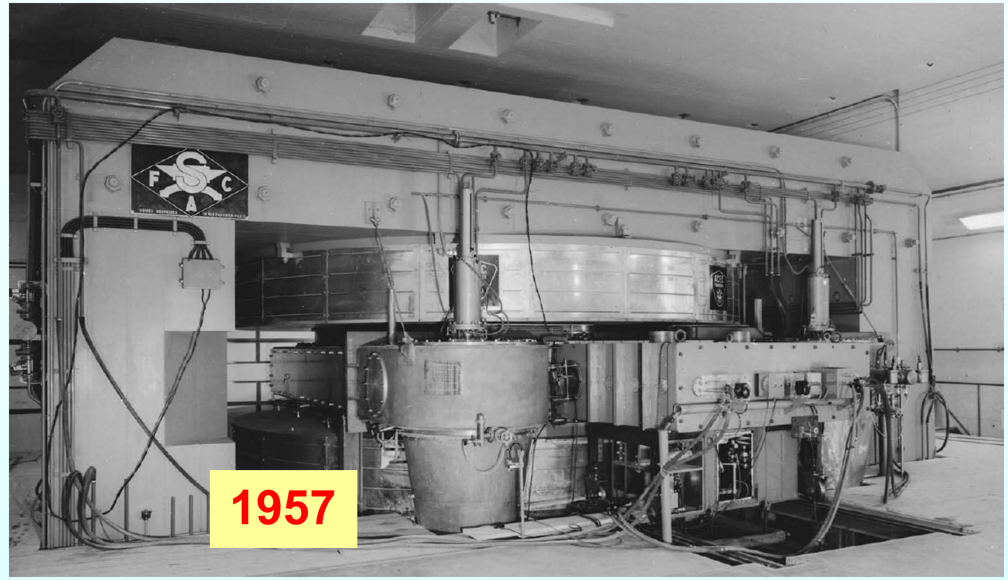

1957

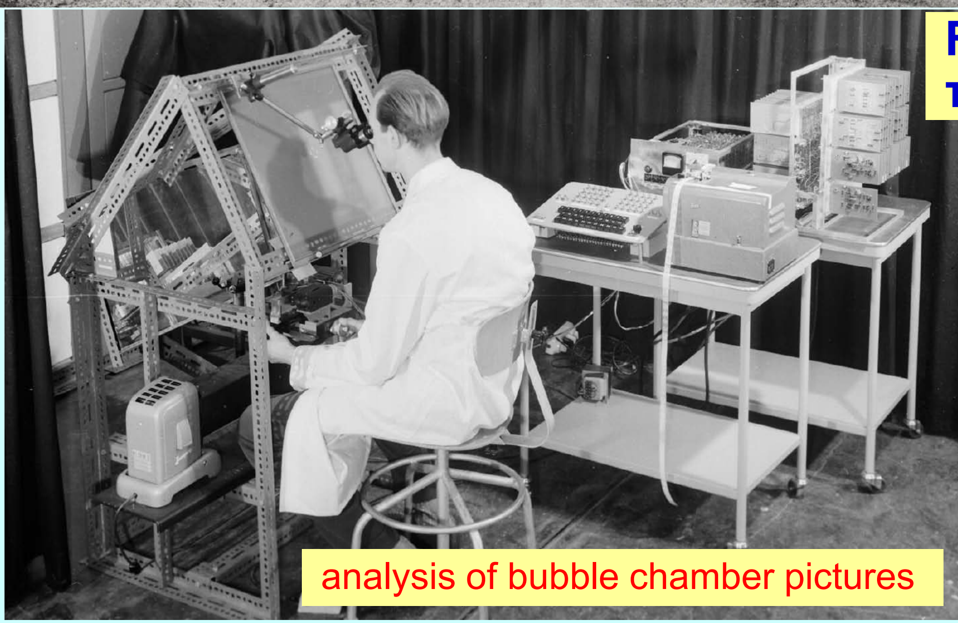

analysis of bubble chamber pictures

First physics result in 1958:
$\pi \rightarrow e\,\nu$ BR = 10^{-4}

G. Fidecaro,
(is the first INFN
Trieste director)

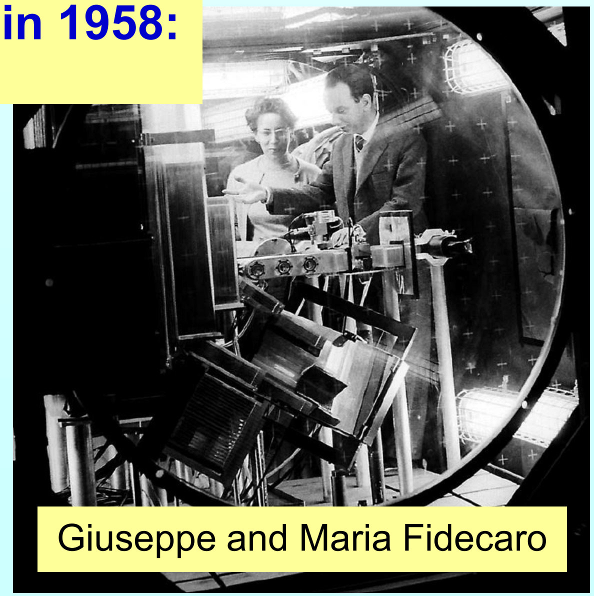

Giuseppe and Maria Fidecaro

The Proton-Syncrotron and the ISR

24 Nov. 1959

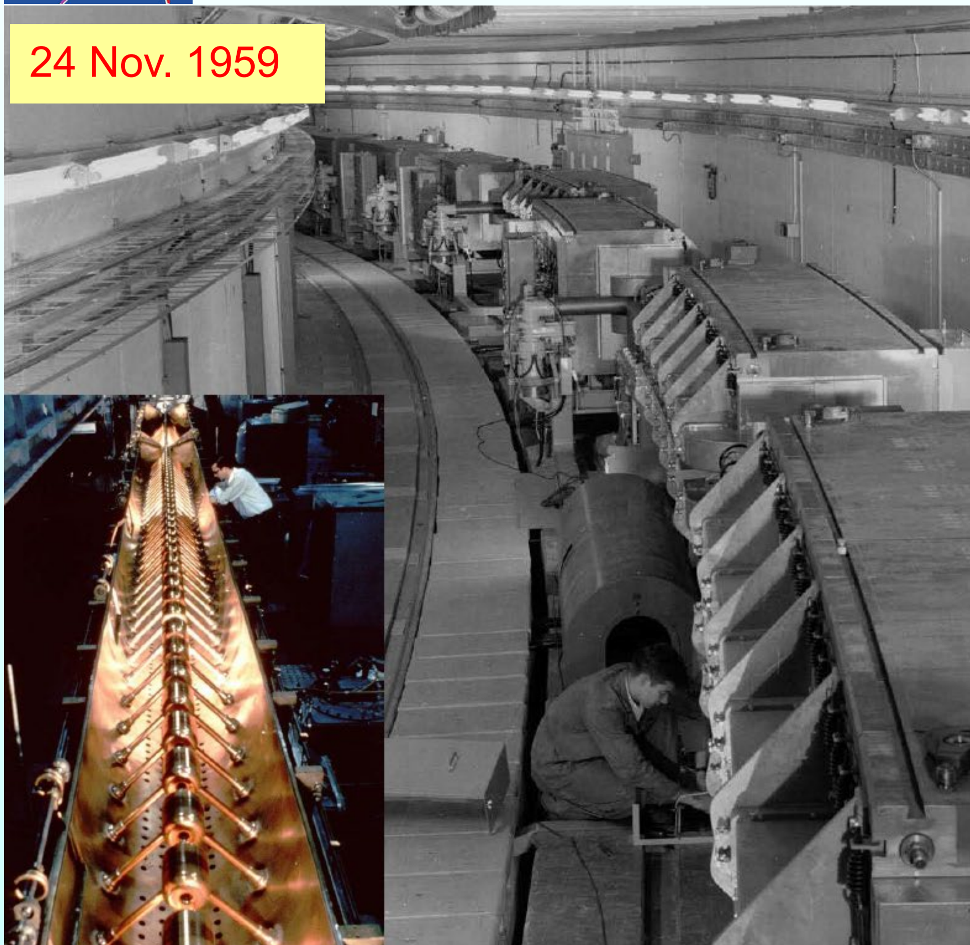

the PS delivers a 24 GeV/c proton beam

27 Jan. 1971

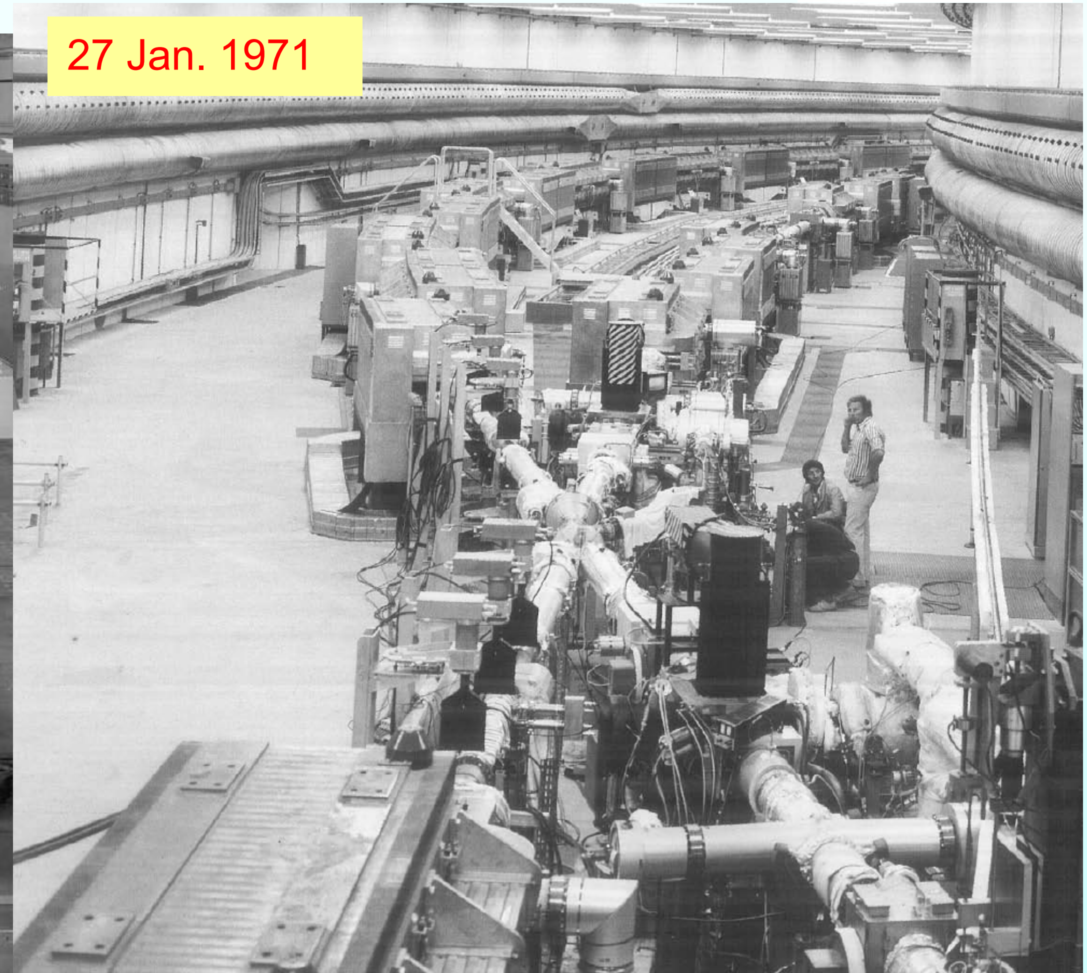

Two proton beams collide for the first time in the world.

The ISR reached a luminosity 1000 times larger than the project design one.

The Super-Proton-Syncrotron

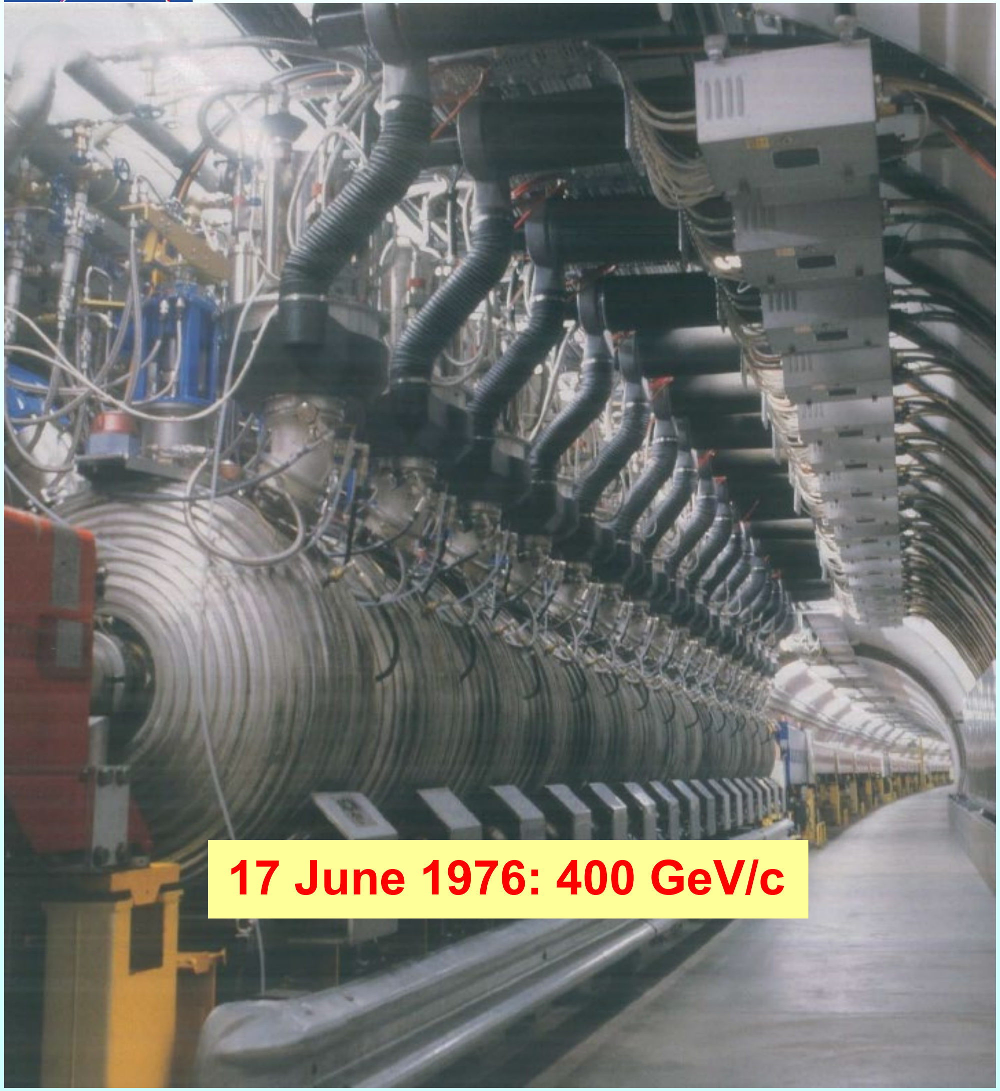

17 June 1976: 400 GeV/c

1981: The SPS is the first proton-antiproton collider

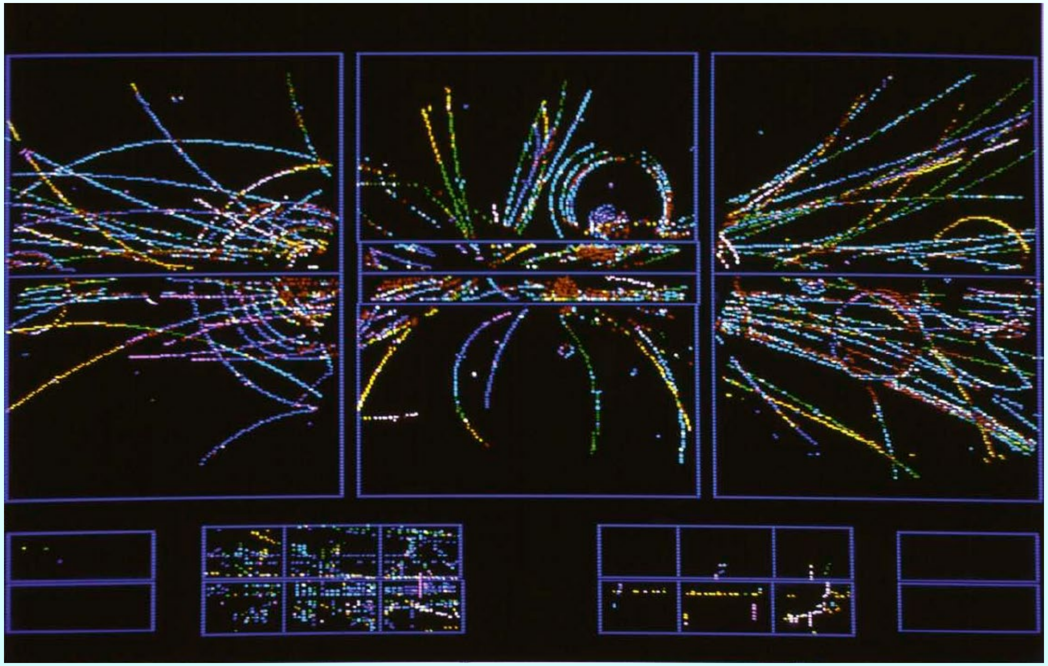

1983: an event in the UA1 detector

The Large Electron-Positron Collider

High precision W and Z measurement

Between 1985 and 1988 1.4 M m^3 were escavated at a depth of 100 m for a length of 27 km: the largest European civil engineering work of that period

The largest accelerator in the world

2012: discovery of the Higgs boson

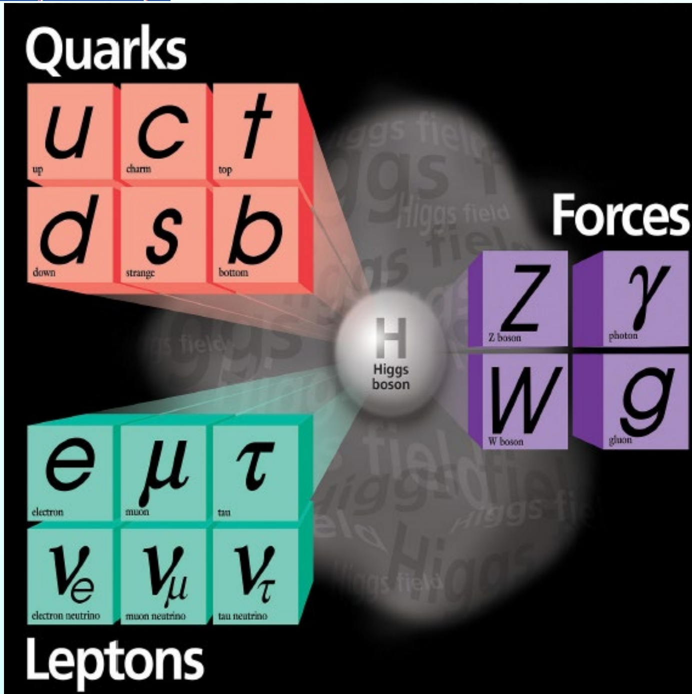

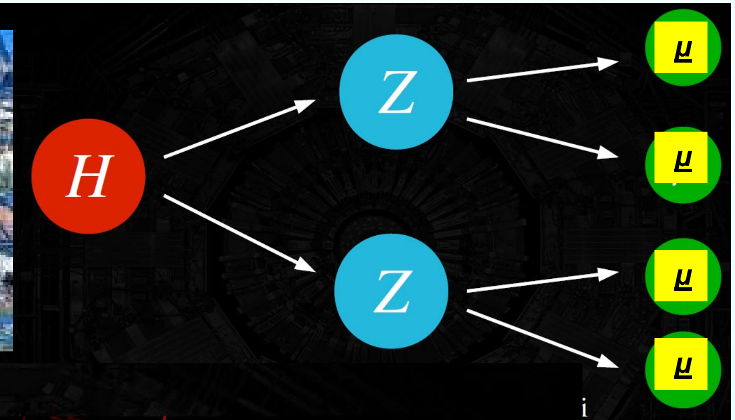

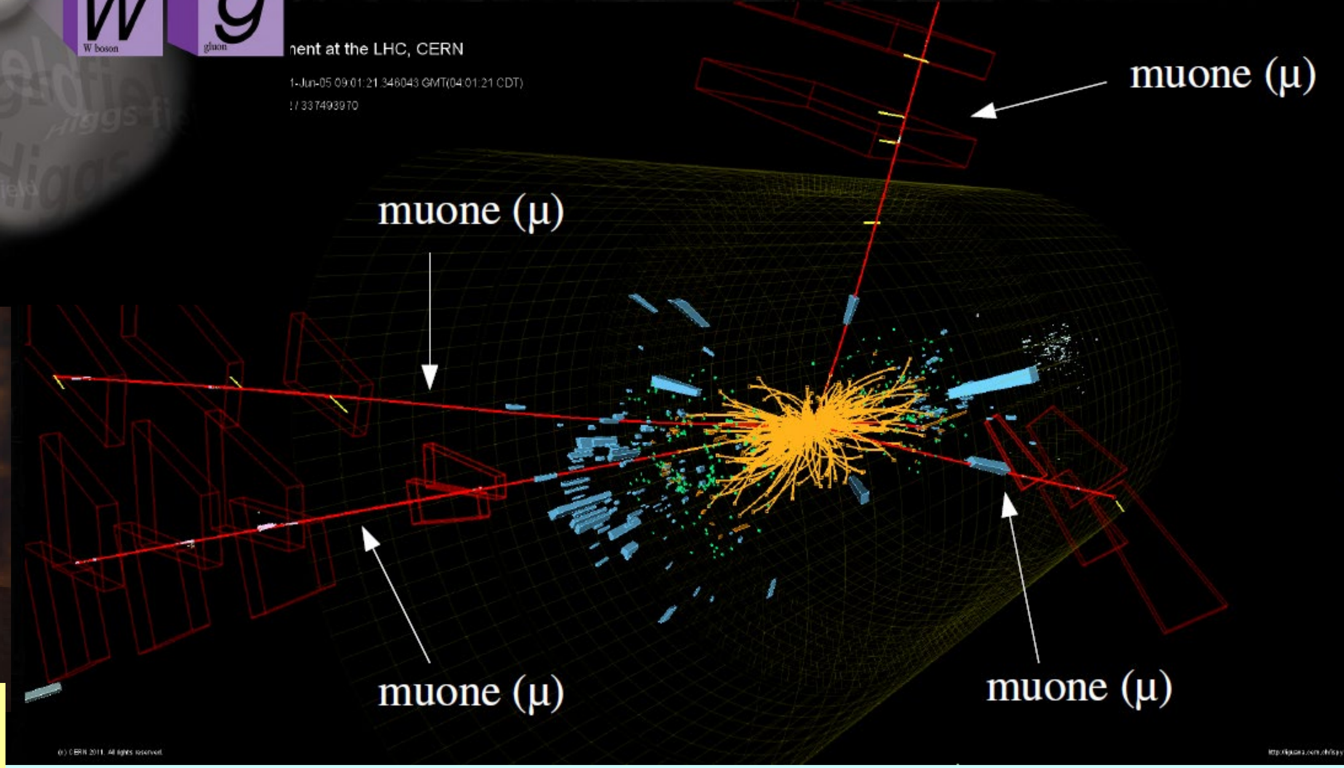

Peter Higgs,
Nobel Prize 2013

The antihydrogen

The Low Energy Antiproton Ring

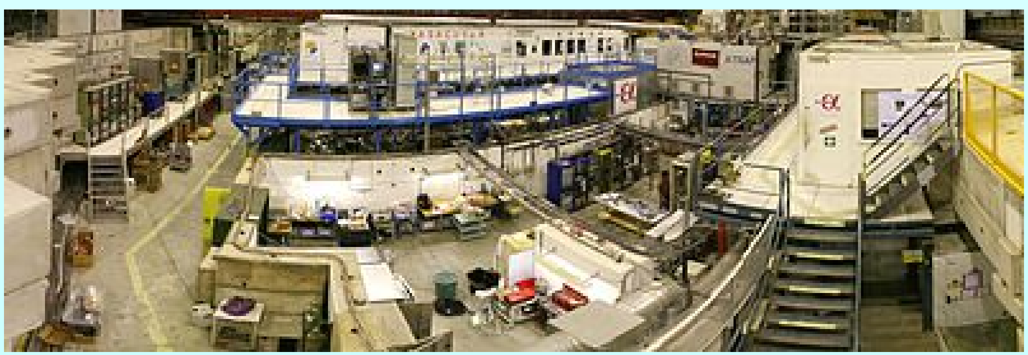

16 Dec. 2016
first antimatter spectroscopy

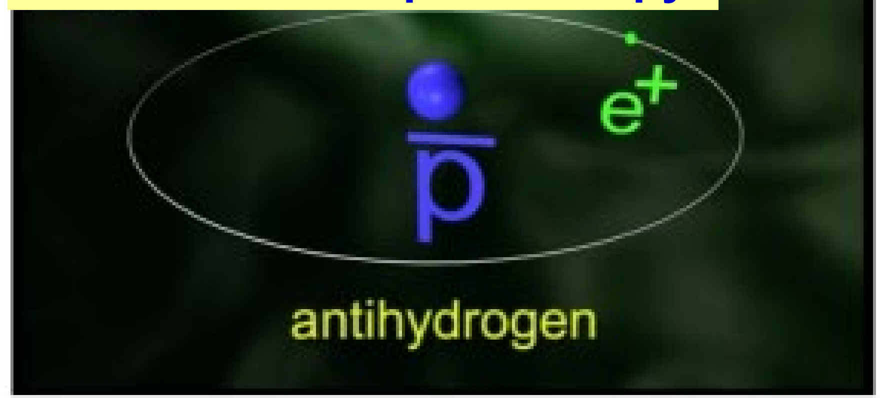

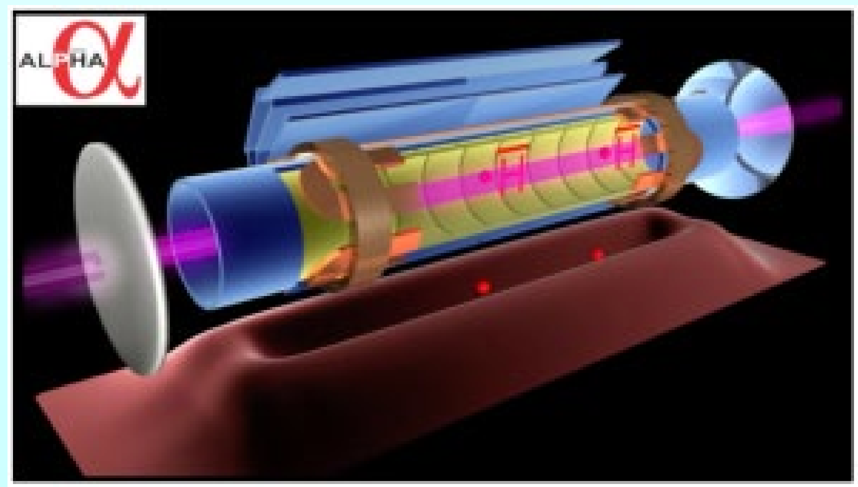

Tim Bernes-Lee invented the www

in 1990 the web is born!

Tim Berners Lee

The web was invented at CERN! The machine used by Tim Berners-Lee in 1990 to develop and run the first WWW server, multi-media browser and web editor.

fundamental contribution to the informatics revolution

A modern experiment

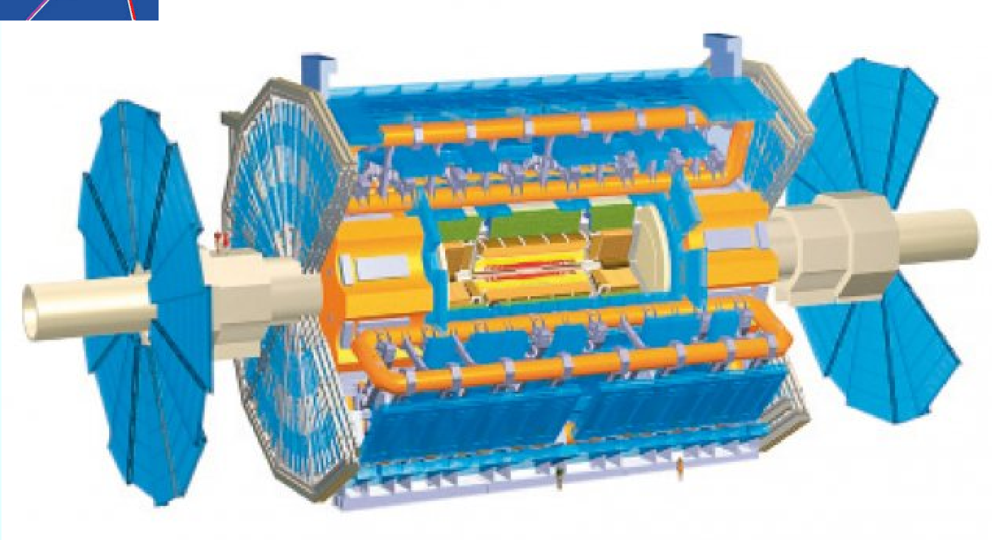

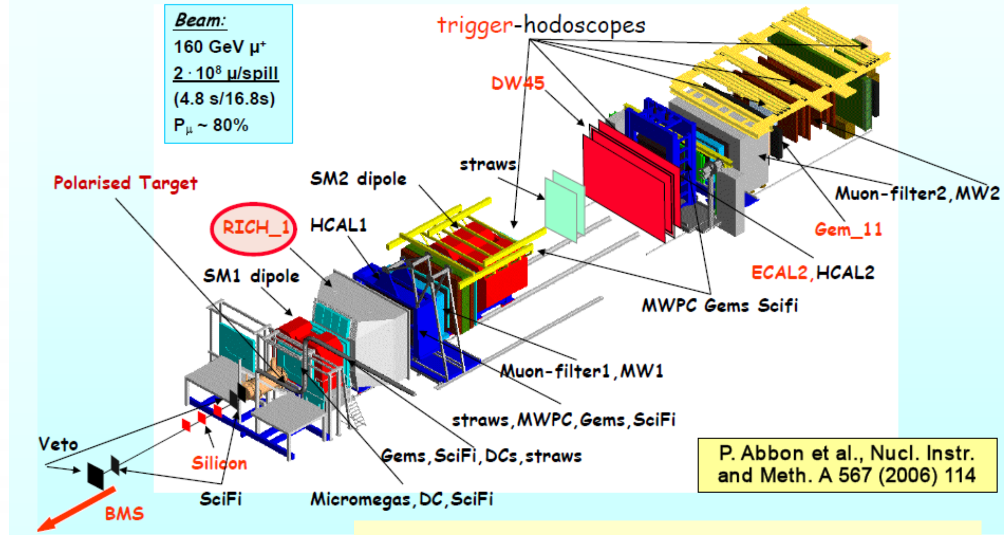

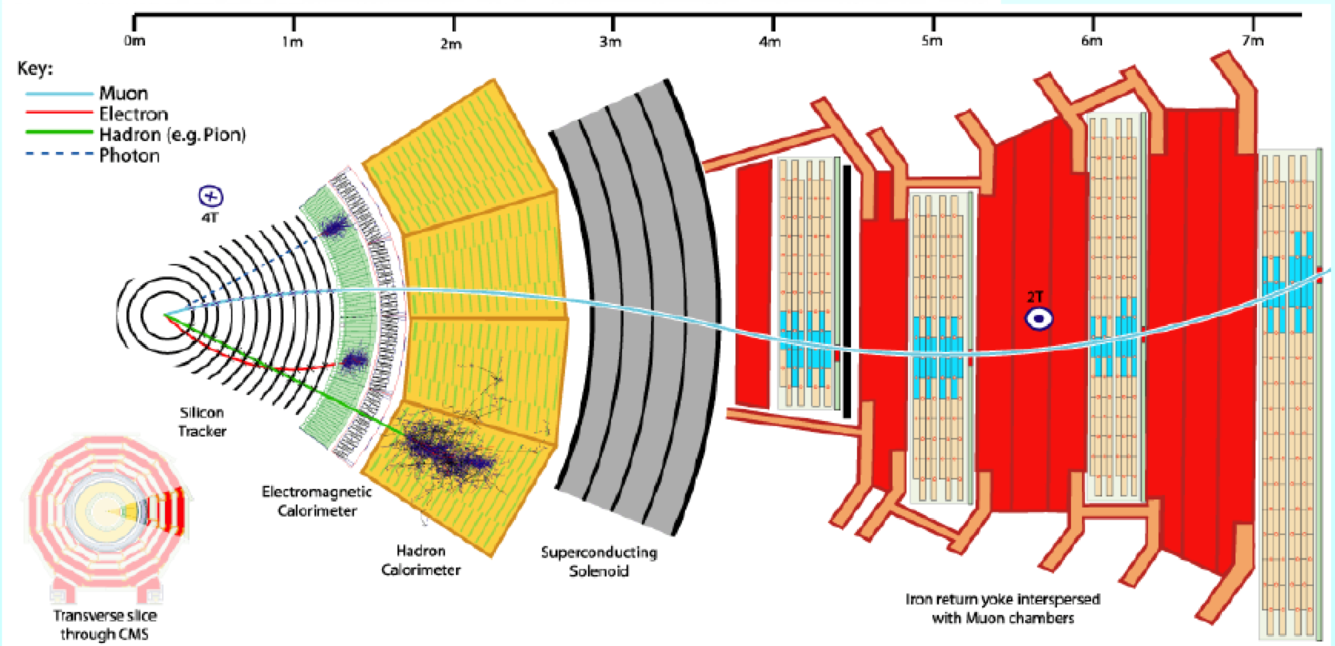

uses a combination of different detectors, combines the information from all of them and fully reconstructs the characteristics of the interesting event which took place

Different particles are seen by different detectors

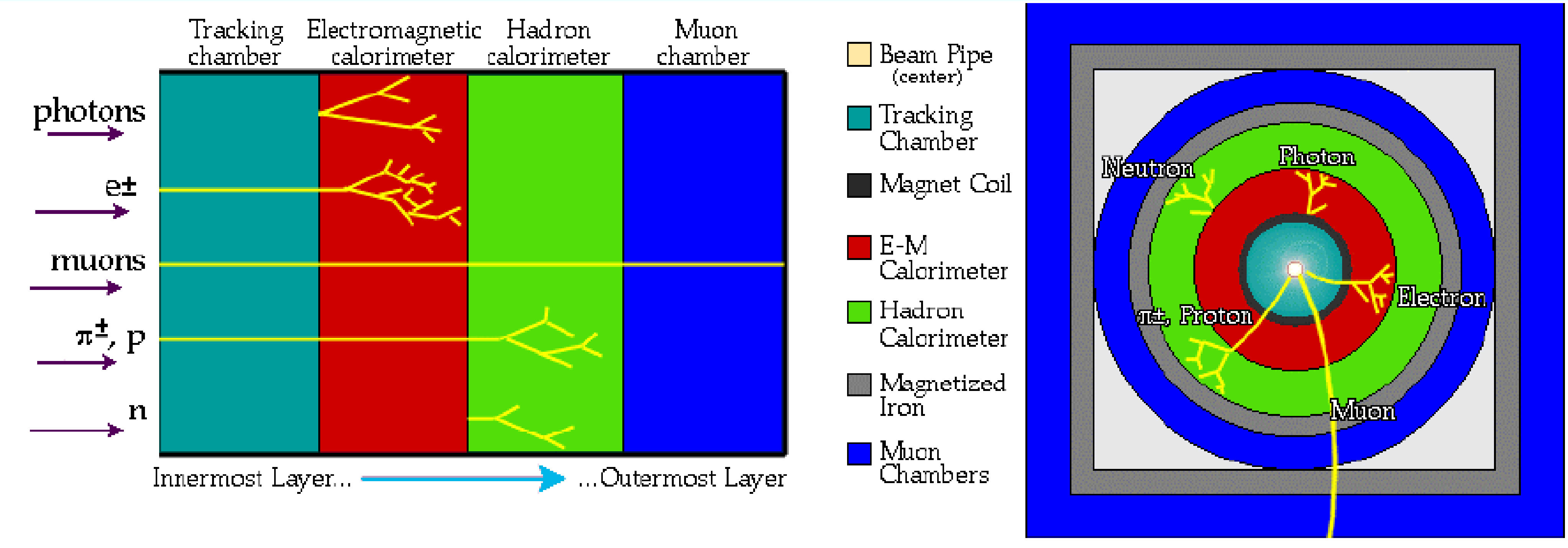

Scintillation detectors

Particle Detection via Luminescence

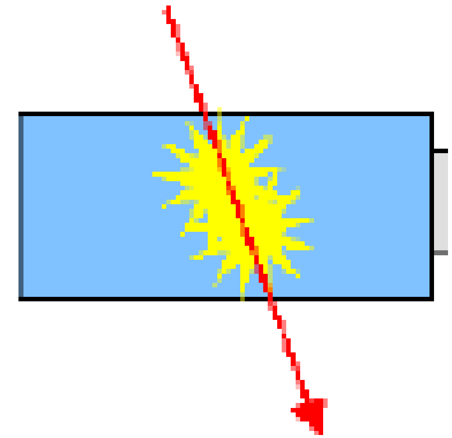

Scintillators – General Characteristics

Principle:

dE/dx converted into visible light
Detection via photosensor
[e.g. photomultiplier, human eye ...]

Main Features:

Sensitivity to energy
Fast time response
Pulse shape discrimination

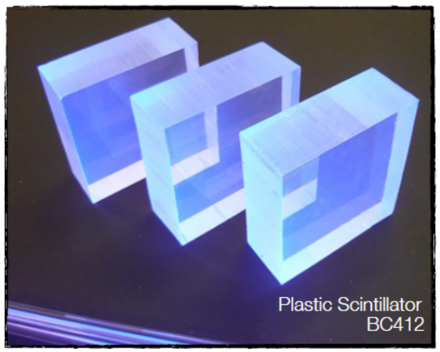
Plastic Scintillator
BC412

Requirements

High efficiency for conversion of excitation energy to fluorescent radiation
Transparency to its fluorescent radiation to allow transmission of light
Emission of light in a spectral range detectable for photosensors
Short decay time to allow fast response

Scintillators – Basic Counter Setup

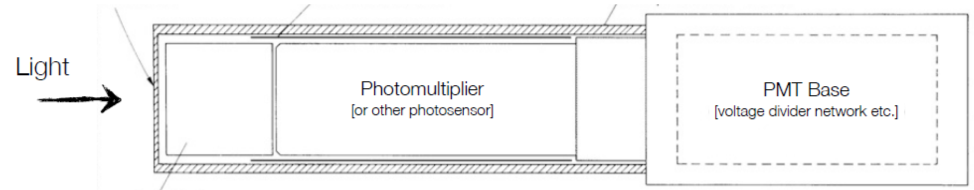

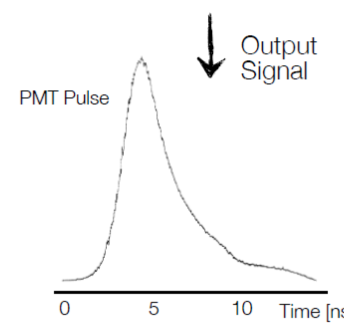

Scintillator Types:

Organic Scintillators
Inorganic Crystals
Gases

Photosensors

Photomultipliers
Micro-Channel Plates
Hybrid Photo Diodes
Visible Light Photon Counter
Silicon Photomultipliers

Scintillation detectors

Particle Detection via Luminescence

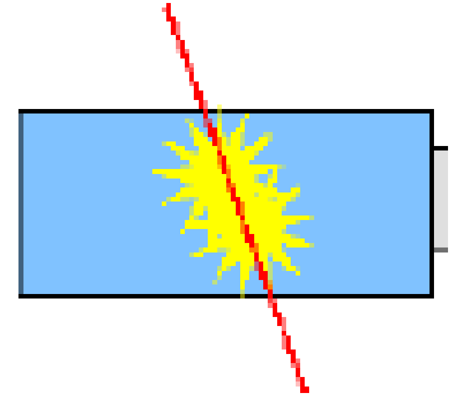

Inorganic Crystals

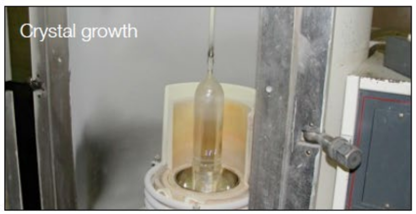

Example CMS
Electromagnetic Calorimeter

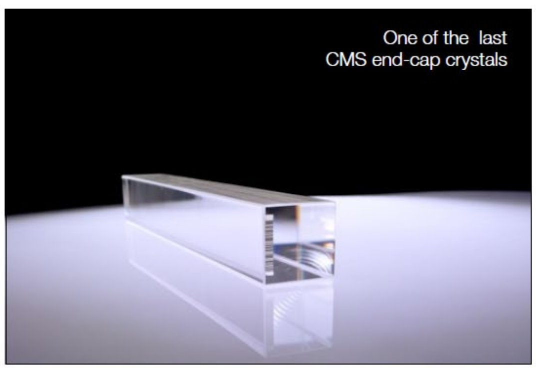

Large light yield, good energy resolution

Plastic and Liquid Scintillators

In practice use ...

solution of organic scintillators
[solved in plastic or liquid]

+ large concentration of primary 'fluor'
+ smaller concentration of secondary 'fluor'
+ ...

Scintillator requirements:

Solvable in base material

High fluorescence yield

Absorption spectrum must overlap with emission spectrum of base material

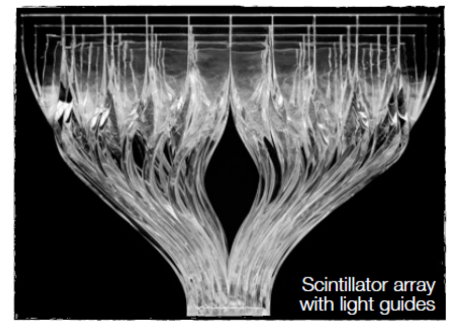

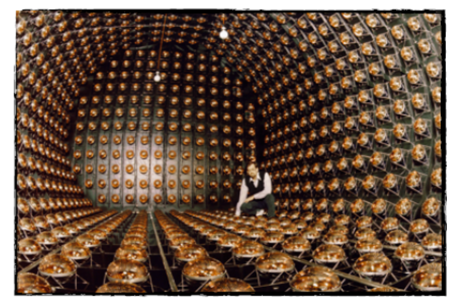

LSND experiment

Fast and cheaper

Scintillating Fibers hodoscopes

Scintillating Fibers Hodoscopes

9 stations: 21 coordinates

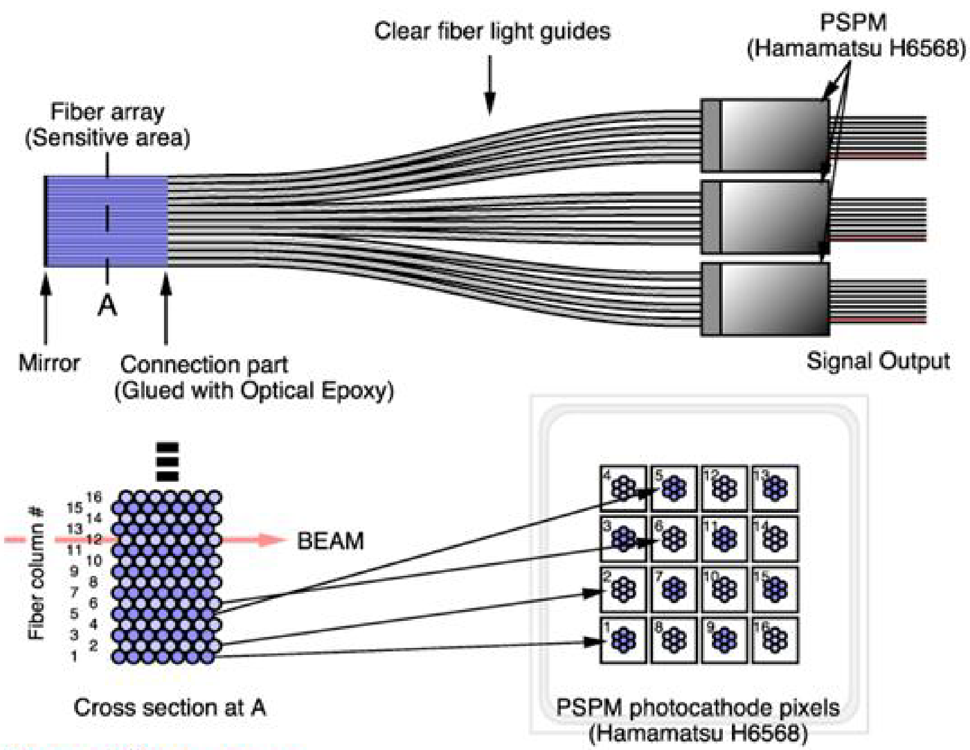

Rate capability > 5 MHz per channel

Efficiency: 99%

Space resol. 130 – 250 μm

Time resol. < 400 ps

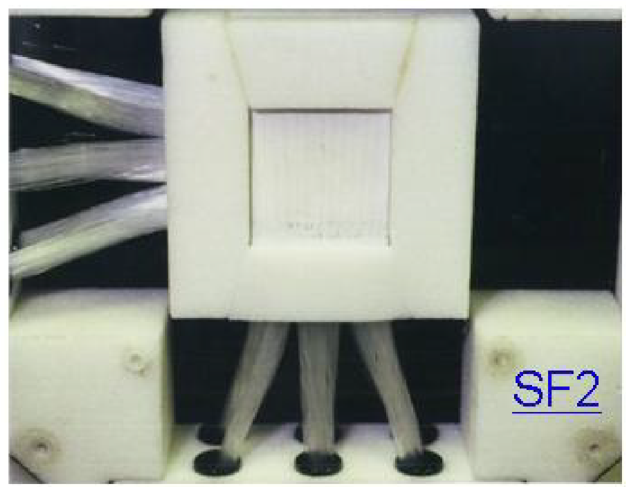

Sensitive area:

7-layers of Kuraray SCSF-78MJ 0.5 mm Ø

Photomultipliers

Photomultipliers

Principle:

Electron emission
from photo cathode

Secondary emission
from dynodes; dynode gain: 3-50 [f(E)]

Typical PMT Gain: > 10^6
[PMT can see single photons ...]

PMT Collection

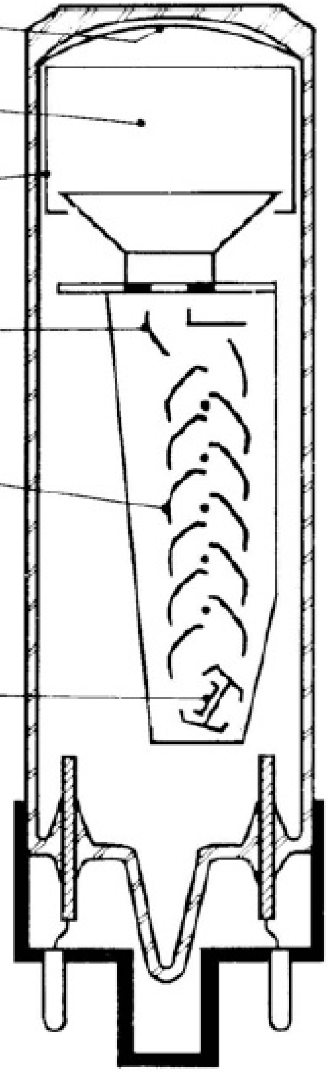

Photocathodes

Bialkali: SbRbCs; SbK_2Cs

γ-conversion
via photo effect ...

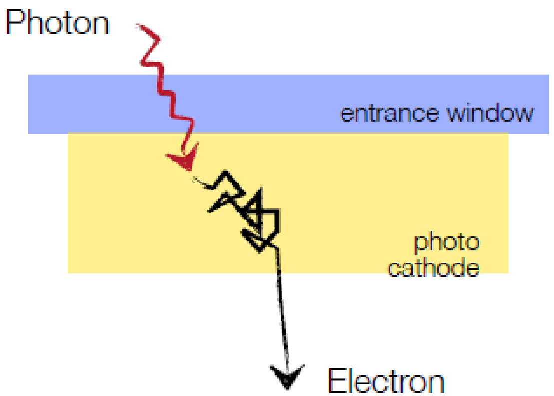

3-step process:

- Electron generation via ionization
- Propagation through cathode
- Escape of electron into vacuum

Q.E. ≈ 10-30%
[need specifically developed alloys]

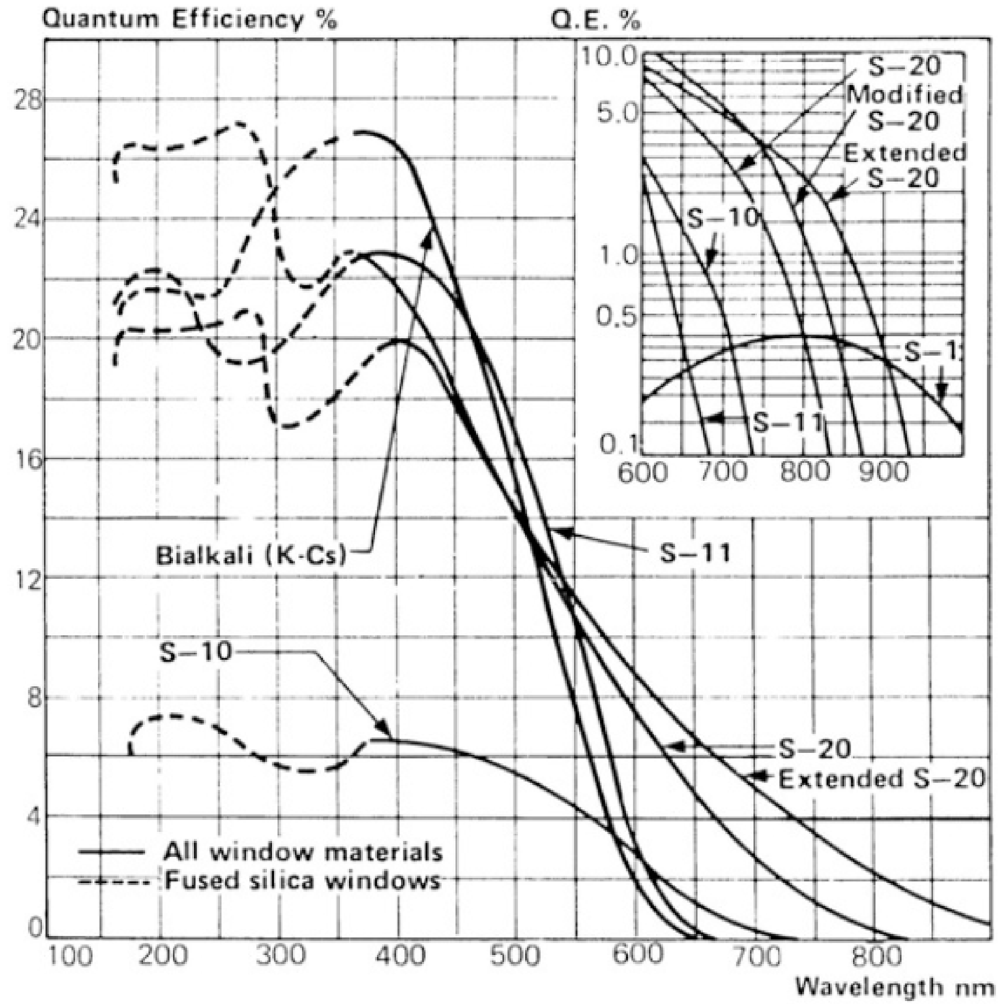

Micro-Channel Plates

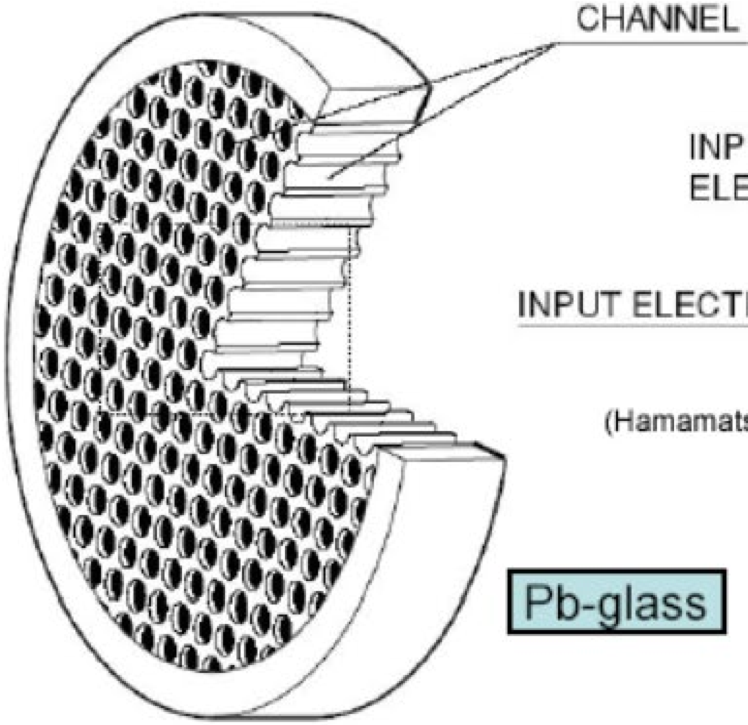

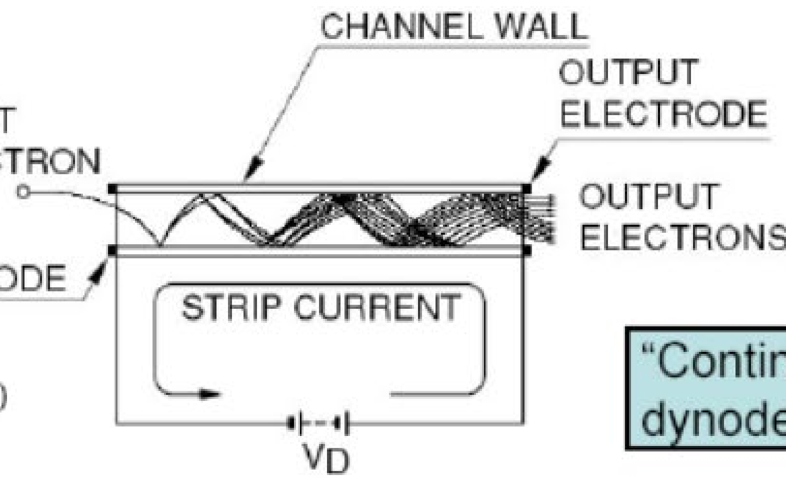

(Hamamatsu)

"Continuous" dynode chain

Pb-glass

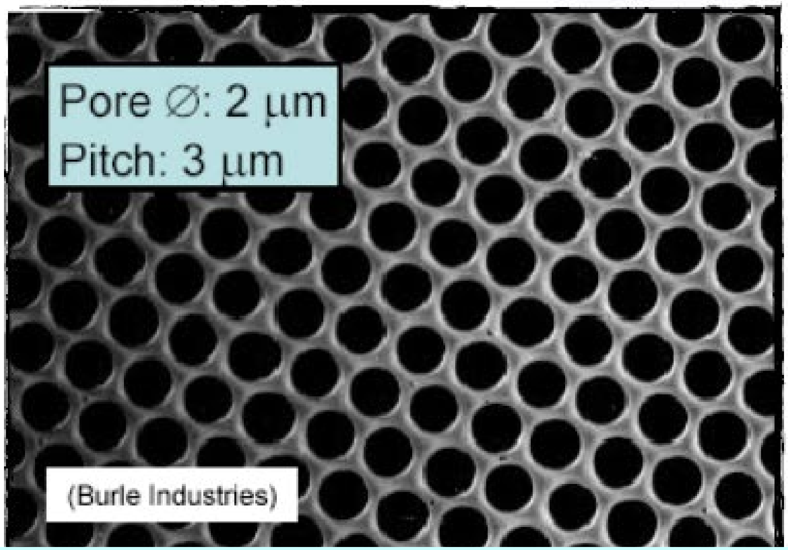

"2D Photomultiplier"

Gain: $5 \cdot 10^4$

Fast signal [time spread ~ 50 ps]

B-Field tolerant [up to 0.1T]

Si PMs

Silicon Photomultipliers

Principle:

Pixelized photo diodes
operated in Geiger Mode

Single pixel works as a binary device

Energy = #photons seen by
summing over all pixels

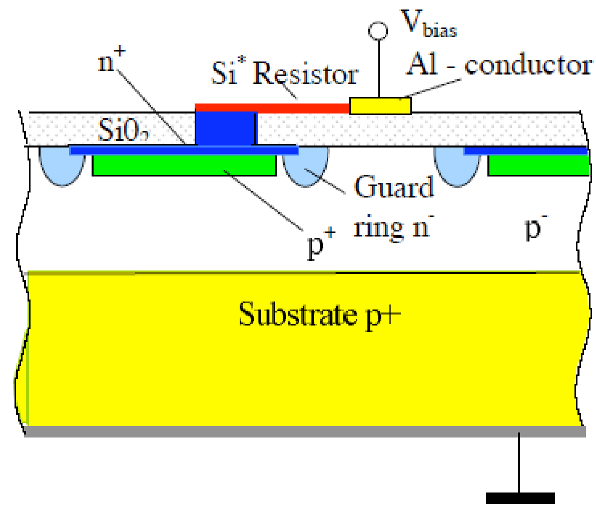

Features:

Granularity	:	10^3 pixels/mm^2
Gain	:	10^6
Bias Voltage	:	< 100 V
Efficiency	:	ca. 30 %

Insensitive to magnetic fields!
Works at room temperature ...

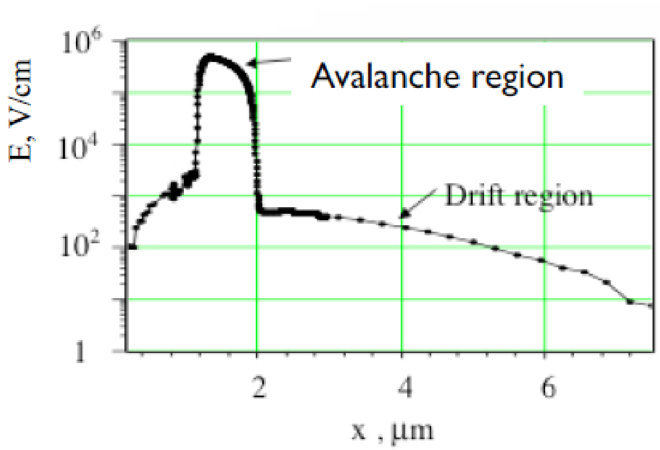

CCD

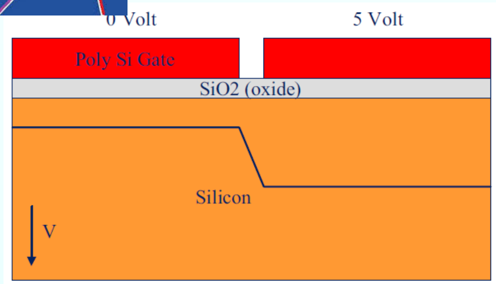
0 Volt
5 Volt
Poly Si Gate
SiO2 (oxide)
Silicon
V

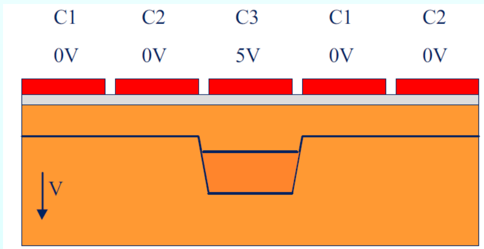
C1
C2
C3
C1
C2
0V
0V
5V
0V
0V
V

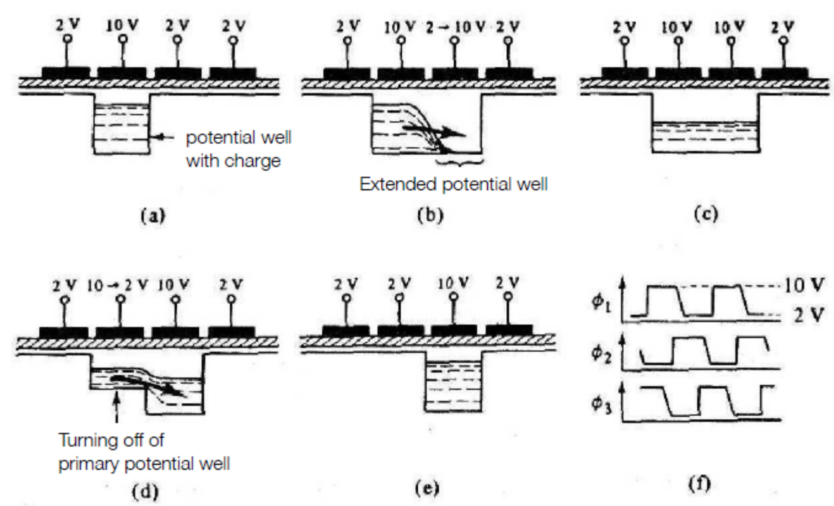
potential well with charge
(a)
Extended potential well
(b)
(c)
Turning off of primary potential well
(d)
(e)
(f)
10 V
2 V


The Nobel Prize in Physics 2009
"for groundbreaking achievements concerning the transmission of light in fibers for optical communication"
"for the invention of an imaging semiconductor circuit – the CCD sensor"
Charles K. Kao
Willard S. Boyle
George E. Smith

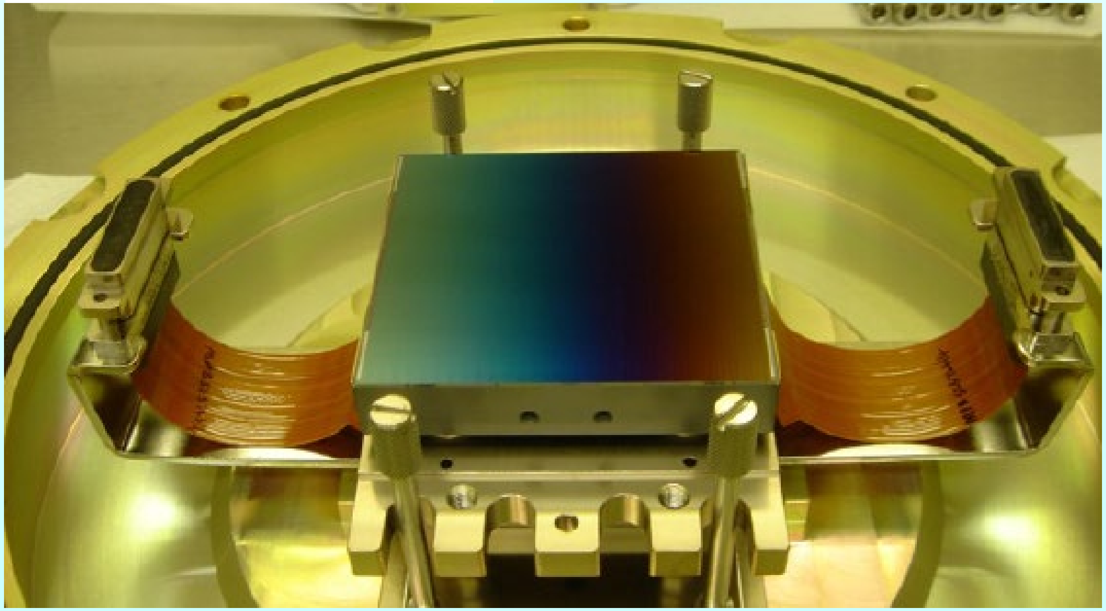

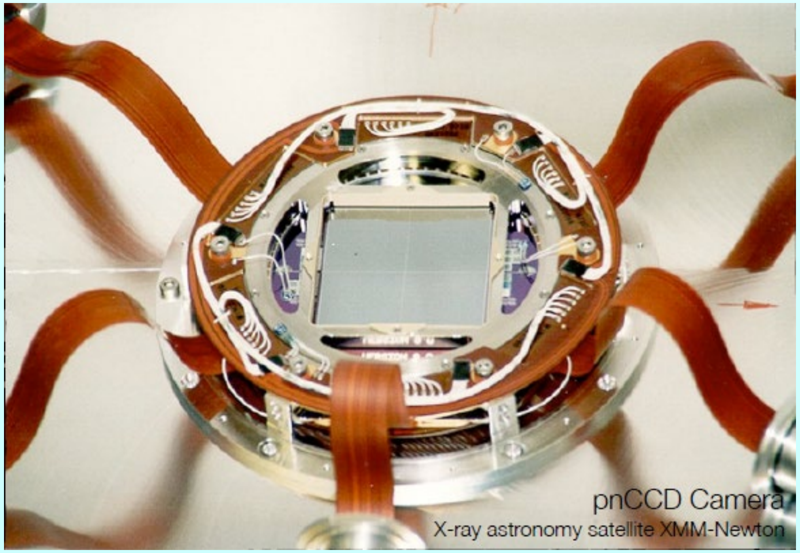
pnCCD Camera
X-ray astronomy satellite XMM-Newton

CMOS Image Pixel Sensors

- While 1980s were dominated by CCDs (camcorder market)
- The 1990s/2000s have shown an increasing demand for CMOS imaging sensors due to the camera phone market

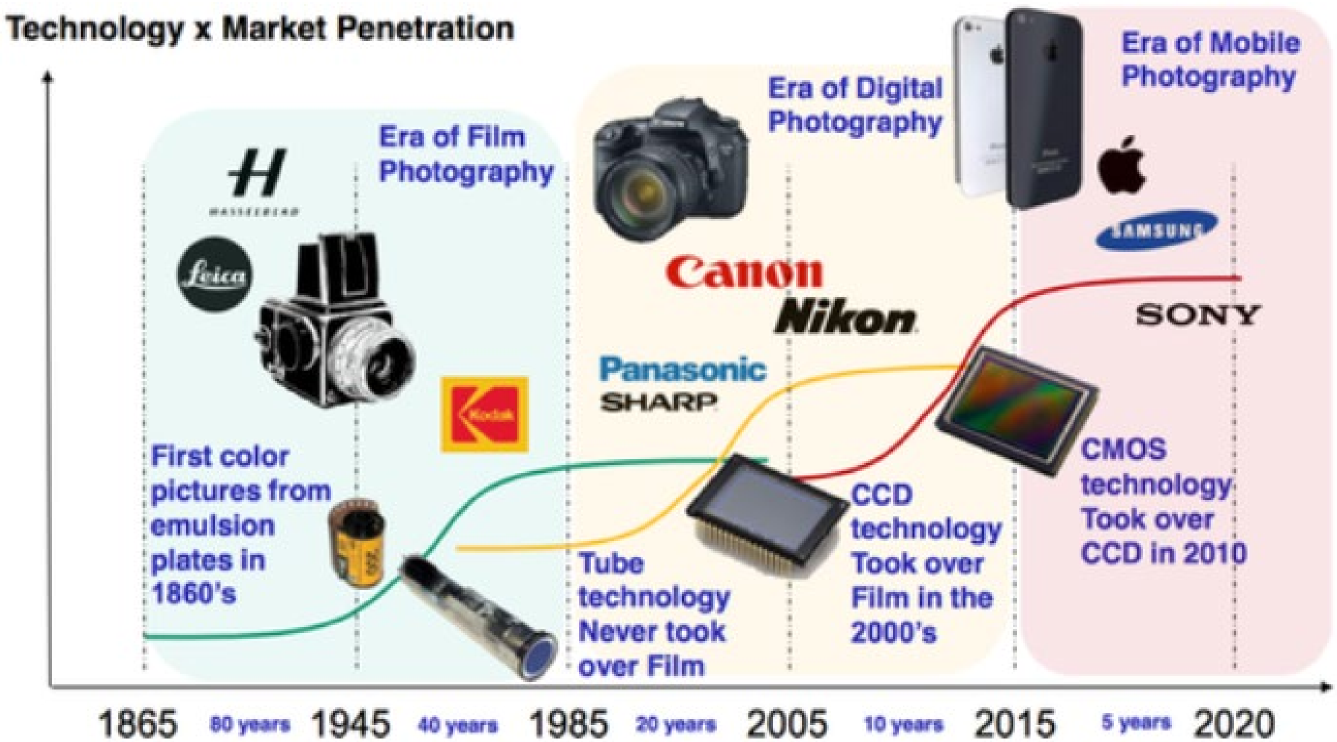

Si microstrips

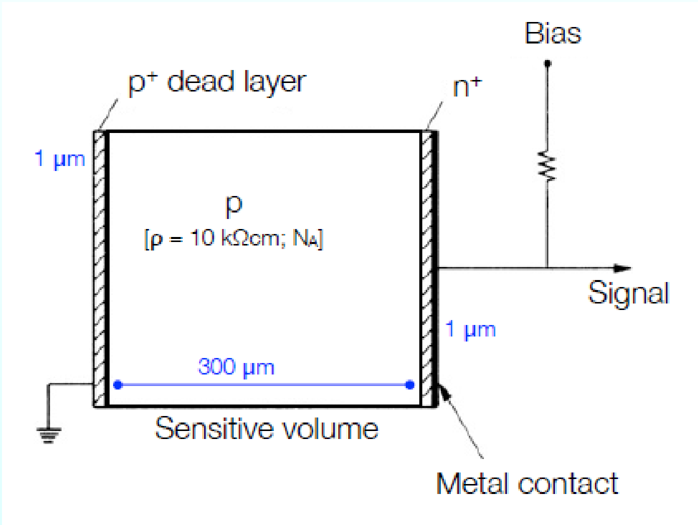

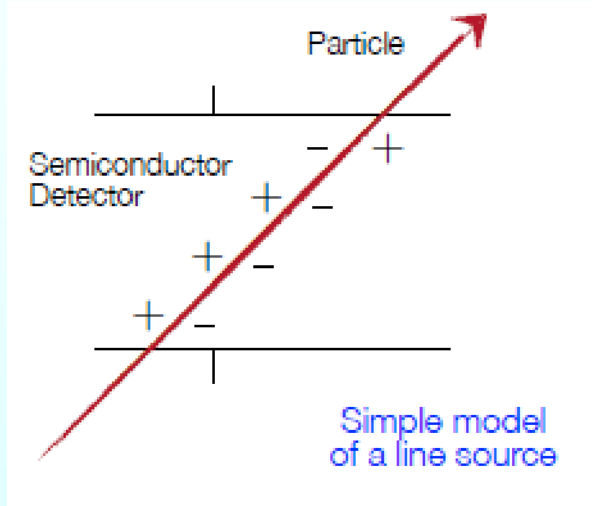

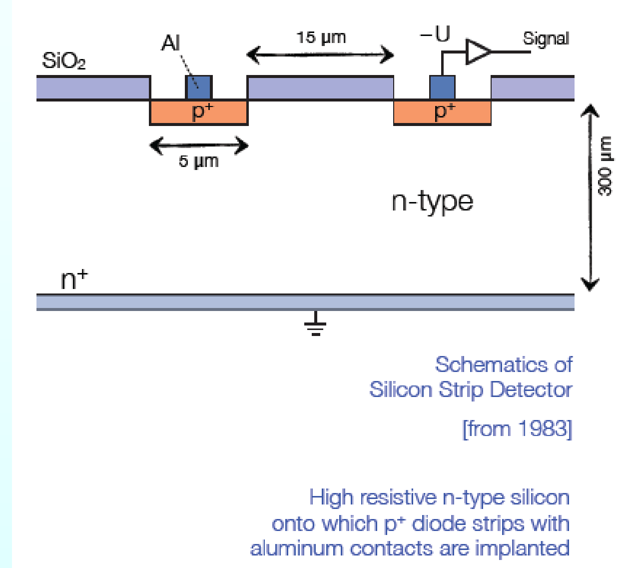

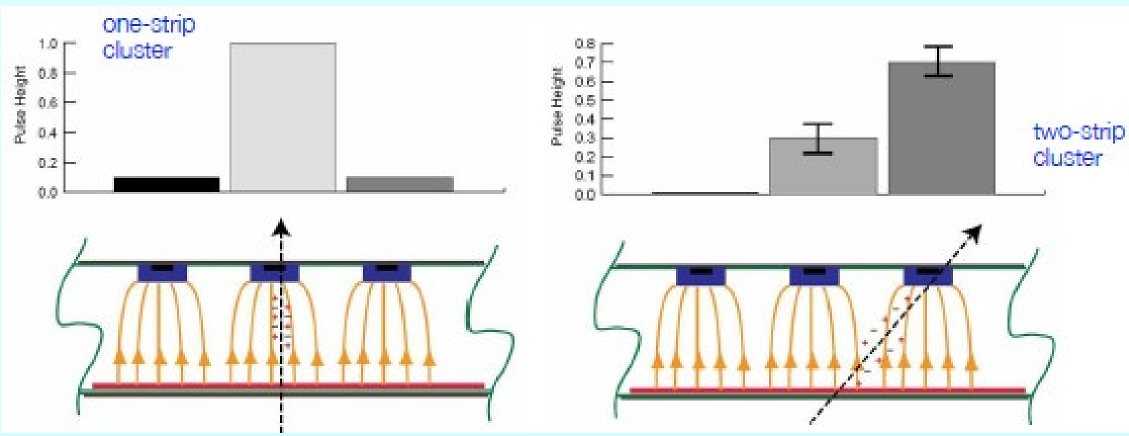

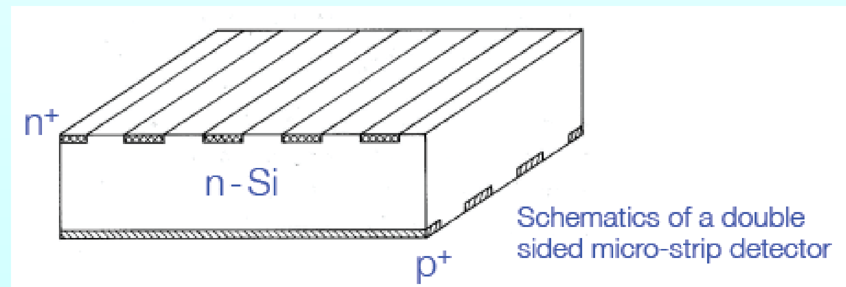

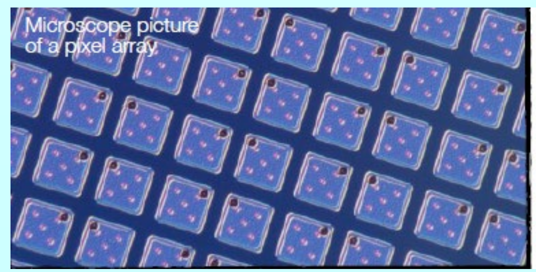

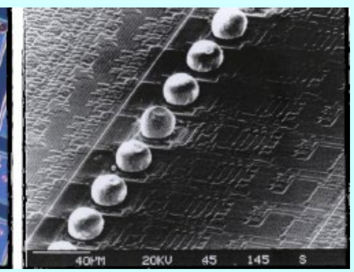

Si detectors

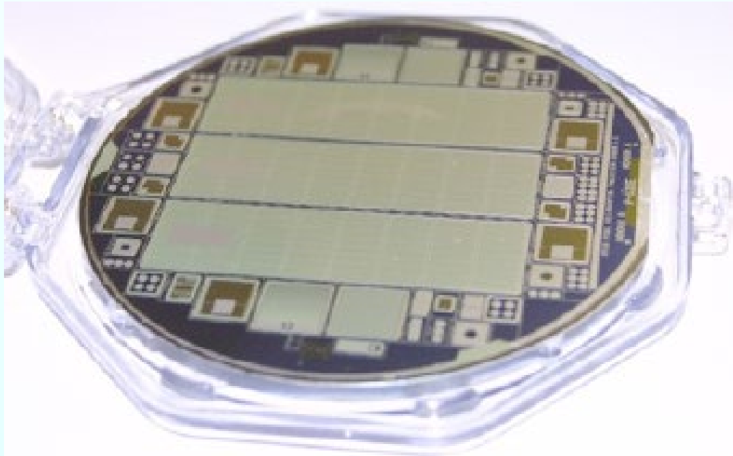

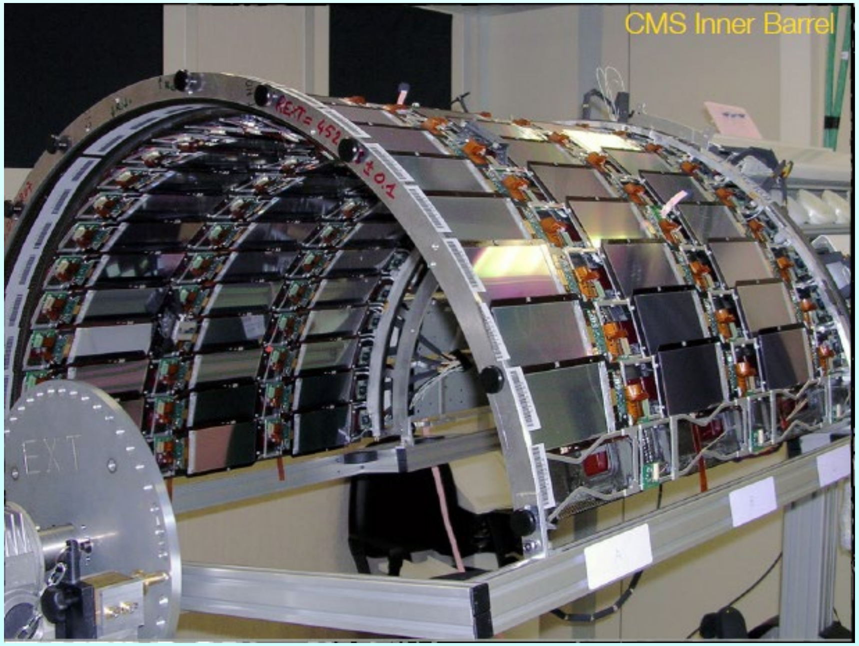

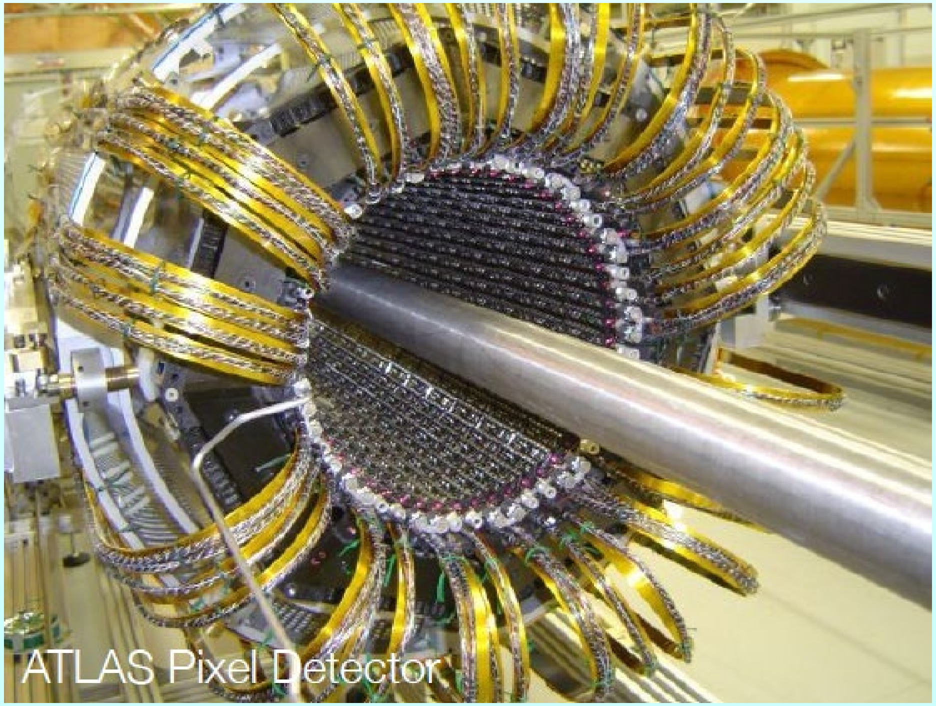

ALICE inner tracker upgrade

MAPS (Monolithic Active Pixel Sensors) for Imaging and More

Many developments in the field of CMOS imaging sensors and MAPS in general within the community!

Example:
Wafers scale (8") imaging sensor developed by the RAL team (stitched)

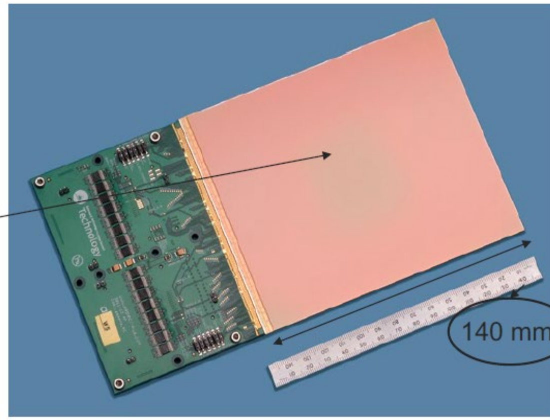

N. Guerrini, RAL, 5th school on detectors, Legnaro, April 2013

Developments lead by IPHC created a number of monolithic pixel sensors of the MIMOSA family:

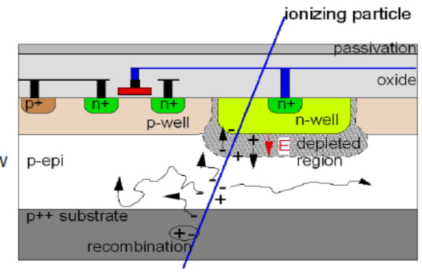

- Epitaxial wafers with collection diode and few transistors per cell (size ~ 20 x 20 μm²)
- 0.35 μm CMOS technology with only one type of transistor (NMOS)
- Rolling shutter architecture (readout time O(100 μs))
- **Charge collection mostly by diffusion**
- Limited radiation tolerance (< 10^{13} n_{eq} cm^{-2})

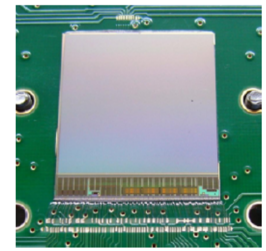

ULTIMATE chip for STAR HFT (IPHC Strasbourg)

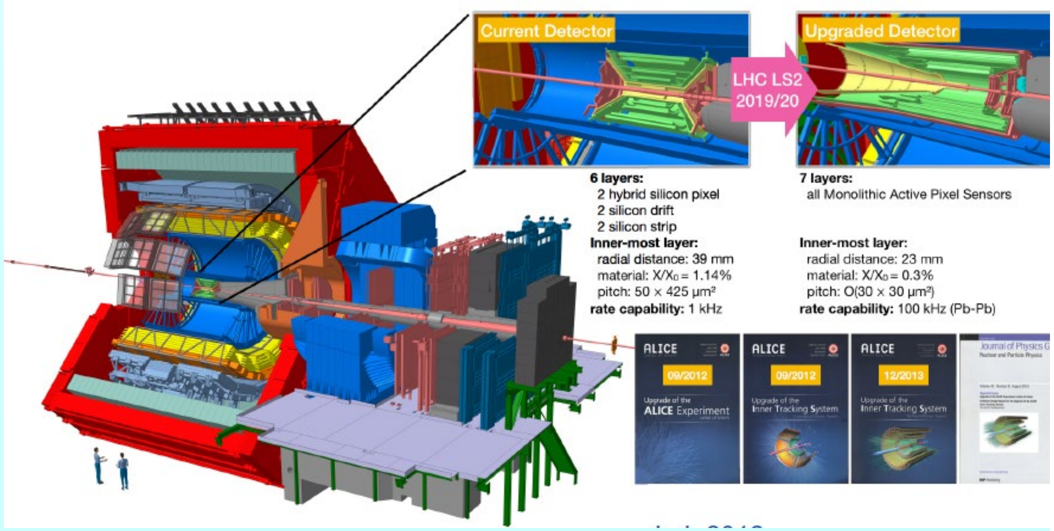

ALICE ITS upgrade

- Complete removal of the **present inner tracking system and installation of a new tracker based on monolithic silicon pixel** sensors (~ 10m²)
- **Change of technology** compared to the present system: hybrid pixels silicon drift, silicon strips → **monolithic CMOS sensors**
- **First use of monolithic pixel detectors in an LHC experiment.**

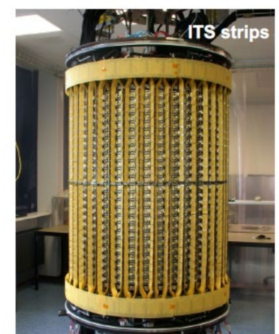

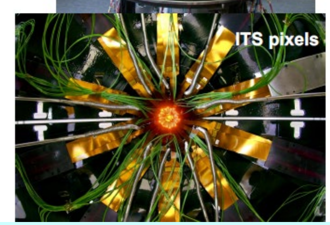

Glorious tradition: 100 years of gaseous detector developments

1908: FIRST WIRE COUNTER
USED BY RUTHERFORD IN THE STUDY OF NATURAL RADIOACTIVITY

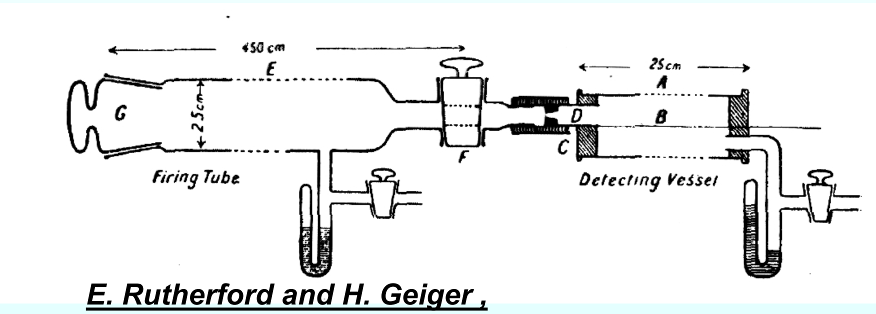

E. Rutherford and H. Geiger ,
Proc. Royal Soc. A81 (1908) 141

Nobel Prize in Chemistry in 1908

1911: CLOUD CHAMBER

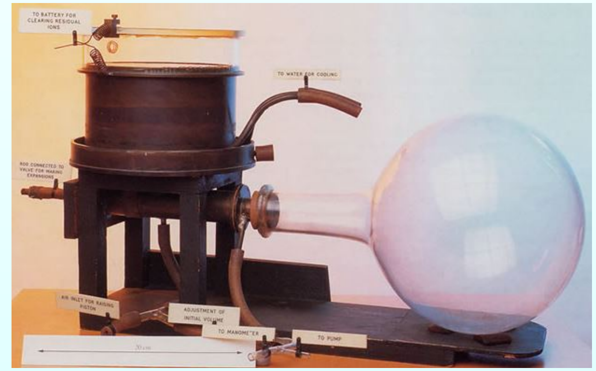

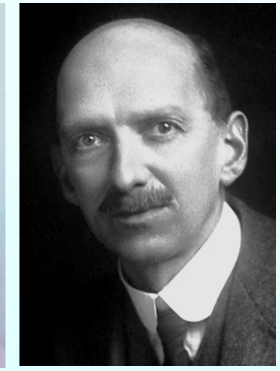

Charles T.R. Wilson
Nobel Prize in 1927

1928: GEIGER COUNTER
SINGLE ELECTRON SENSITIVITY

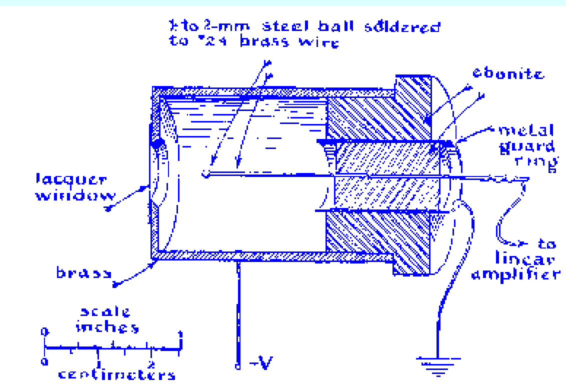

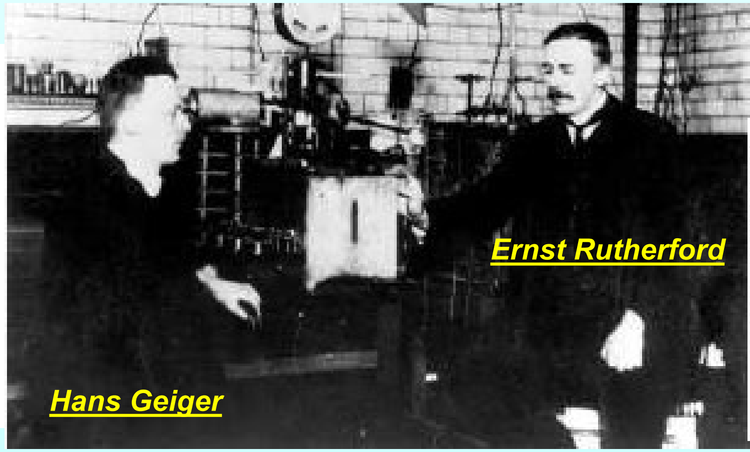

Ernst Rutherford

Hans Geiger

H. Geiger and W. Müller,
Phys. Zeits. 29 (1928) 839

COINCIDENCE METHOD

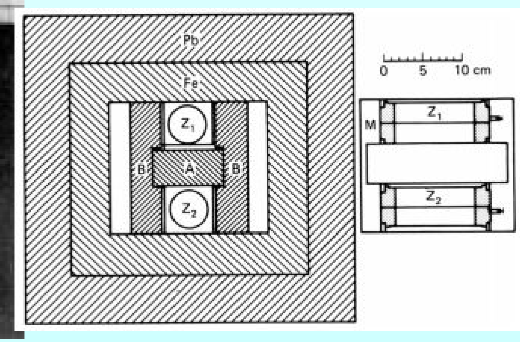

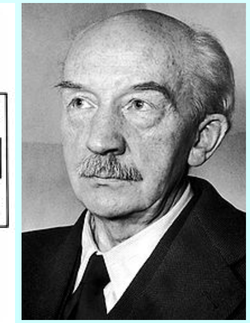

Walther Bothe
Nobel Prize in 1954

Glorious tradition: 100 years of gaseous detector developments

SPARK CHAMBER

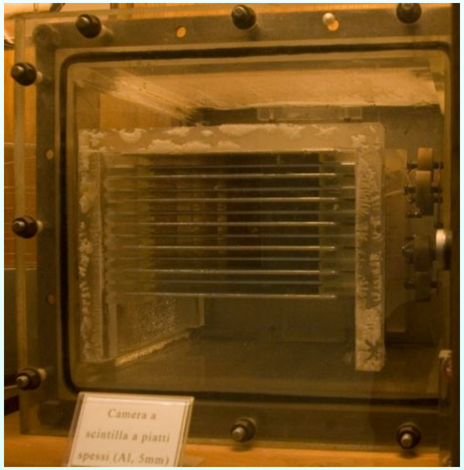

1952: BUBBLE CHAMBER

Donald A. Glaser
Nobel Prize in 1992

1968: MULTIWIRE PROPORTIONAL CHAMBER

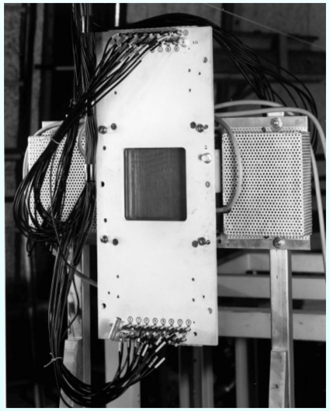

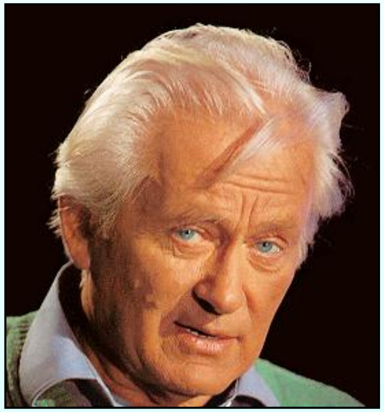

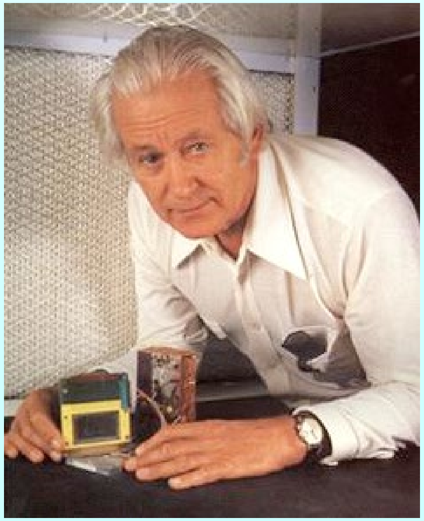

George Charpak
Nobel Prize in 1992

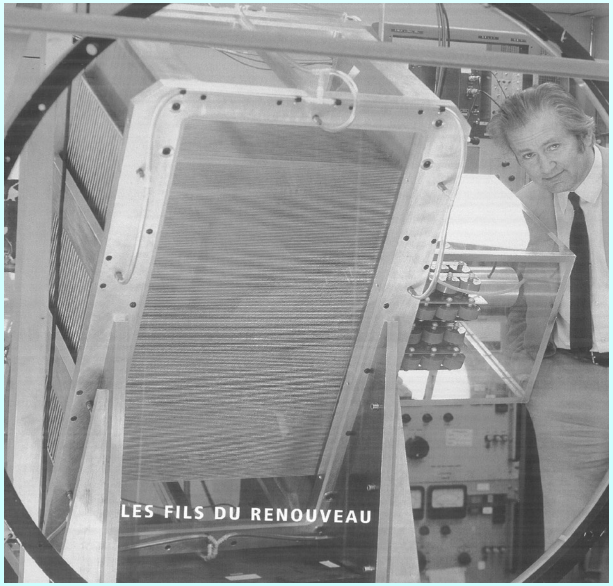

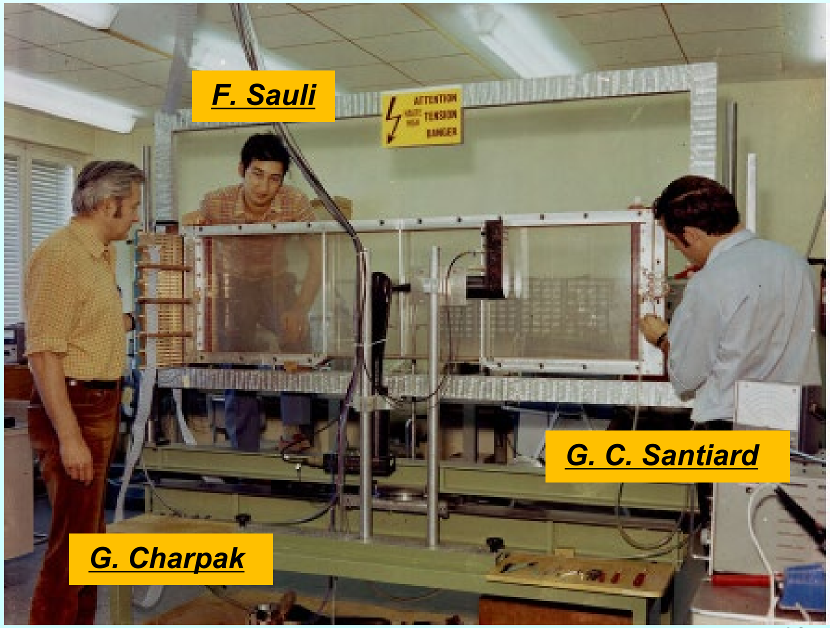

Glorious tradition: 100 years of gaseous detector developments

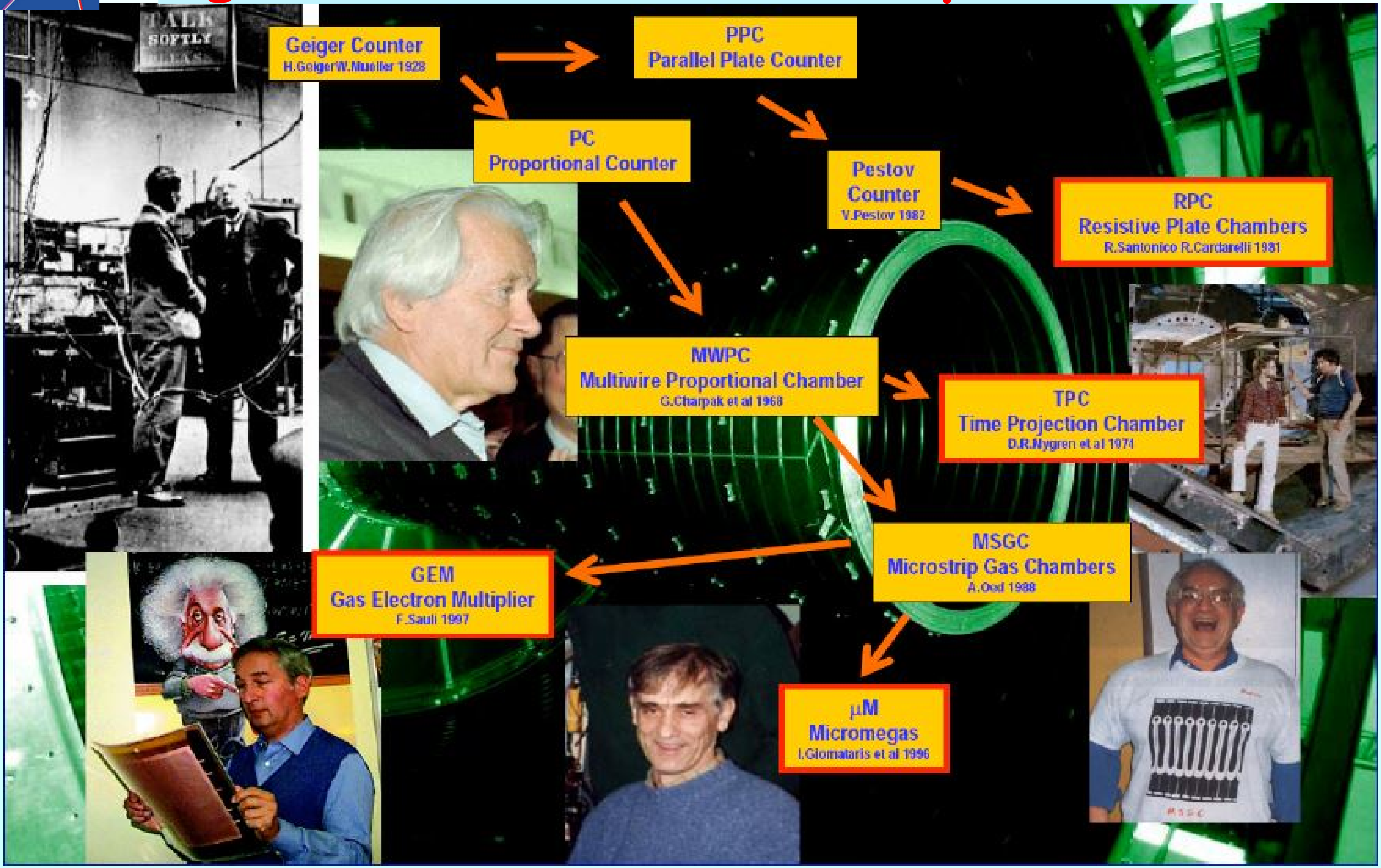

Tip Counter, Geiger 1914

Charges create a discharge of a needle which is at HV with respect to a cylinder.

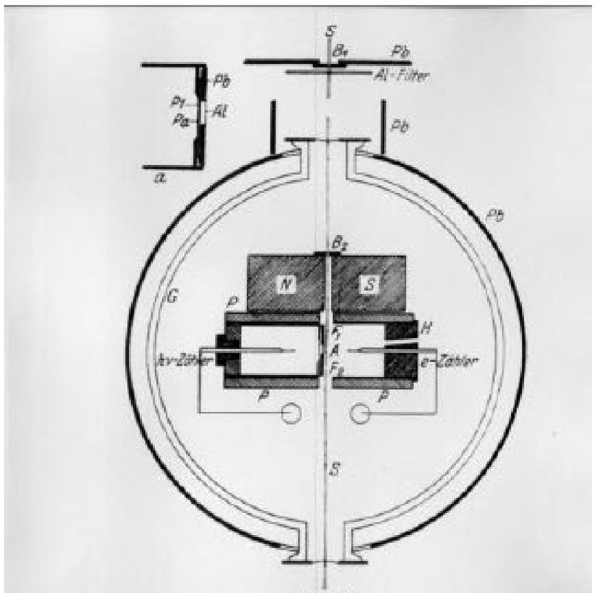

Fig. 2.

The needle is connected to an electroscope that can detect the produced charge.

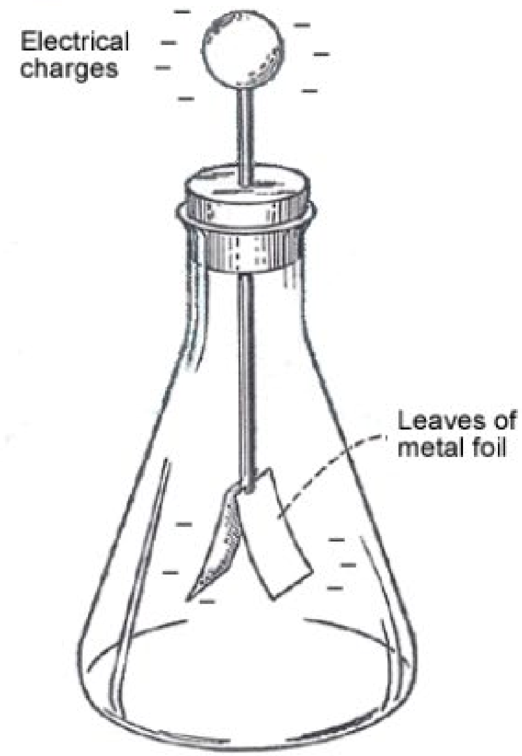

E(a)rnest Rutherford
(1871-1937)

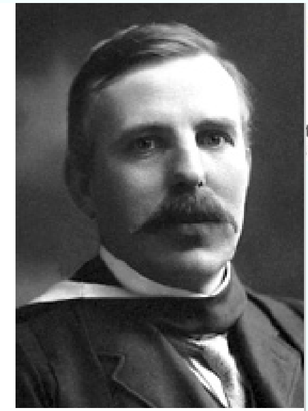

Geiger counter

- Detects radiation by discharge;
- can count α, β and γ particles (at low rates ...);
- no tracking capability.
- 1908: Ernest Rutherford and Hans Geiger
- 1928: Hans Geiger and Walther Müller

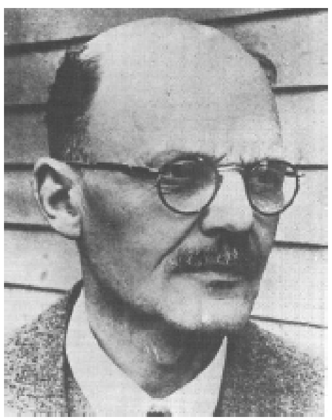

Hans Geiger
(1882-1945)

Walt(h)er Müller
(1905-1979)

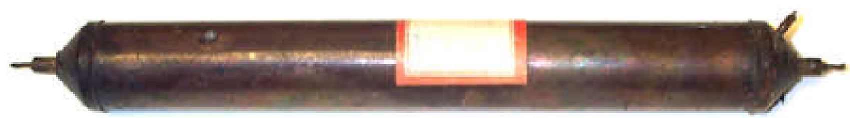

A Geiger-Muller counter built in 1939 and used in the 1947-1950 for cosmic ray studies in balloons and on board B29 aircraft by Robert Millikan et al.

Made of copper, 30 cm long

Electric Registration of Geiger Müller Tube Signals

azionale
Nucleare

Charges create a discharge in a cylinder with a thin wire set to HV. The charge is measured with a electronics circuit consisting of tubes → electronic signal.

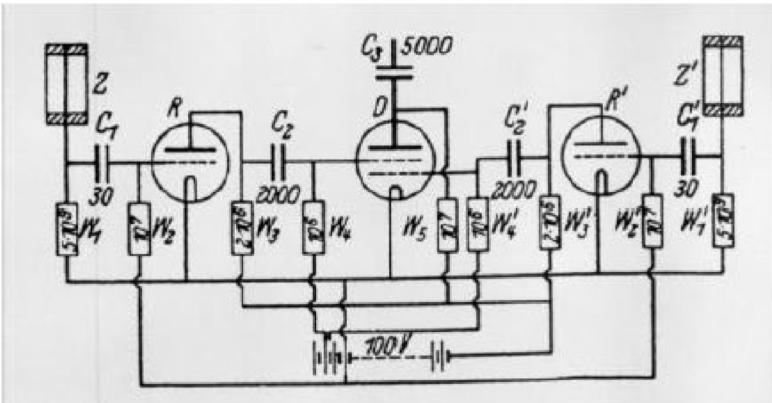

W. Bothe, 1928

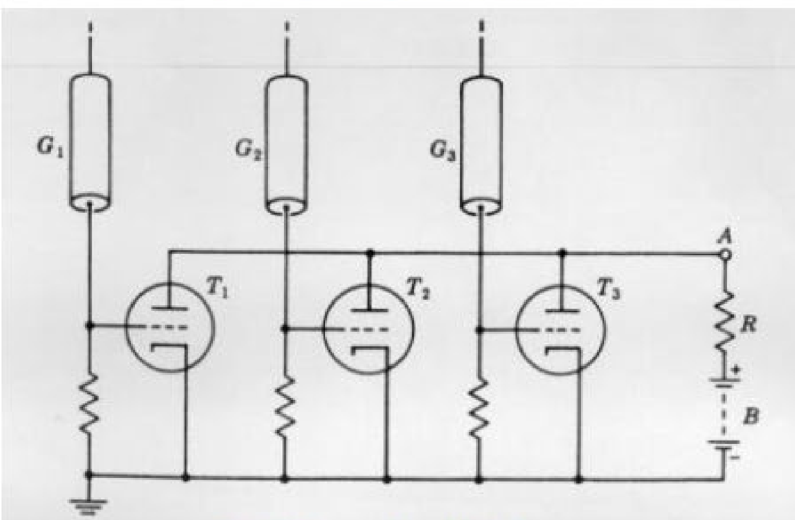

B. Rossi, 1932

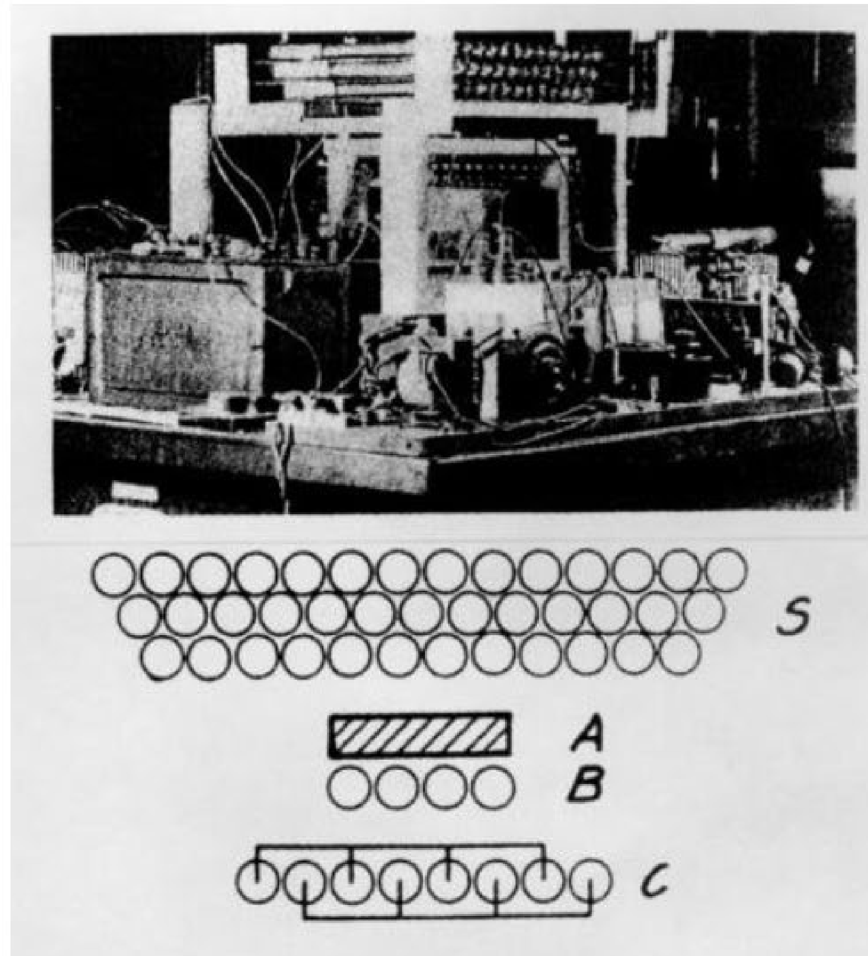

Cosmic Ray Telescope 1930ies

Spark Chamber, 1960ies

Charges create 'conductive channel' which initiates a spark in case HV is applied.

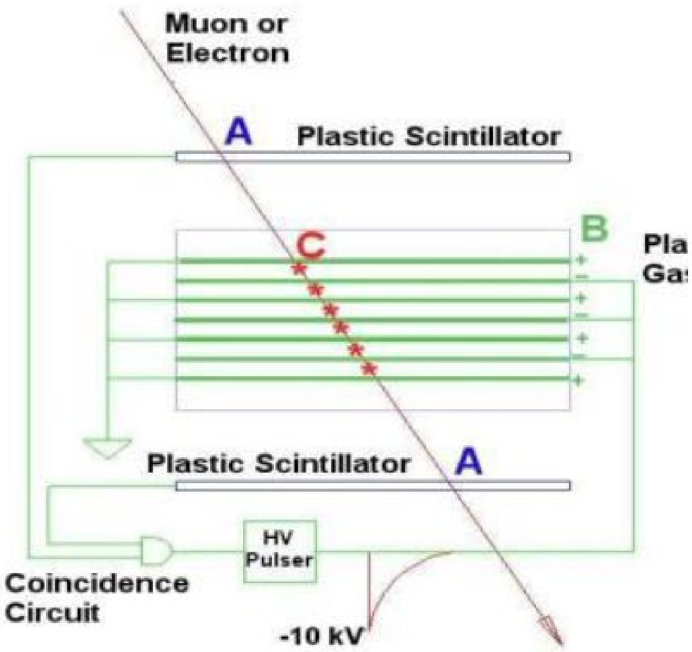

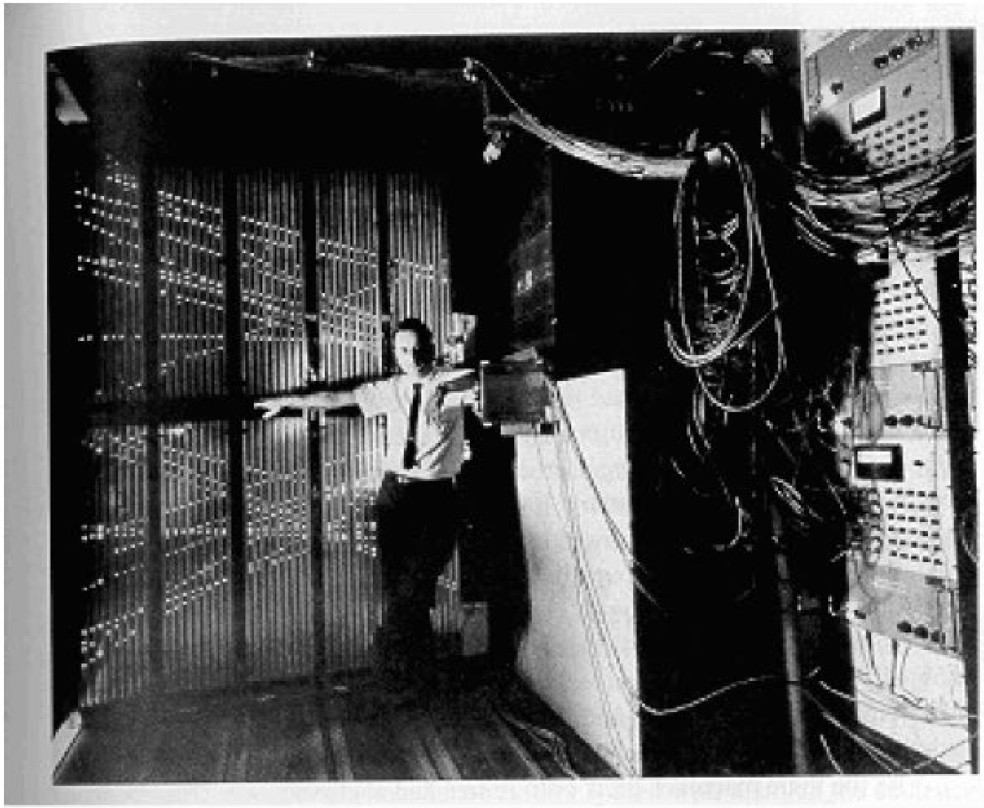

Discovery of the Muon Neutrino 1960ies

CAMERA PROPORZIONALE MULTIFILI

VERSAILLES 1968

colloque international sur l'électronique nucléaire

*

international symposium on nuclear electronics

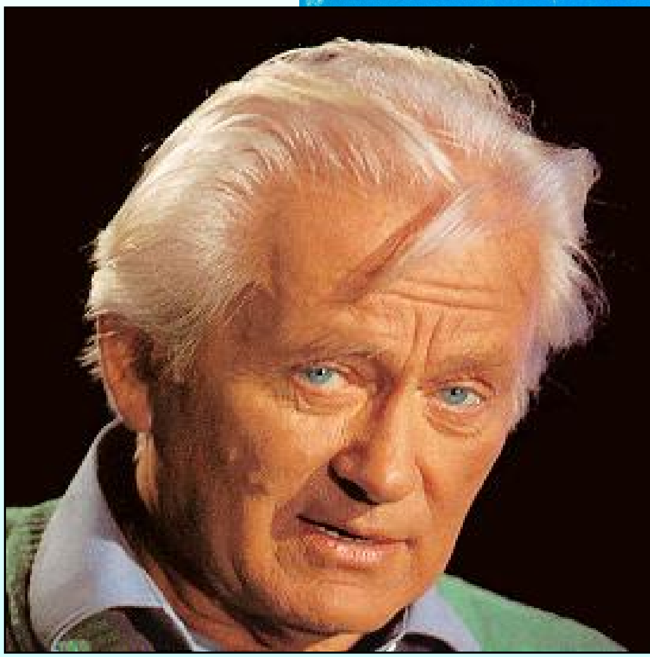

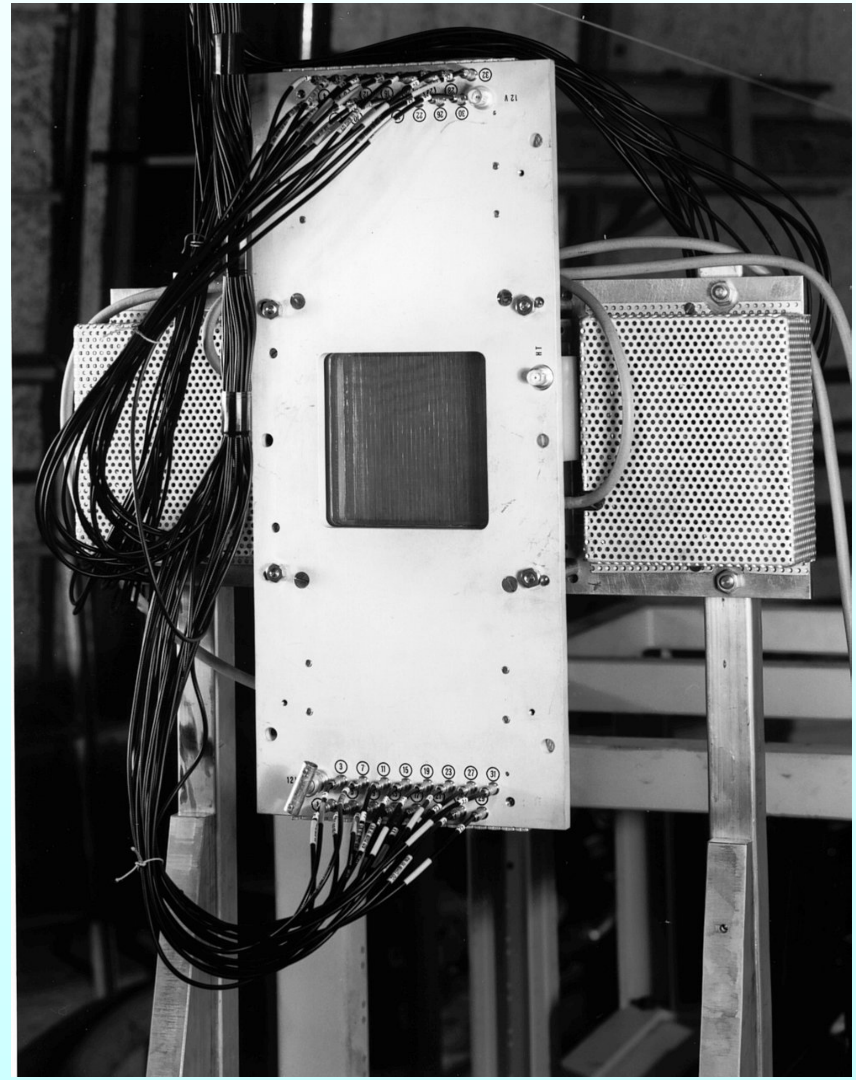

Chambres à Etincelles

Spark chambers

Rapporteur **M. CHARPAK**
Reporter **CERN - GENEVE (Suisse)**

G. Charpak, Proc. Int. Symp. Nuclear Electronics (Versailles 10-13 Sept 1968)

George Charpak in his lab with one of the big Multi-Wire Proportional Chambers

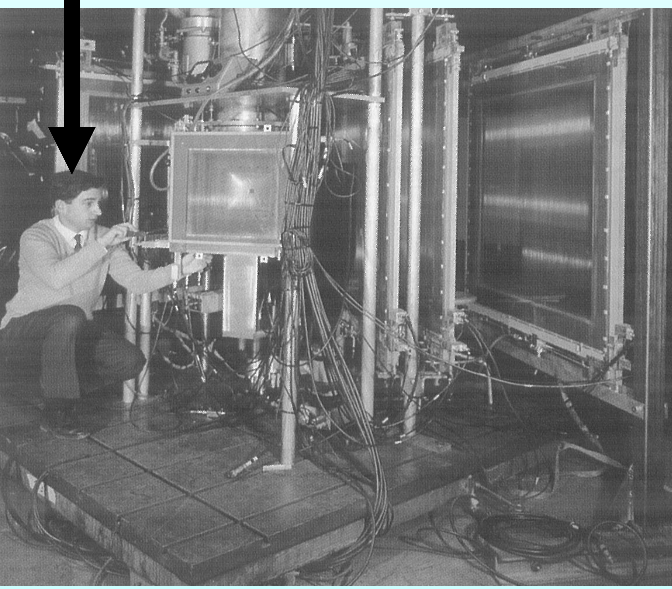

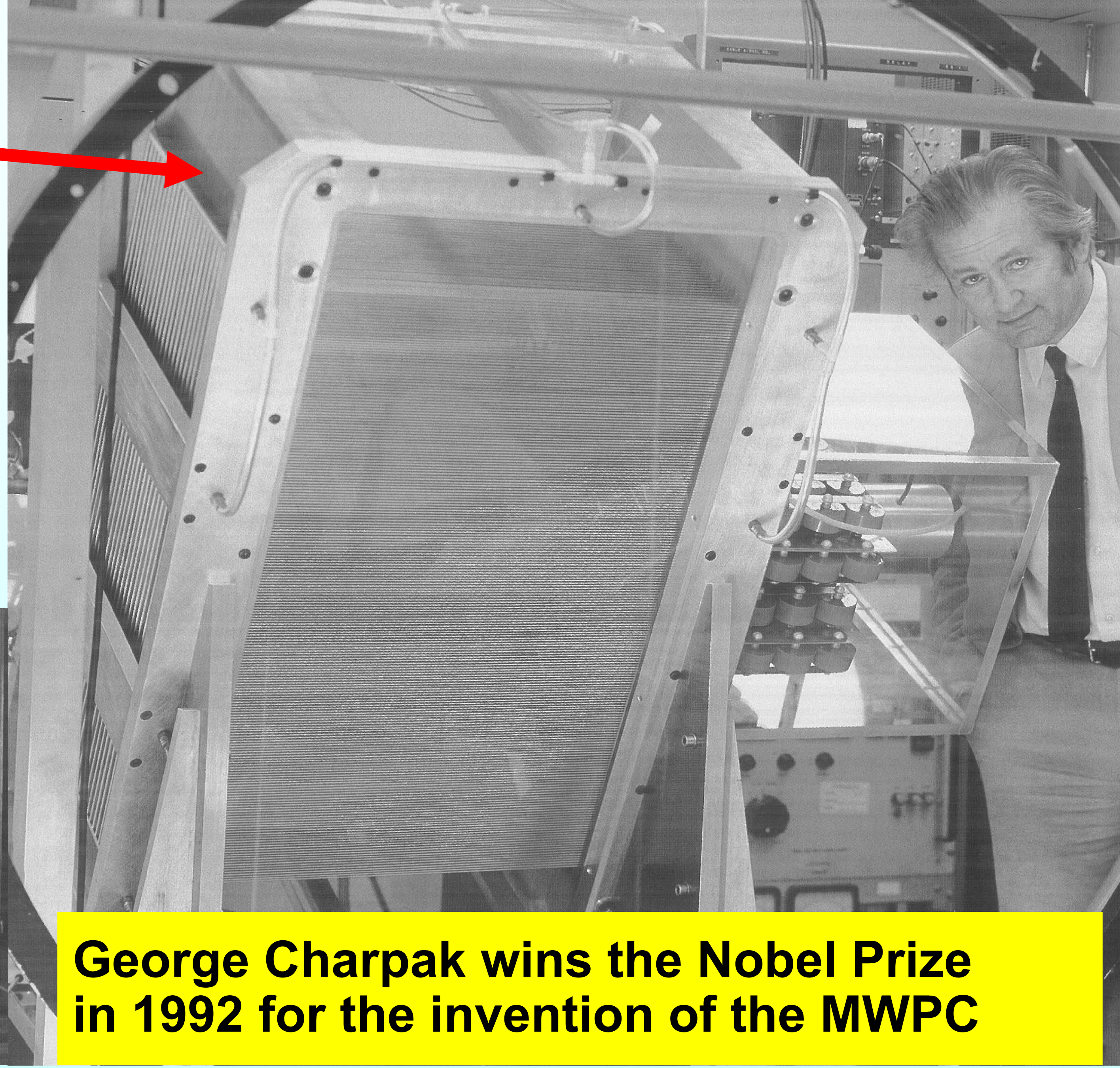

George Charpak wins the Nobel Prize in 1992 for the invention of the MWPC

Multi-Wire Proportional Chamber

WIRE COUNT:
DIGITAL MWPC

TIME MESUREMENT:
DRIFT CHAMBERS

INDUCED CHARGE:
2-D READOUT

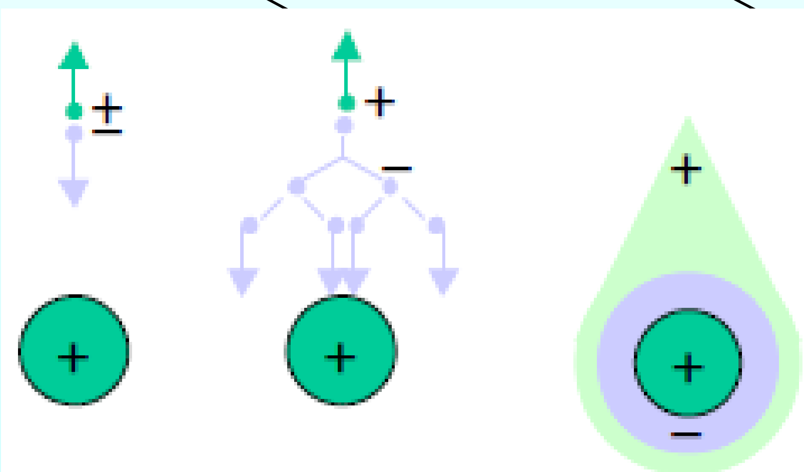

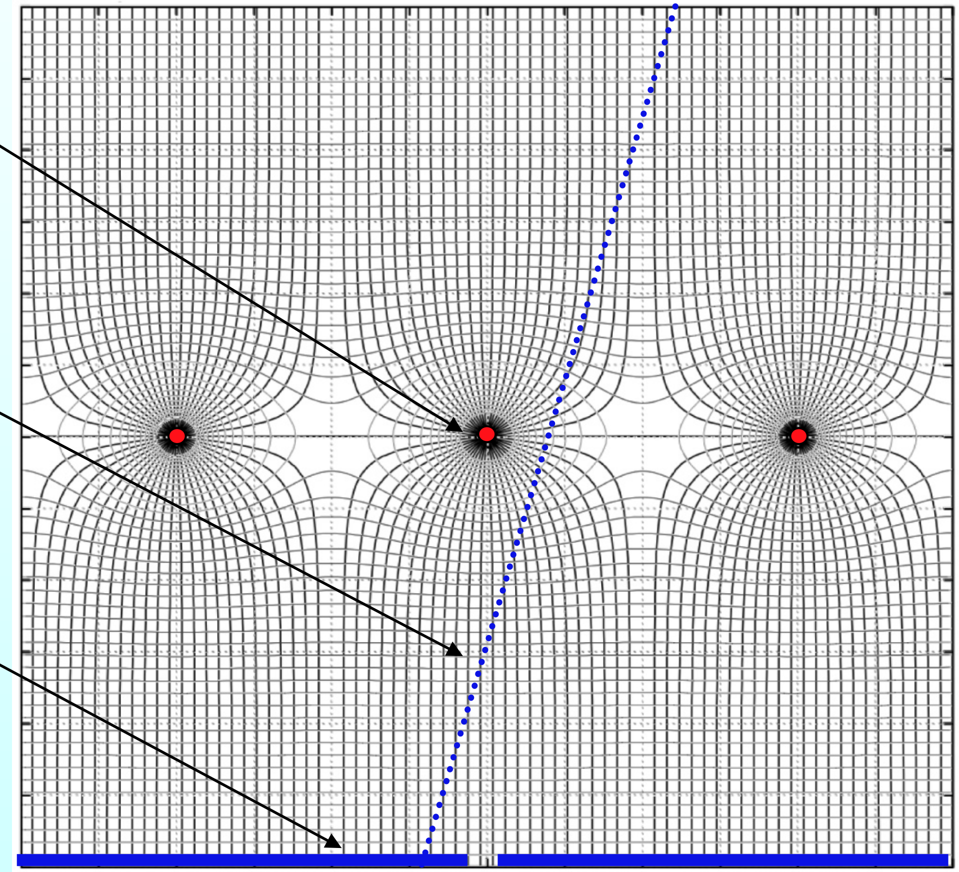

was the only approach to achieve good space resolution before introducing the Si trackers

TIME AND INDUCED CHARGE ON PADS:
TIME PROJECTION CHAMBERS

Old ALICE TPC

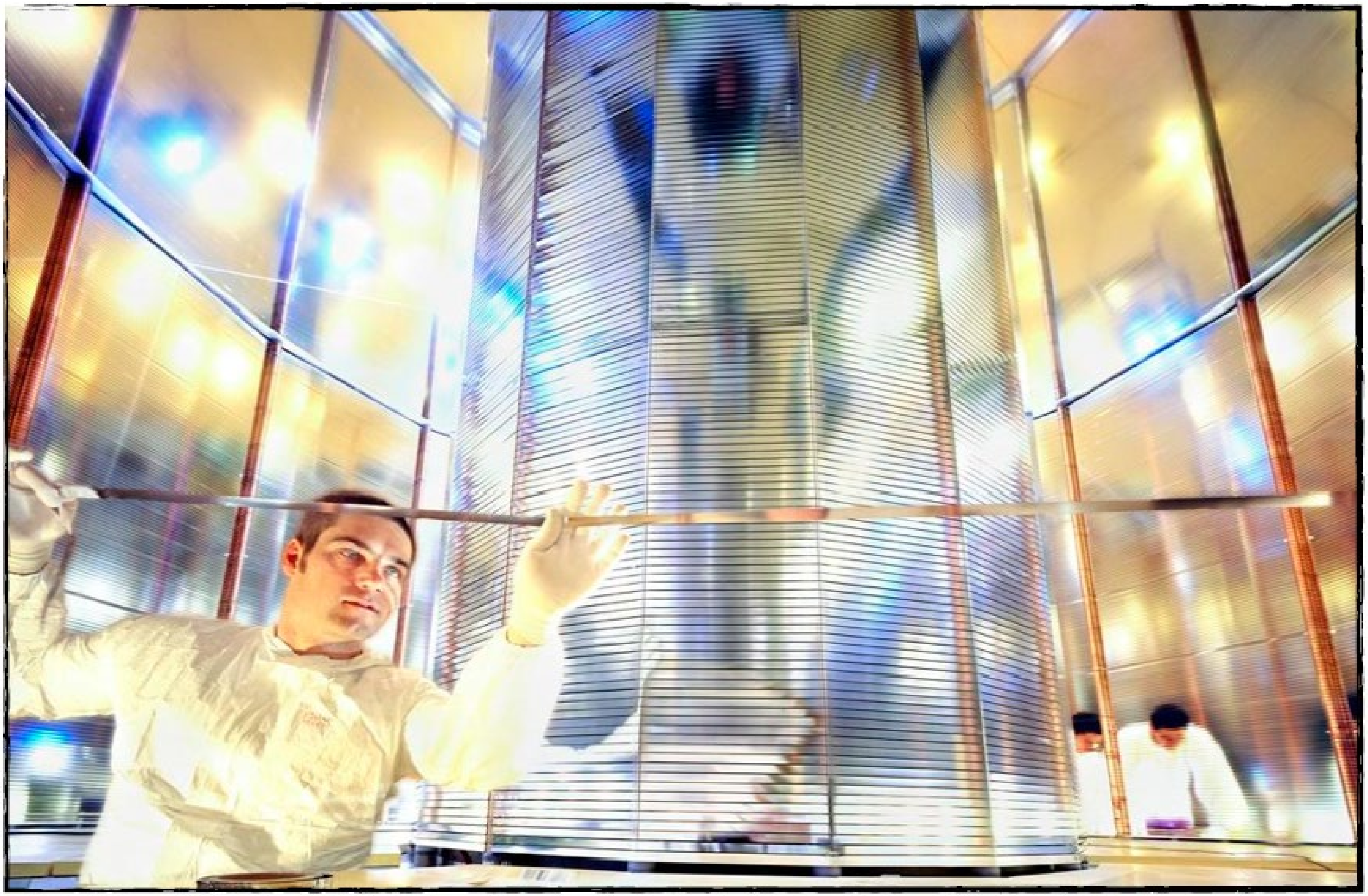

MicroStrip Gas Chamber

MWPC

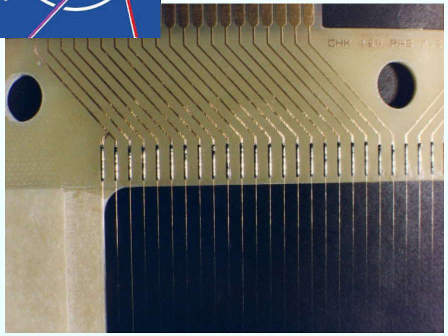

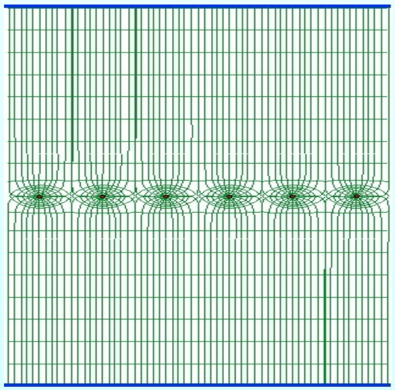

Typical distance between wires limited to 1 mm

MSGC

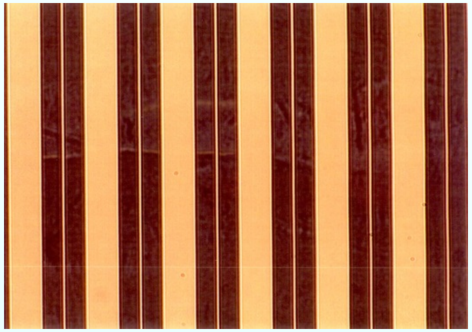

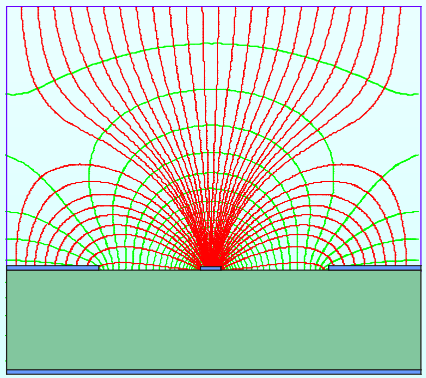

Typical distance between anodes 200 μm thanks to semiconductor etching technology

Semiconductor industry technology:

Photolithography
Etching
Coating
Doping

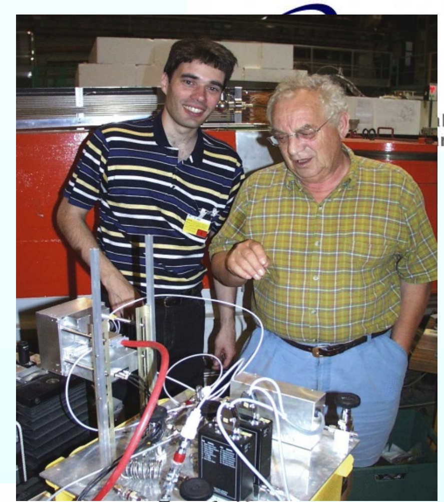

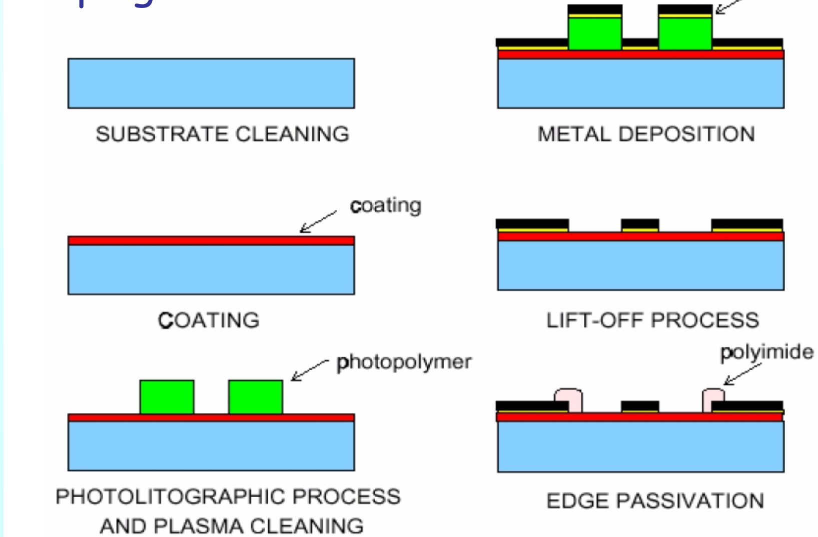

A. Oed, Nucl. Instr. and Meth. A263 (1988) 351.

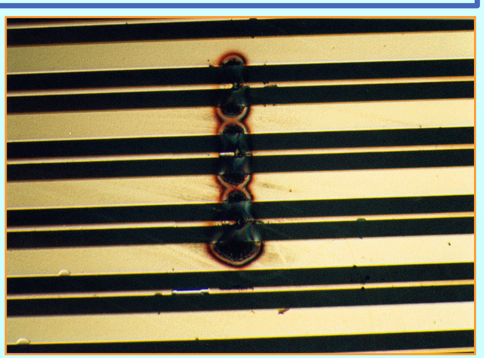

In the early days:
high E-values at the edge between insulator and strips → damages
Charge accumulation at the insulator
→ gain evolution vs time

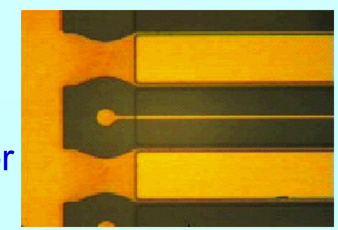

Later (~ 1999-2000): Passivation of the cathode edges → MSGC operational

Several different MPGDs have been developed

MICRO-GAP CHAMBER

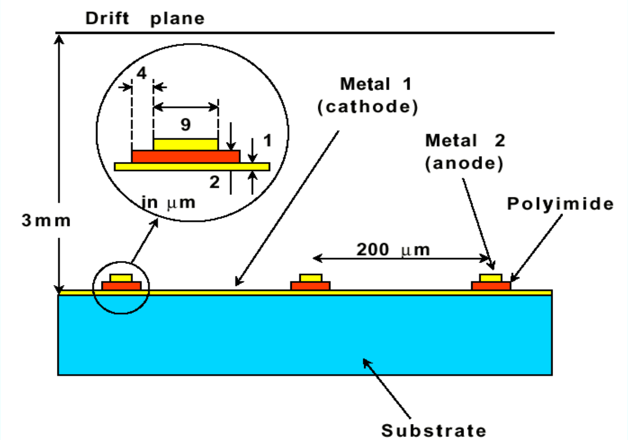

MICRO-GROOVE CHAMBER

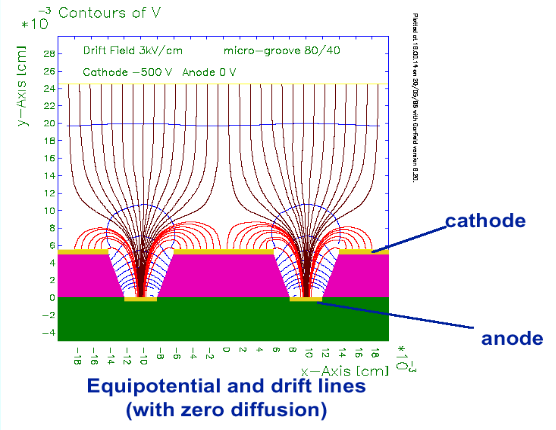

MICRO-PIN ARRAY

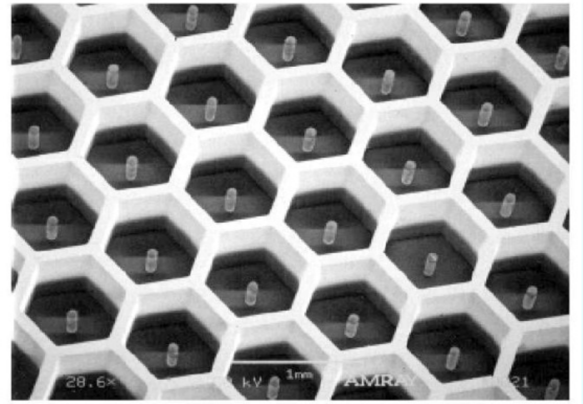

MICRO-WIRE CHAMBER

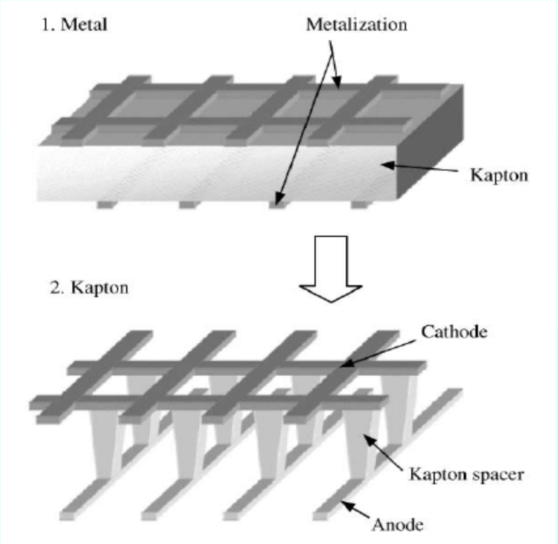

COMPTEUR A TROUS

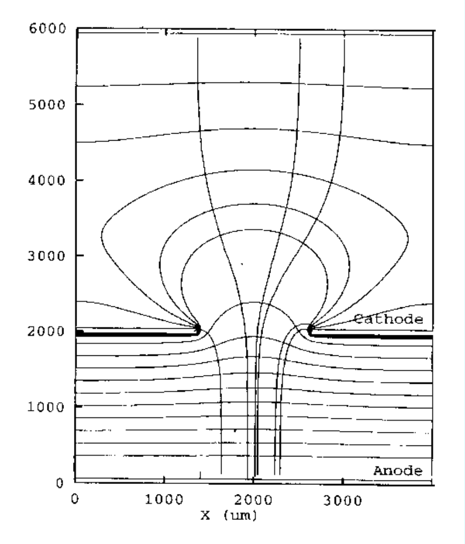

MICRO-PIXEL CHAMBER

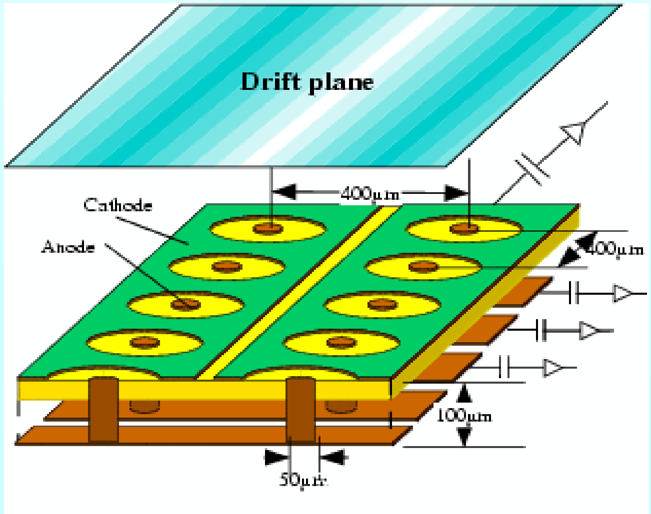

Micromegas

MICROMEGAS: THIN-GAP PARALLEL PLATE COUNTER

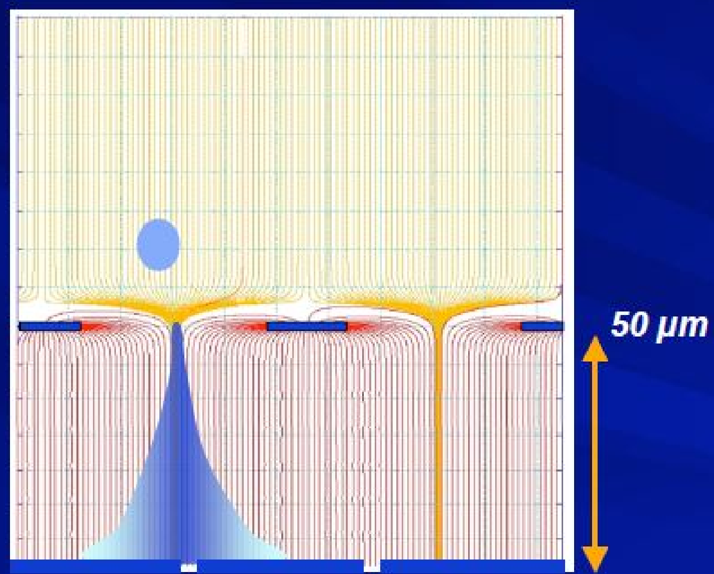

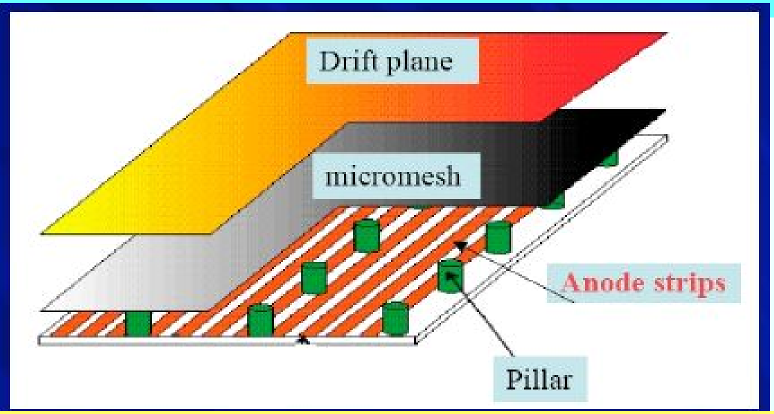

Micromesh mounted above readout structure (typically strips).
E field similar to parallel plate detector.
E_a/E_i ~ 50 to secure electron transparency and positive ion backflow supression.

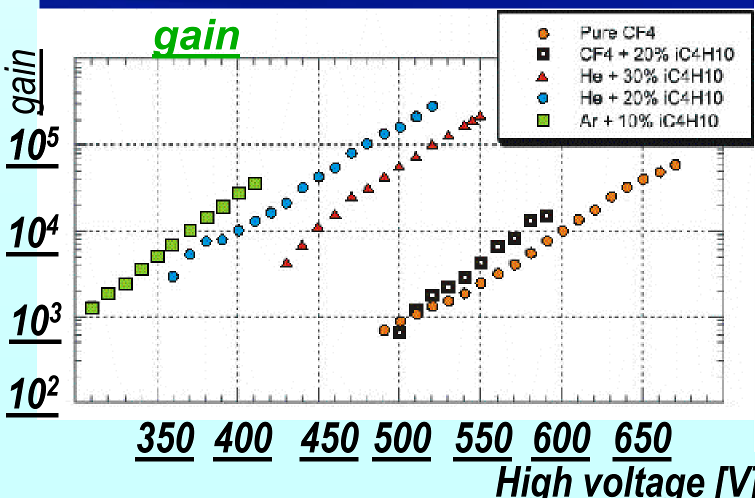

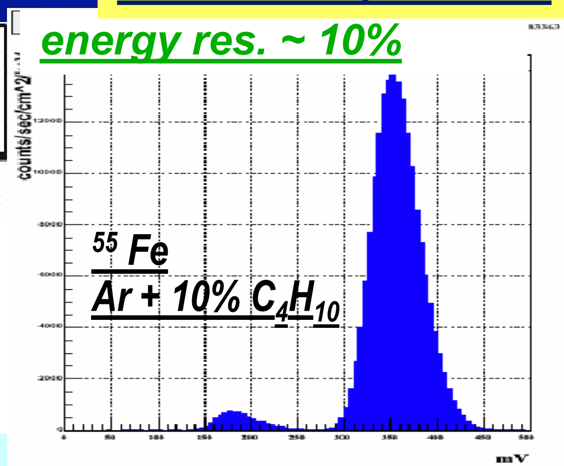

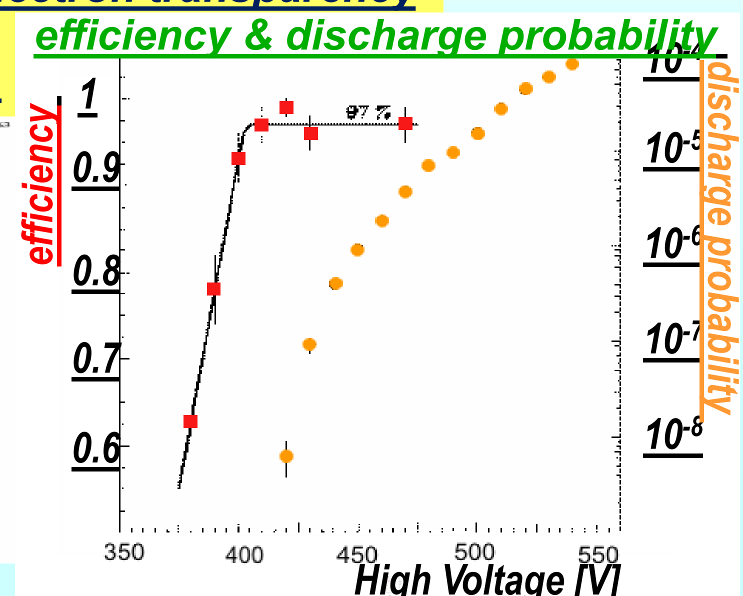

Bulk Micromegas technology

Y. Giomataris
R. de Oliveira

M. Chefdeville

T2K TPC, A. Delbart, M. Zito

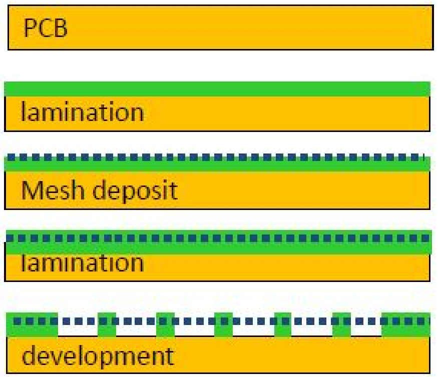

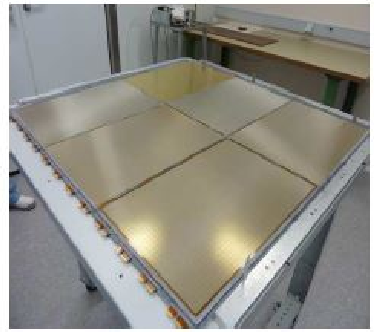

- Fine segmentation 1cm², thickness 8mm for ILC Hadronic calorimetry
- Tested in the RD51 1 kHz beam

Bulk Micromegas ILC DHCAL first m²
LAPP Annecy

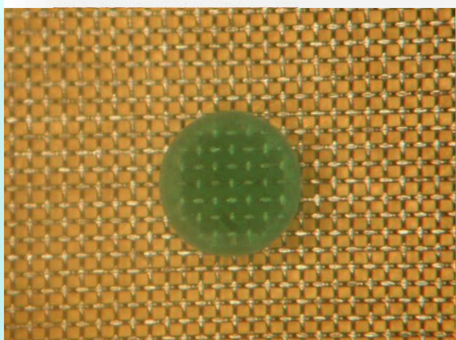

woven mesh

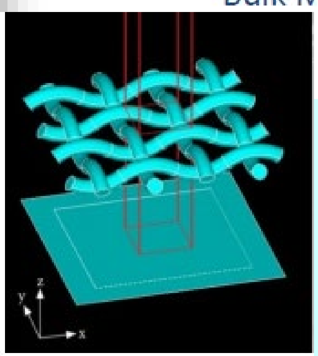

INGRID

Integrated Micromegas and Pixel Sensor
Postprocessing of the TIMEPIX chip to build a metal mesh on insulating pillars

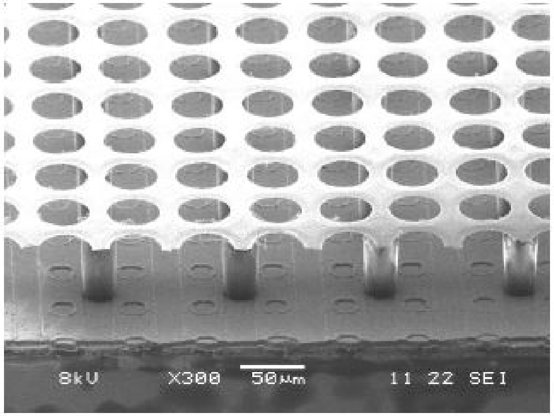

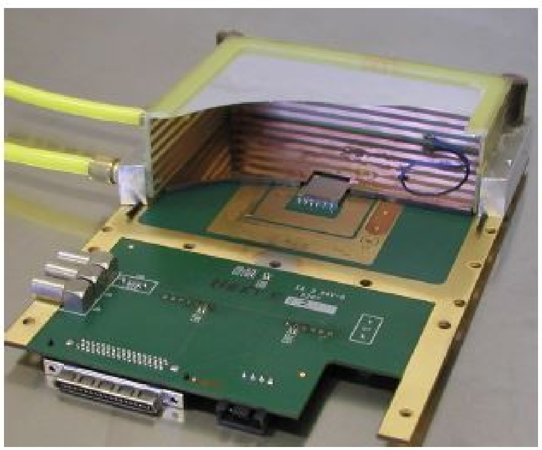

Electron tracks from ^{90}Sr in magnetic field (0.2 T):

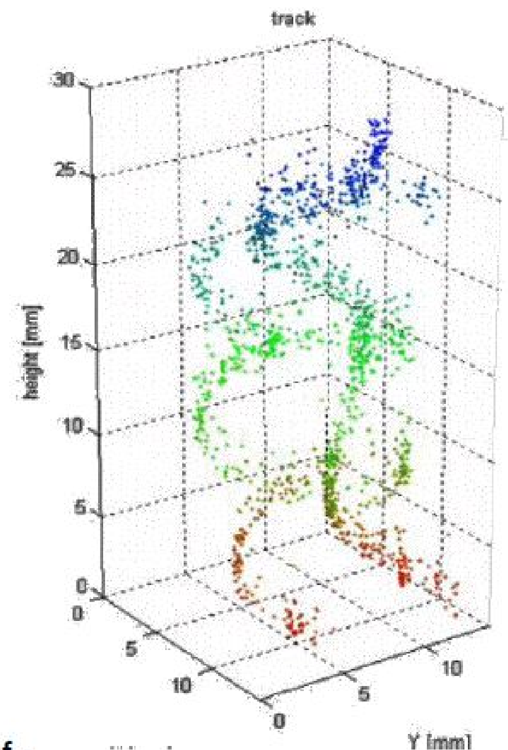

H. Van der Graaf ,
IEEE Nucl. Sci. Symp. Conf. Rec. (Dresden, October 2008)

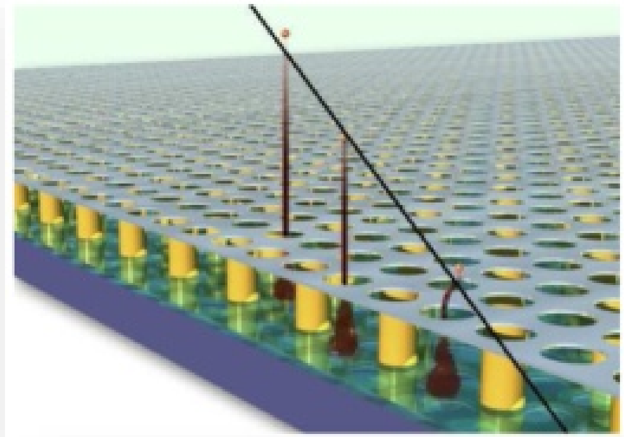

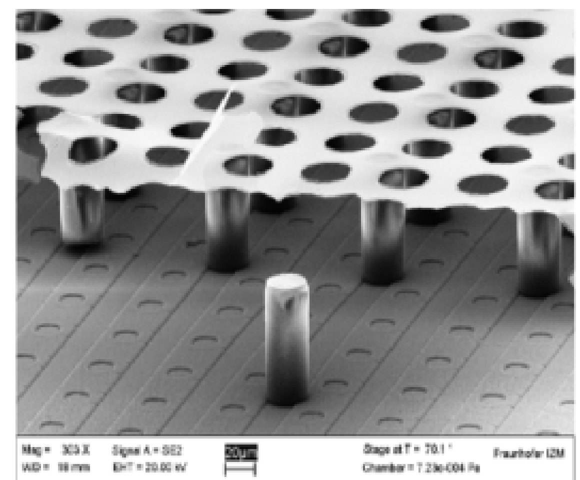

GEM

Thin metal-coated polymer foil pierced by a high density of holes (50-100/mm^2)
Typical geometry: 5 µm Cu on 50 µm Kapton, 70 µm holes at 140 µm pitch

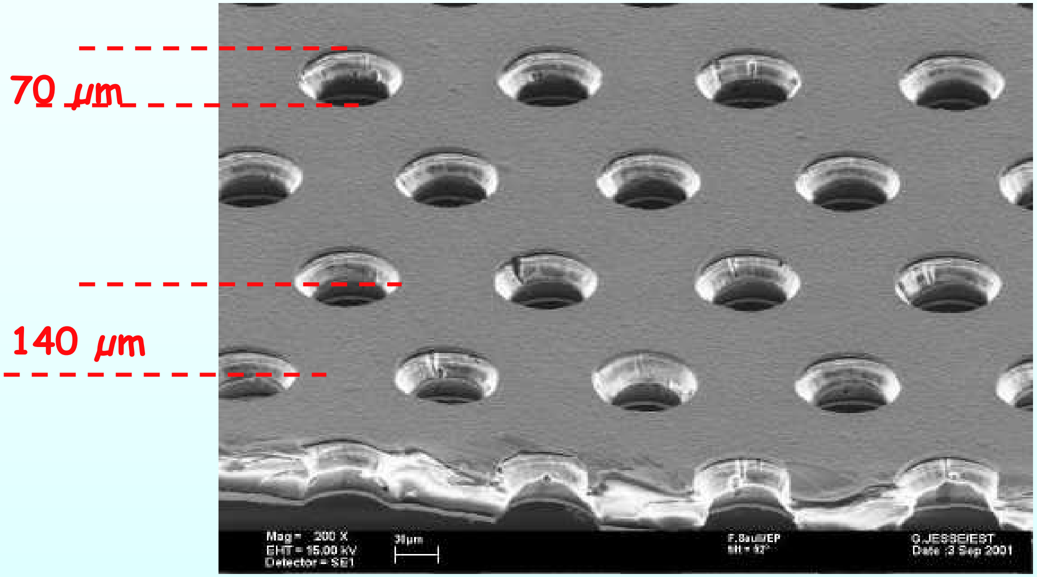

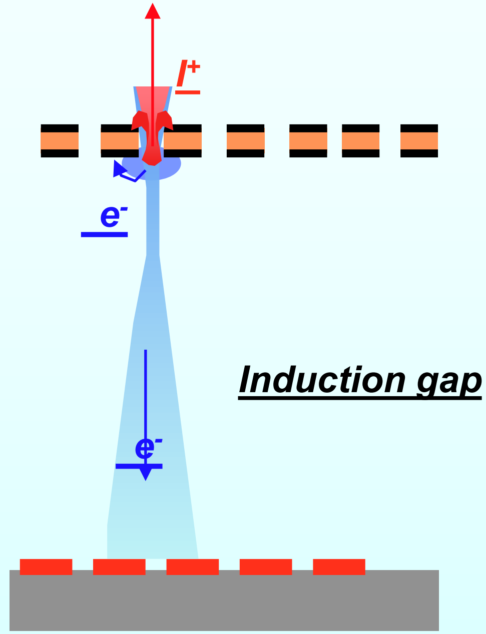

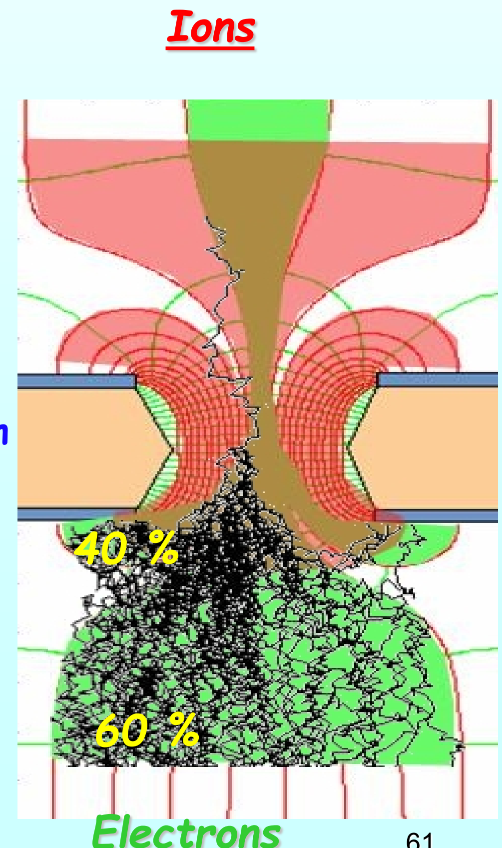

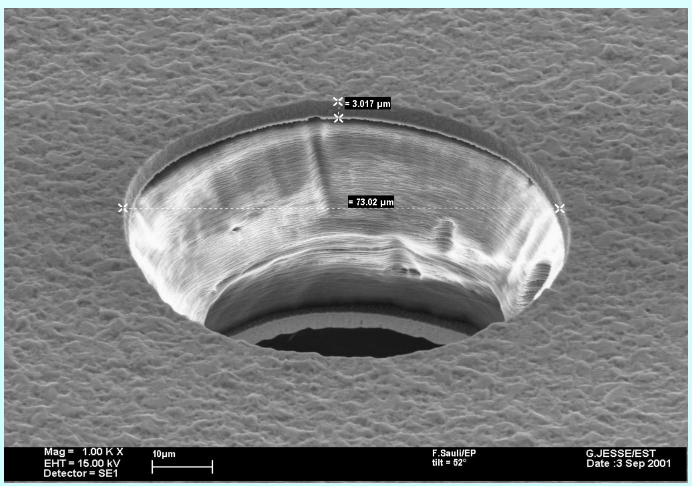

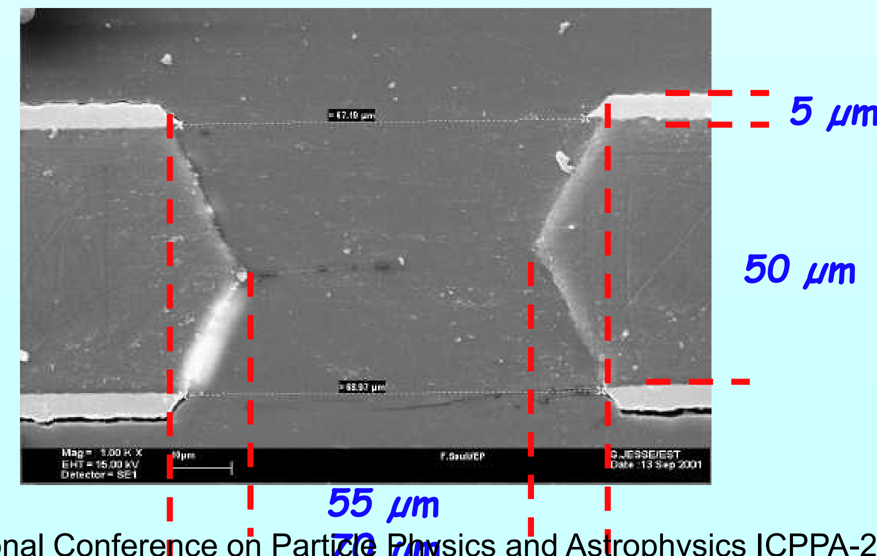

GEM Manufacturing

GEM foils are produced at CERN using proprietary process.

Rui De Oliveira
CERN-EST-DEM

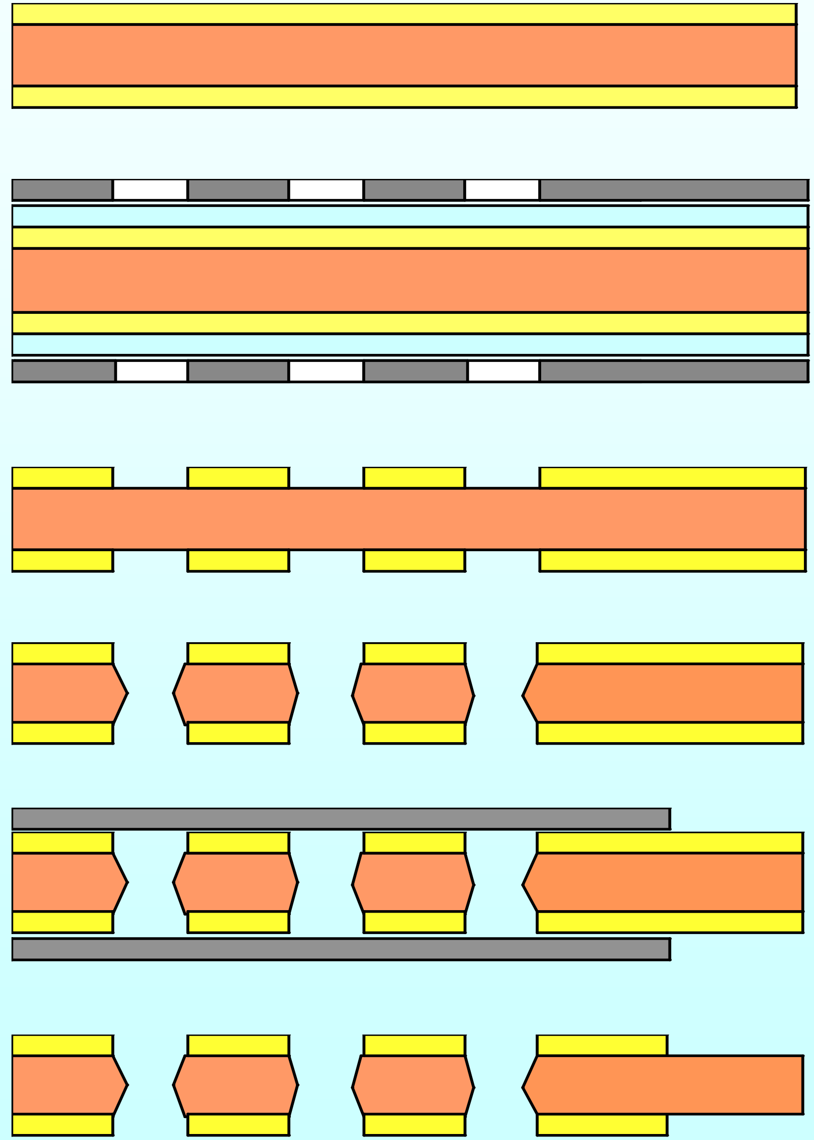

50 μm Kapton
5 μm Cu both sides

Photoresist coating, masking and exposure to UV light

Metal etching

Kapton etching

Second masking

Metal etching and cleaning

GEM – Gas Electron Multiplier

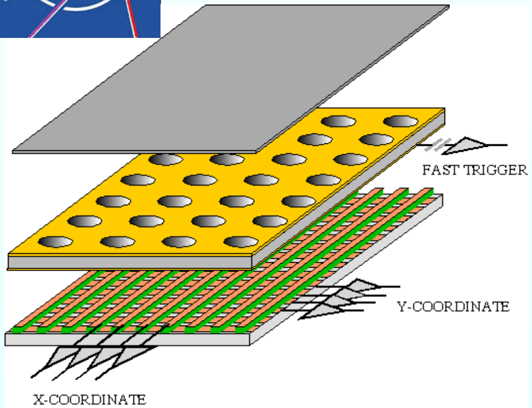

Full decoupling of the charge amplification structure from the charge collection and readout structure.
Both structures can be optimized independently !

A. Bressan et al, Nucl. Instr. and Meth. A425(1999)254

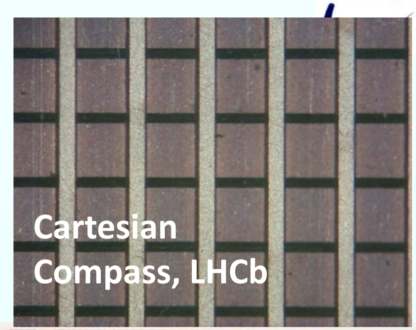

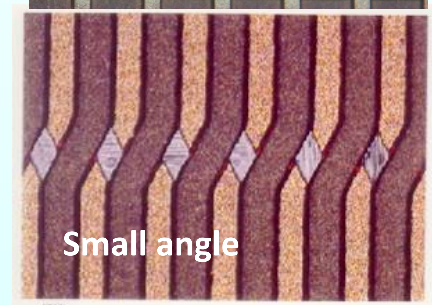

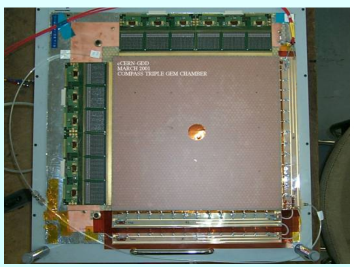

Different flat shapes

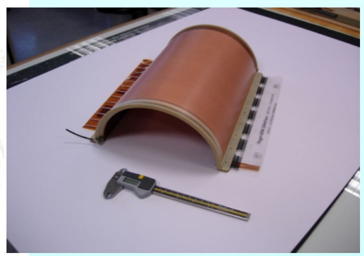

cylindrical

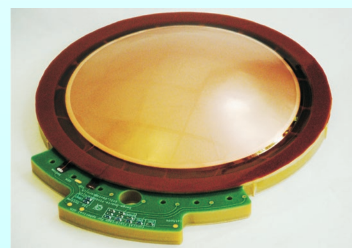

spherical

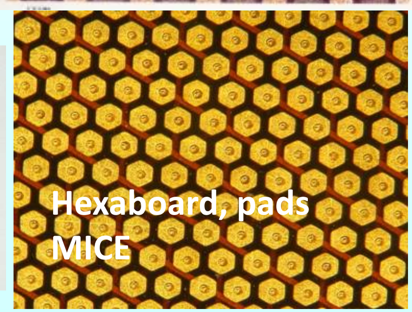

Most of the detectors use three GEM foils in cascade for amplification to reduce discharge probability by reducing field strength.

How do gaseous detectors work?

- a charged particle passing through the gas ionises some of the gas molecules;
- the electric field in the gas volume transports the ionisation electrons and provokes multiplication;
- the movement of electrons and ions leads to induced currents in electrodes;
- the signals are processed and recorded.

Simulation example (from R. Veenhof)

At the 100 μm scale

- Example:
  - CSC-like structure,
  - Ar 80 % CO_2 20 %,
  - 10 GeV μ.
- The electron is shown every 100 collisions, but has been tracked rigorously.
- Ions not shown.

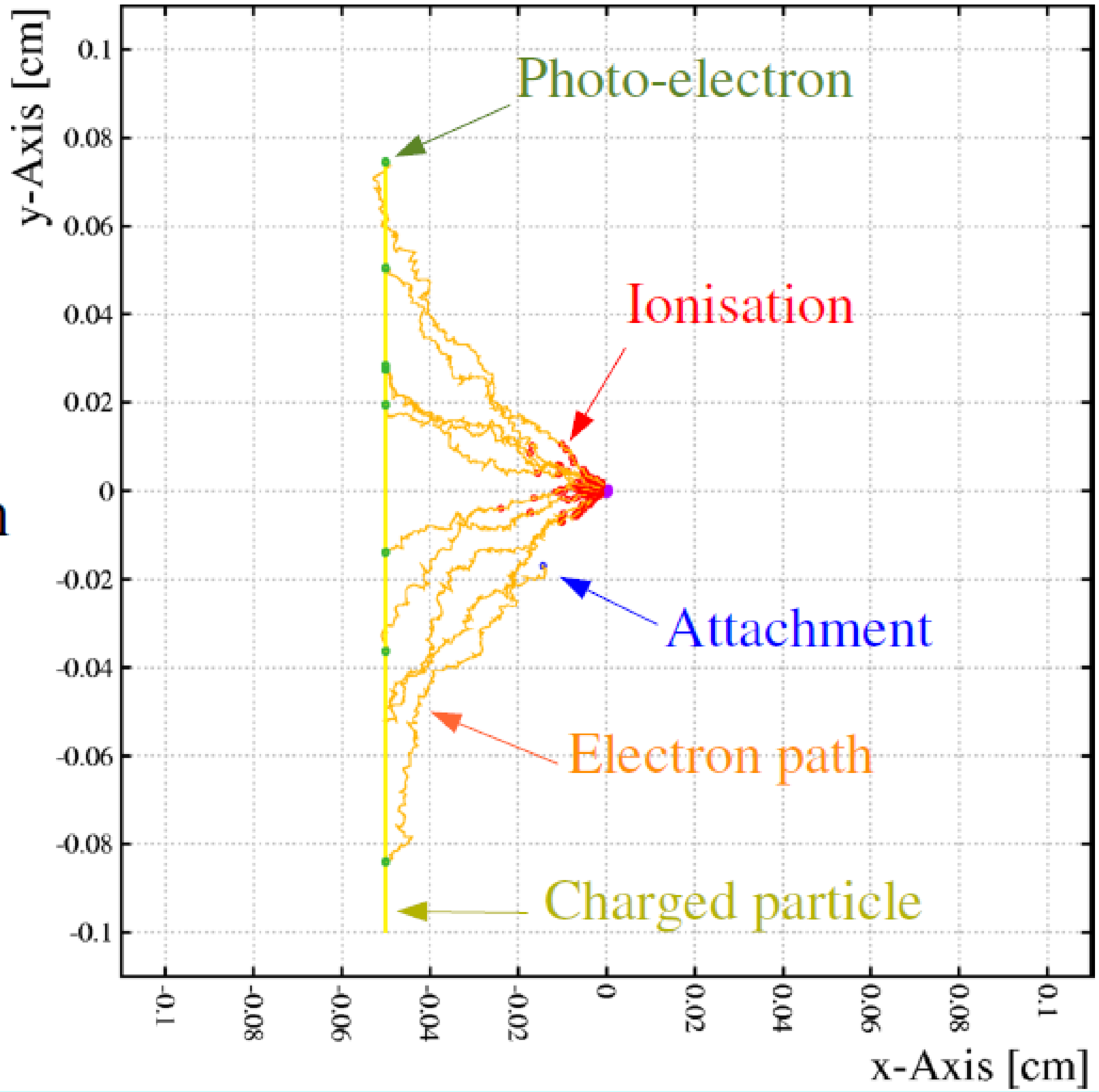

Ionization

- gas-based detectors: ~50 e⁻-ion⁺ pairs/cm;
- lH_2 bubble chamber: ~100 bubbles/cm;
- semi-conductor (Si): ~10^6 e⁻/h pairs/cm

Virtual photon exchange

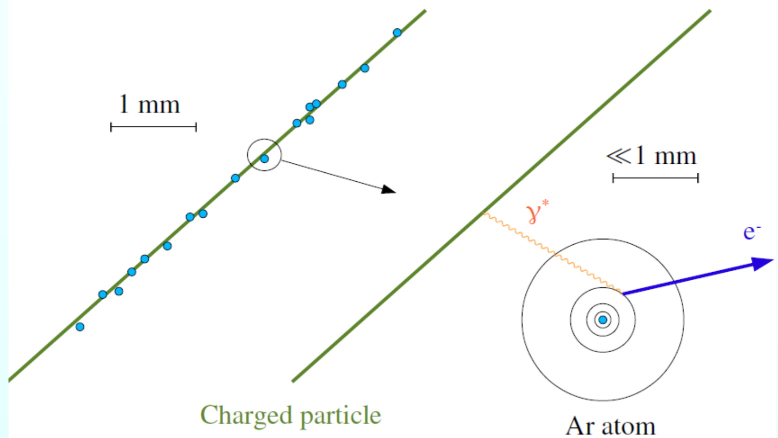

6. ATOMIC AND NUCLEAR PROPERTIES OF MATERIALS

Table 6.1 Abridged from pdg.lbl.gov/AtomicNuclearProperties by D. E. Groom (2007). See web pages for more detail about entries in this table including chemical formulae, and for several hundred other entries. Quantities in parentheses are for NTP (20° C and 1 atm), and square brackets indicate quantities evaluated at STP. Boiling points are at 1 atm. Refractive indices n are evaluated at the sodium D line blend (589.2 nm); values ≫1 in brackets are for $(n-1)\times 10^6$ (gases).

Material	Z	A	$\langle Z/A \rangle$	Nucl.coll. length λ_T {g cm^{-2}}	Nucl.inter. length λ_I {g cm^{-2}}	Rad.len. X_0 {g cm^{-2}}	$dE/dx\|_{\min}$ { MeV g^{-1}cm^2}	Density {g cm^{-3}} ({gℓ^{-1}})	Melting point (K)	Boiling point (K)	Refract. index (@ Na D)
H_2	1	1.00794(7)	0.99212	42.8	52.0	63.04	(4.103)	0.071(0.084)	13.81	20.28	1.11[132.]
D_2	1	2.01410177803(8)	0.49650	51.3	71.8	125.97	(2.053)	0.169(0.168)	18.7	23.65	1.11[138.]
He	2	4.002602(2)	0.49967	51.8	71.0	94.32	(1.937)	0.125(0.166)		4.220	1.02[35.0]
N_2	7	14.0067(2)	0.49976	61.1	89.7	37.99	(1.825)	0.807(1.165)	63.15	77.29	1.20[298.]
O_2	8	15.9994(3)	0.50002	61.3	90.2	34.24	(1.801)	1.141(1.332)	54.36	90.20	1.22[271.]
F_2	9	18.9984032(5)	0.47372	65.0	97.4	32.93	(1.676)	1.507(1.580)	53.53	85.03	[195.]
Ne	10	20.1797(6)	0.49555	65.7	99.0	28.93	(1.724)	1.204(0.839)	24.56	27.07	1.09[67.1]
Ar	18	39.948(1)	0.45059	75.7	119.7	19.55	(1.519)	1.396(1.662)	83.81	87.26	1.23[281.]
Xe	54	131.293(6)	0.41129	100.8	172.1	8.48	(1.255)	2.953(5.483)	161.4	165.1	1.39[701.]

- A minimum-ionising particle loses (only !)

$$1.519\,\mathrm{MeV\,cm^2/g}\times 1.662\times 10^{-3}\,\mathrm{g/cm^3} = 2.5\,\mathrm{keV/cm}$$

Ionization

Electrons are not evenly spaced, not even exponentially:

- 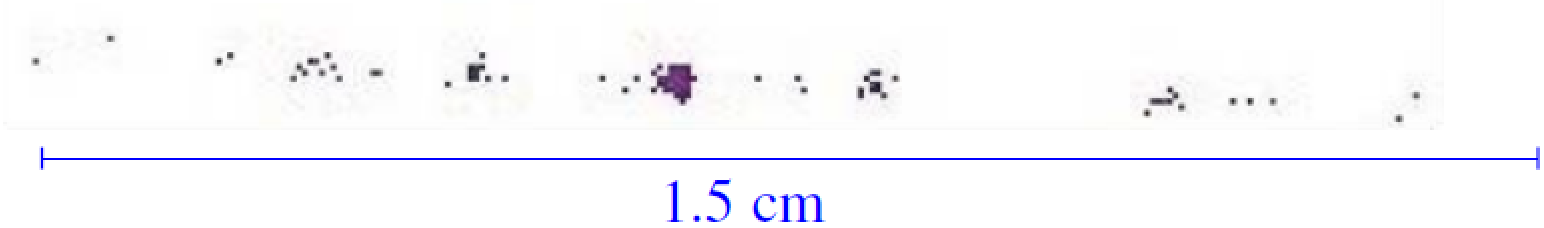

- 25-30 clusters/cm

δ-electrons

- Deposits are not always "lumps":

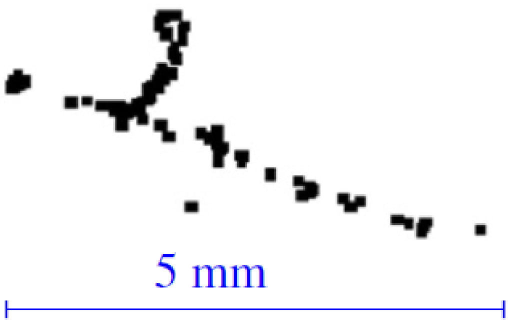

Number of primary ionising interactions per cm in Ar,

- by $\mu^{\pm}$ at minimum ionising energy,
- at 300 K and 1 atm,

according to

Degrad:	23.1 / cm
Heed:	24.1 / cm
Rieke-Prepejchal:	24.3 / cm
CERN 77-9:	29.4 / cm

Electron transport simulation

Electrons in Ar/CO_2 at E=1 kV/cm

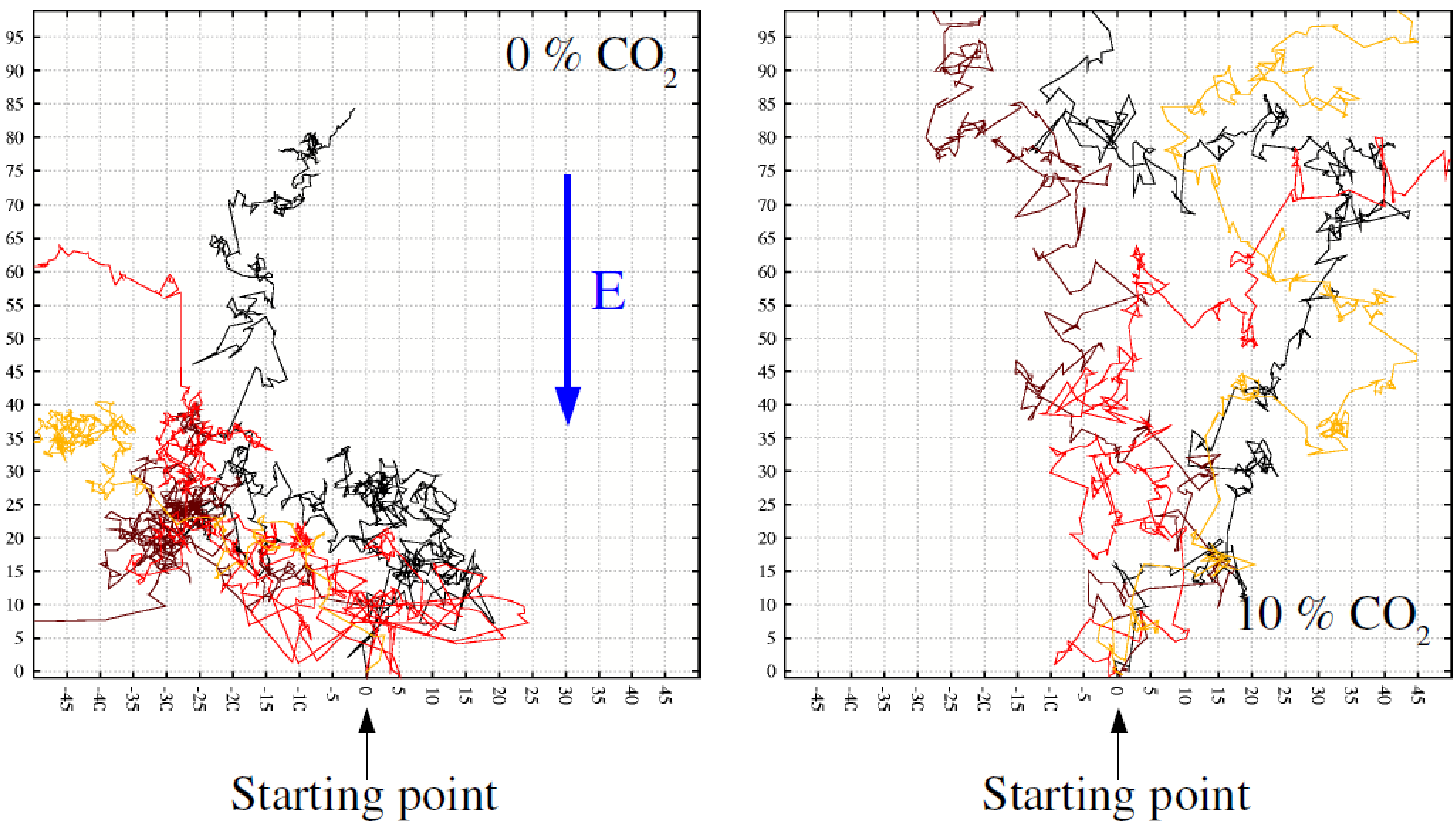

Electron transport simulation

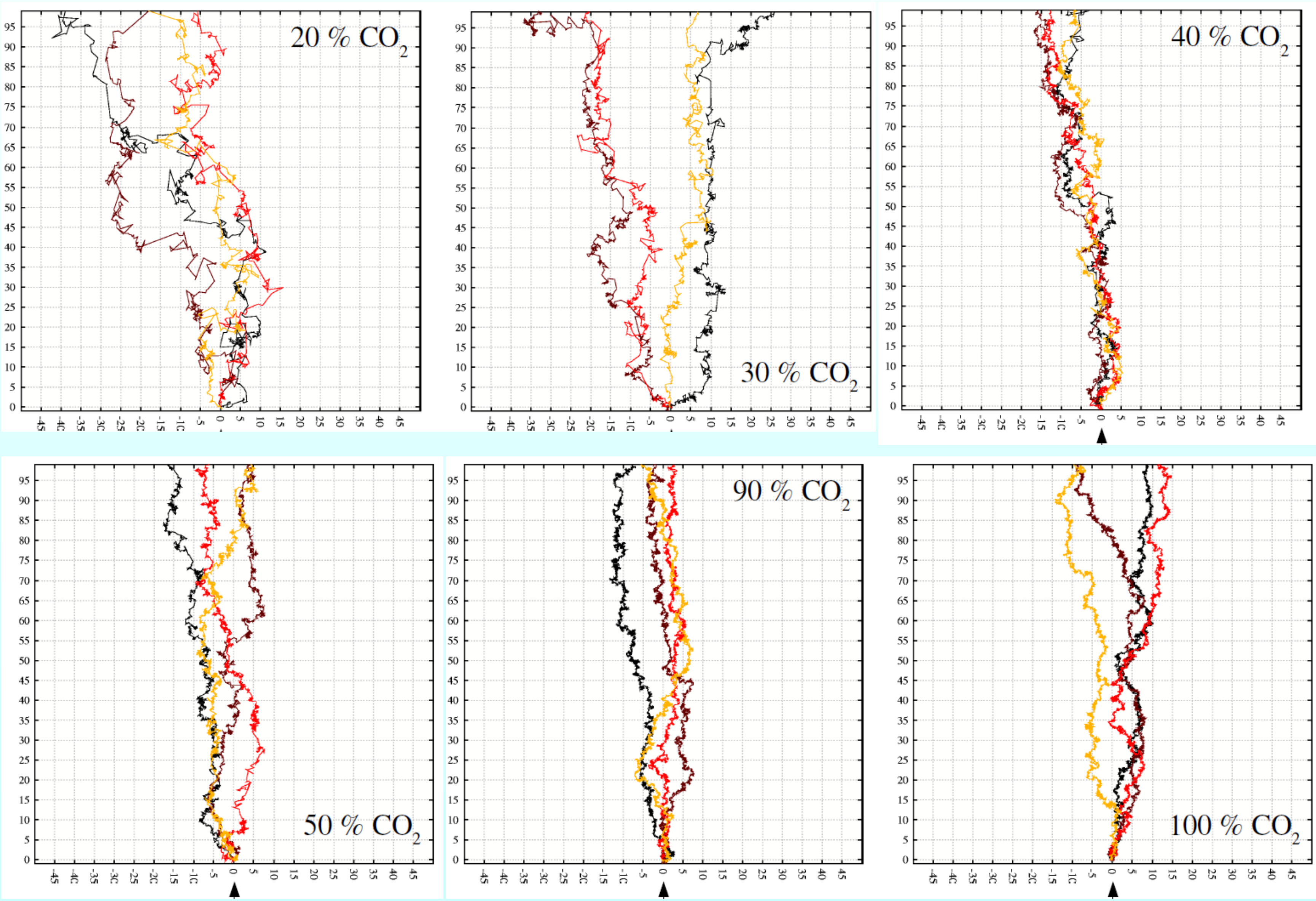

Electron Cross-section

Energy dependence of e⁻ scattering

- Elastic scattering:
  - dominant contribution for much of the energy range that concerns us;
  - only term < 15.7 eV (ionisation threshold).
- Non-trivial structure:
  - Ramsauer dip.

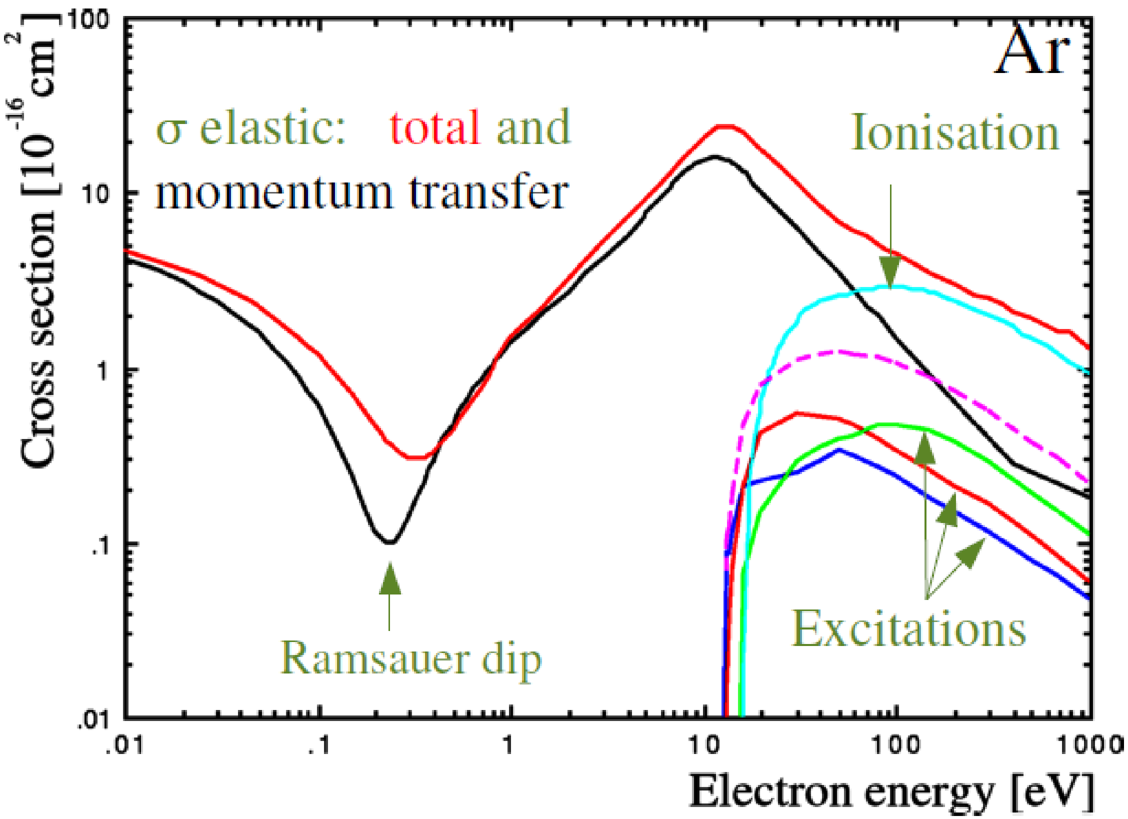

Gaseous detectors regimes

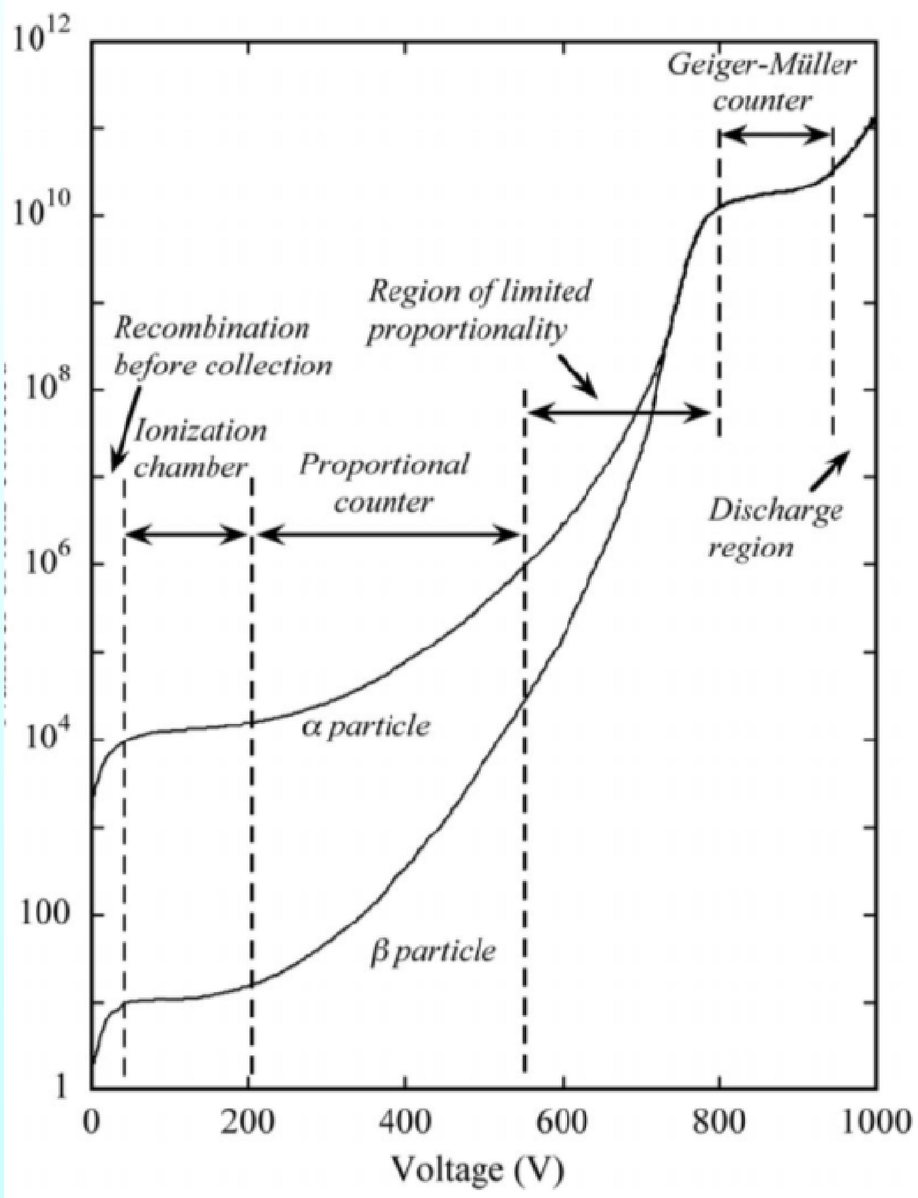

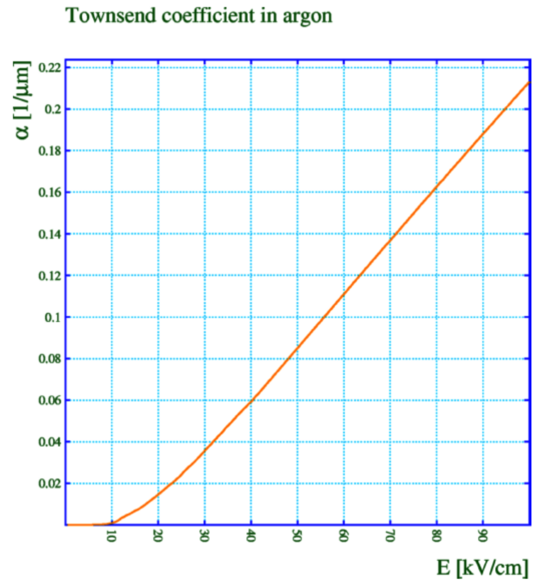

- Energy after a distance λ_e:
  - $\epsilon = E\lambda_e, \quad \lambda_e \approx 2.5\,\mu m$
- ionisation energy of argon:
  - IP ~ 15.7 eV
- ionisation would occur at:
  - $E > 60$ kV/cm,
  - indeed a typical field for multiplication, avalanches start much earlier, though.
- α: Townsend coefficient, # new e^- per unit length.
- Townsend coefficient α: probability per unit length that an electron creates an additional electron.
- Avalanches grow proportionally to their size:

$$dn(x) = n(x)\alpha(x)\,dx$$

$$n(x) = n(0)\,e^{\int_0^x \alpha(y)\,dy}$$

Ar atom radius: ~ 70 pm
distance between Ar atoms: ~ 4 nm
mean free path of electron: ~2 μm

Induction signals

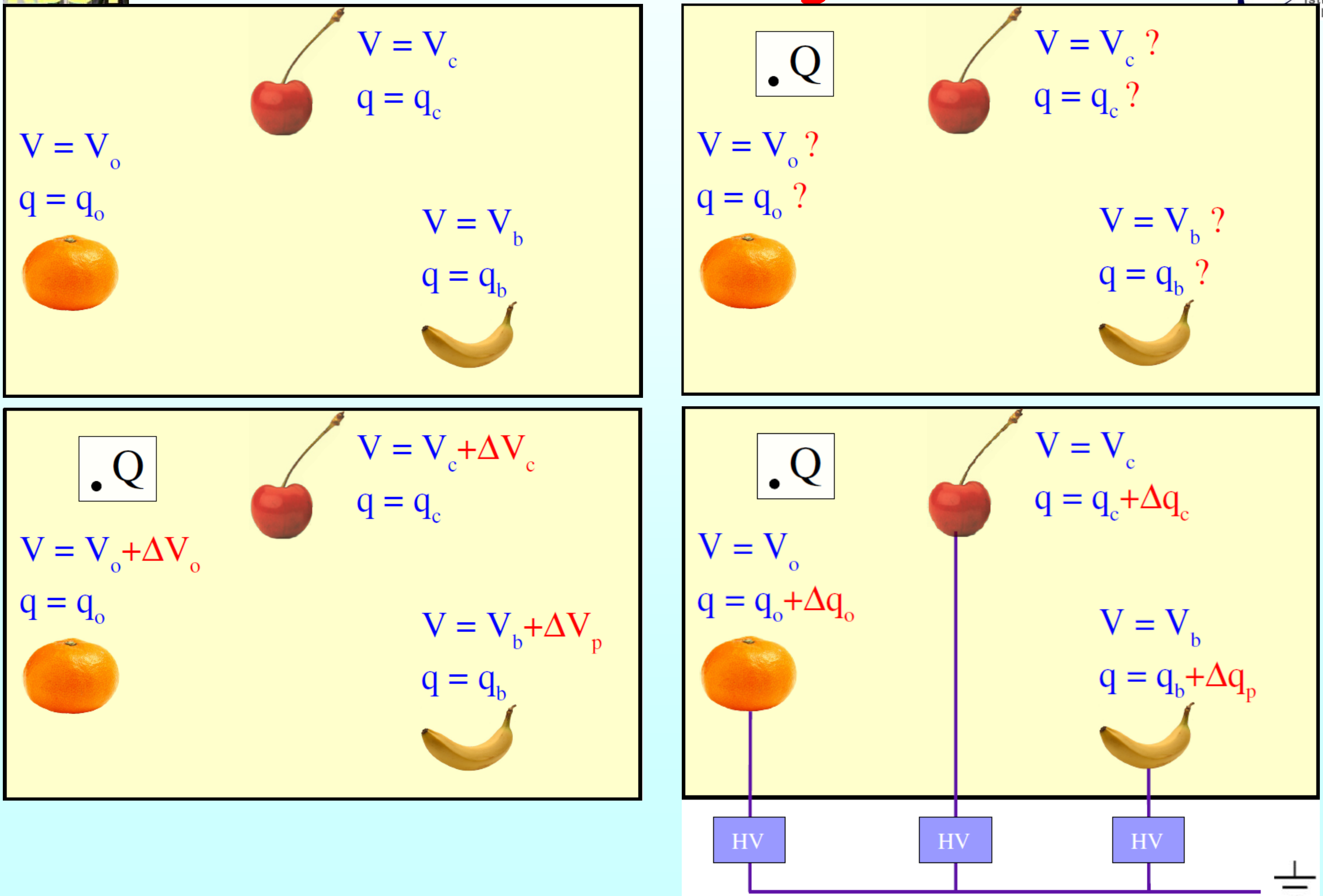

Induced charges

A point charge q at a distance z_0 above a grounded metal plate 'induces' a surface charge.

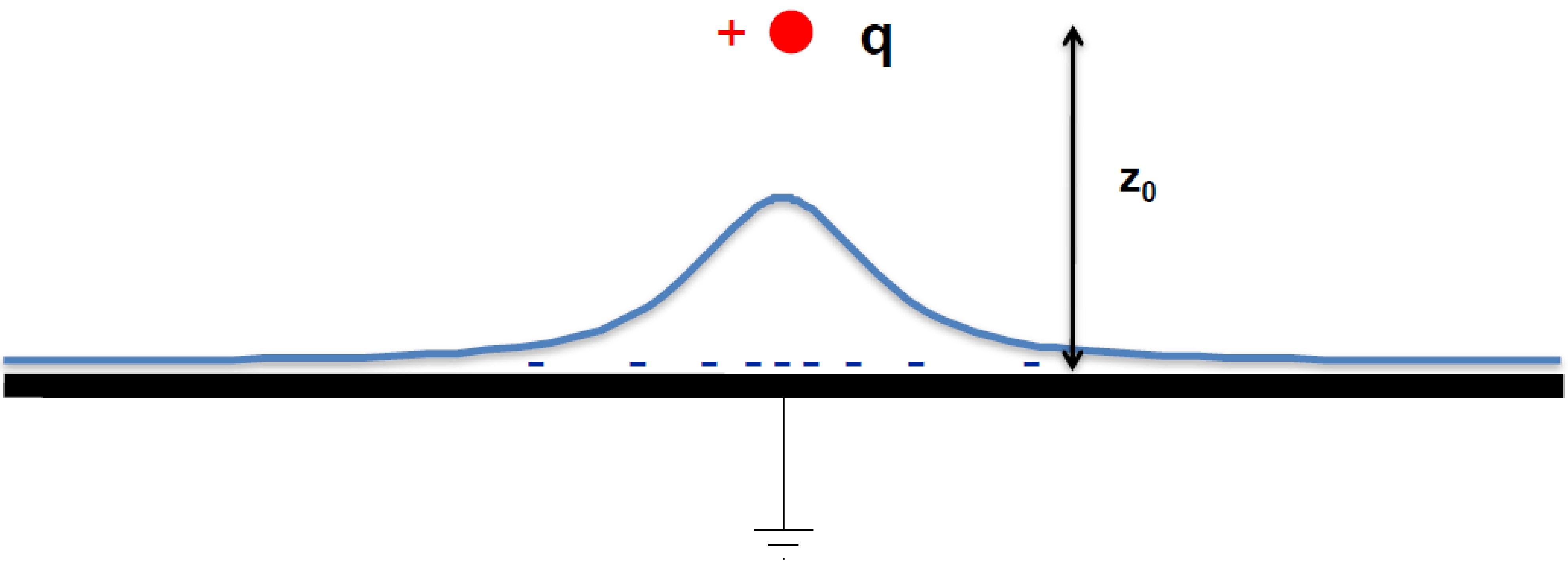

Induced charges

The total charge induced by a point charge q on an infinitely large grounded metal plate is equal to –q, independent of the distance of the charge from the plate.

The surface charge distribution is however depending on the distance z_0 of the charge q.

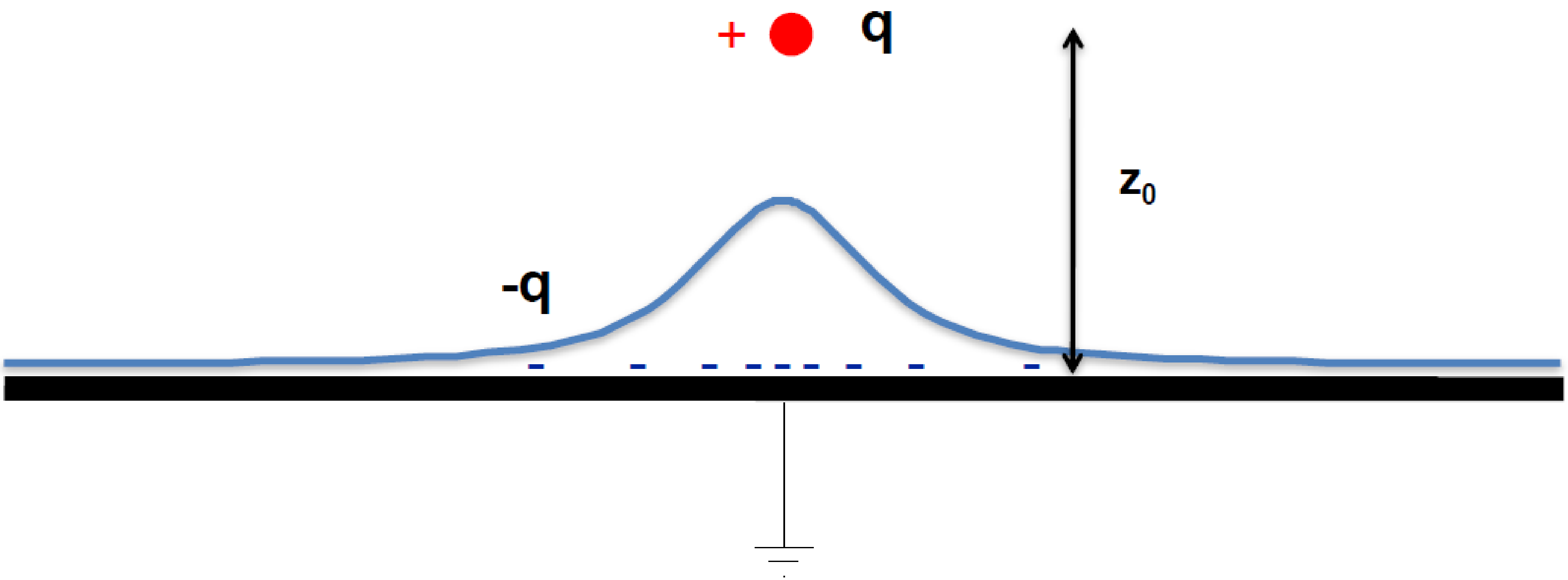

Induced charges

Moving the point charge closer to the metal plate, the surface charge distribution becomes more peaked, the total induced charge is however always equal to –q.

$$\sigma(x,y) = -\frac{q z_0}{2\pi(x^2+y^2+z_0^2)^{\frac{3}{2}}}$$

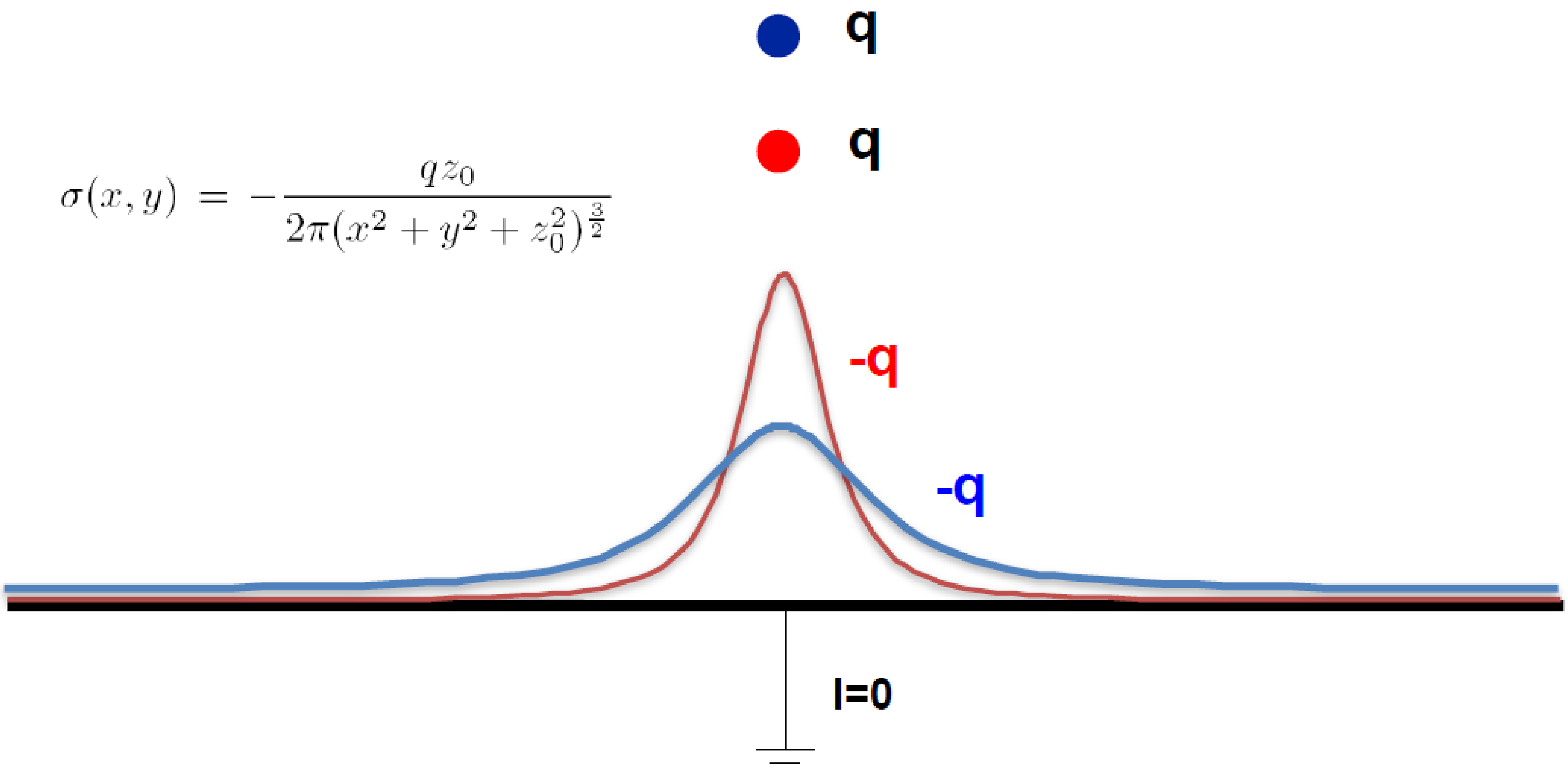

Induced charges

If we segment the grounded metal plate and if we ground the individual strips, the surface charge density doesn't change with respect to the continuous metal plate.

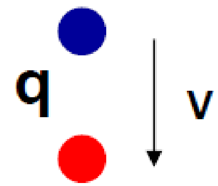

The charge induced on the individual strips is now depending on the position z_0 of the charge.

If the charge is moving there are currents flowing between the strips and ground.

→ The movement of the charge induces a current.

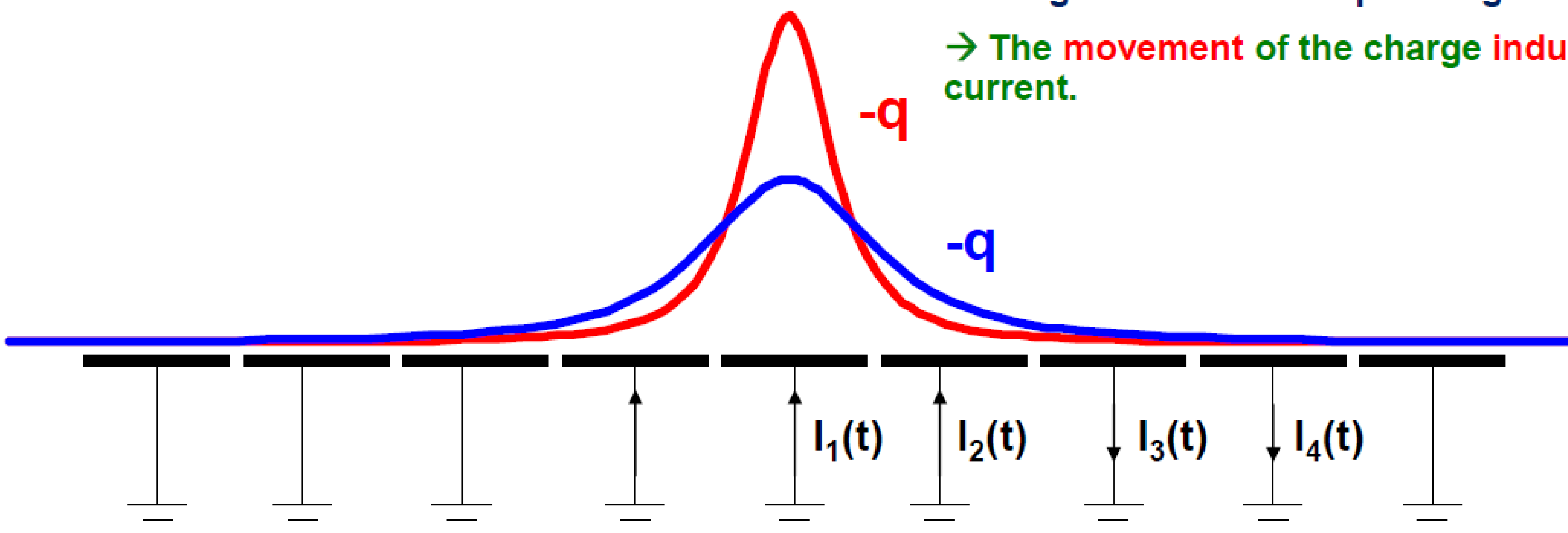

$$Q_1(z_0) = \int_{-\infty}^{\infty}\int_{-w/2}^{w/2}\sigma(x,y)\,dx\,dy = -\frac{2q}{\pi}\arctan\left(\frac{w}{2z_0}\right) \qquad z_0(t) = z_0 - vt$$

$$I_1^{ind}(t) = -\frac{d}{dt}Q_1[z_0(t)] = -\frac{\partial Q_1[z_0(t)]}{\partial z_0}\frac{dz_0(t)}{dt} = \frac{4qw}{\pi[4z_0(t)^2 + w^2]}v$$